MODELING AND SIMULATION OF GENERIC PRESSURE REGULATOR

By

MUHAMMAD RAMZAN

NUST201260251MRCMS64012F

Supervisor

Dr. Adnan Maqsood

RESEARCH CENTRE FOR MODELING & SIMULATION

NATIONAL UNIVERSITY OF SCIENCES AND TECHNOLOGY

2015

MODELING AND SIMULATION OF GENERIC PRESSURE REGULATOR

MUHAMMAD RAMZAN

Research Centre for Modeling & Simulation

A thesis submitted to the National University of Sciences & Technology

in partial fulfillment of the requirement for the degree of

Masters of Science

2015

DECLARATION

I certify that work titled “Modeling and Simulation of Generic Pressure Regulator” is my own work. The work has not been presented elsewhere for assessment. Where material has been used from other sources it has been properly acknowledged or referred.

Signature of Student

Muhammad Ramzan

NUST201260251MRCMS64012F

COPYRIGHT STATEMENT

ACKNOWLEDGEMENTS

I am thankful to you, my Creator Allah Subhana-watala that you guide me throughout this work at every step and for every new thought which you setup in my mind to improve it. Indeed I could have done nothing without your priceless help and guidance, not even I breathe without your intention let alone other endeavors. Whosoever helped me, weather my parents or any other individual was your will, so indeed none be worthy of praise and you be worthy of all praise and thanks.

I am profusely thankful to my beloved parents, sisters and brothers who raised me when I was not capable of walk and continue to support me throughout in every department of my life. I am also highly grateful to my wife Dr. Rubina Siddique for her special support and caring of my kids Esshal Ramzan (2 year old) and Muhammad Ayaan (6 months) during my research time at RCMS.

Special Thanks to my supervisor Dr. Adnan Maqsood for his help throughout my thesis and also for Compressible Fluid Dynamics and Advanced Flight Mechanics courses which he has taught me. I can safely say that I haven't learned any other subjects in such depth than the ones which he has taught.

I would also thank the rest of my thesis committee members Dr. Syed Salman Shahid, Dr. Majid Ali &Mr. Ammar Mushtaq for their valuable feedbacks and suggestions which helped me to improve the thesis. I would like to thank Irfan Ali Khan, Dr. Tariq, Ashraf Ali, Engr. Sikandar Hayat Mirza, Dr. Imran Akhtar and Dr. Ahmed Ejaz Nadeem for providing me the facilities and guidance.

I am also thankful to Khuram Ashraf, Yasir Hussain, and Muhammad Auwais for their support and cooperation.

Finally, I would like to express my gratitude to all the individuals who have rendered valuable assistance to my study.

Summary

Pressure regulator is a commonly used hardware device in industries that regulate the working pressure for plants and machines. It is installed in highly pressurized pipe lines of liquids as well as gases to regulate pressure as per requirement. In this research, dynamic analysis of pressure regulator is carried out. Specifically, the effect of pressure drop, valve opening and mass flow rate on outlet pressure is investigated. Three different approaches are adopted for analysis. Firstly, a non-linear mathematical model of pressure regulator with variable inlet is developed for analysis. Secondly an analytical solution of flow equation is generated based on constant mass flow rate assumption and results of pressure drop and valve opening are compared with nonlinear mathematical formulation. In the third approach, Reynolds-Averaged-Navier-Stokes (RANS) simulations are performed on 3D Computer Aided Design (CAD) of pressure regulator. Simplified 2D axis symmetry geometry is designed for analysis of flow simulation near valve opening. Steady state analysis is carried out for visualizing contours of pressure drop, velocity magnitude and temperature distributions. Valve opening and mass flow rate found with RANS simulation are also compared with non-linear mathematical formulation. Results indicate that the analytical solution adequately follows non-linear mathematical model solution. Moreover, detailed visualization is achieved through high fidelity RANS algorithm. The results of RANS simulations conform very close to nonlinear mathematical model as well. The approach has generated a high degree of confidence in the generic framework proposed in this research. The results will be used in the indigenous design and development of high pressure regulators.

Table of Content

LIST OF FIGURES

CHAPTER 1

Introduction

Pressure regulator is a commonly used device that controls the required working pressure for plants and machines in different industries. It is installed in highly pressurized pipe lines to transfer a relatively lower constant pressure. It is just like a dynamic valve that takes a varying high upstream pressure and reduces it to desired downstream pressure. The basic function of any gas pressure regulator is to ensure a safe supply of demand pressure within an acceptable tolerance, to the system attached with its outlet part.

1.1 Components of pressure regulator

It consists of set screw, working spring, main shaft, valve seat, inlet outlet chamber, sensing orifice, damping chamber, rolling diaphragm plate and return spring.

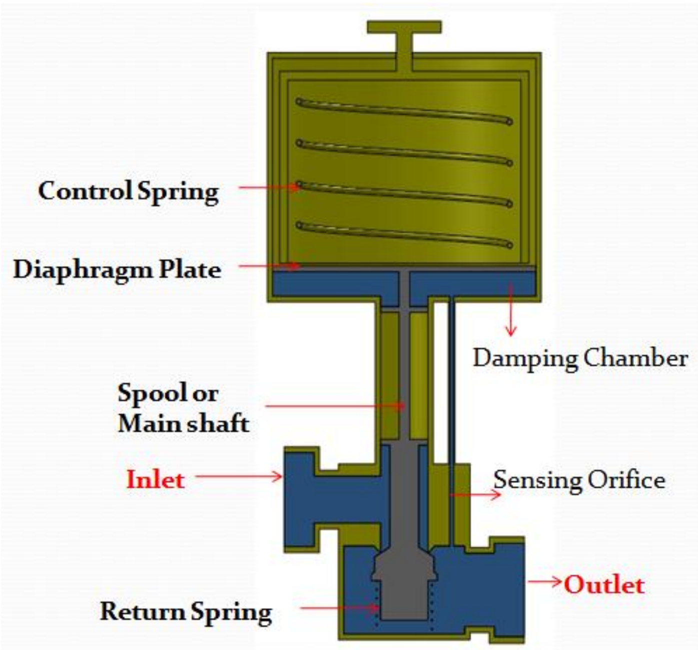

Figure 1.1 Components of pressure regulator

Three basic elements of any type of pressure regulator are restricting element (valve opening or vena contracta), loading element (weight, working spring compression) and measuring element (diaphragm plate, pressure gauges, bellows).In most cases, restricting element consists of a resilient valve seat (plug) and a sharp edge orifice. Function of restricting element is just like a dynamic valve and its basic purpose is to form a restriction to the flow which converts a high upstream pressure to low downstream pressure. Valve provides a major restriction to high inlet pressure so valve flow area is considerably smaller than that of surrounding flow area. In order to meet conservation of mass (continuity equation) the velocity will be greatest near the valve. This maximum velocity point in a flow is called vena contracta. After passing across the valve, fluid flow slows down in the larger downstream region and thus gives the some pressure recovery that was lost across the valve. This pressure recovery is dependent on style of valve.

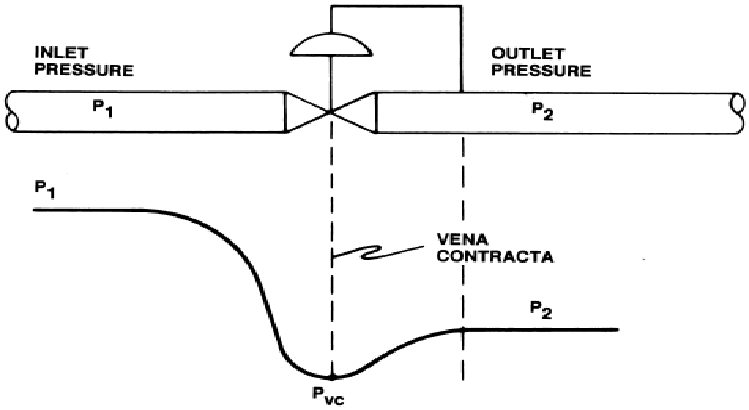

Figure 1.2 Pressure change inside pressure regulator [1]

In gas pressure regulator, gas flows due to pressure differentials across the valve opening. As we increase the pressure differentials across the valve by lowering downstream pressure, we reach a point where the gas velocity reaches to speed of sound at the vena contracta. Since we cannot normally make the gas travels faster than this limiting sonic velocity so we will have a maximum mass flow rate at this critical flow condition.

Restriction in high speed flow is obtained by valve which is connected to the loading element. All new design regulators use spring compression mechanism as a loading element. The spring is compressed downward by a tightening screw. When the screw is tight, the compressed spring gives a loading force on diaphragm plate. The screw is tightened for desired downstream pressure. The specifications of spring are referred with parameters like, type of material, wire diameter, spring diameter, free length, and the number of coils. The spring rate is the main factor which is defined as force required to compress the spring per unit meter.

A measuring element is used to control the downstream pressure. In most universally used gas pressure regulator measuring element is the diaphragm plate. Diaphragm plate provides an effective area for pressure distribution against the loading force. Effective area of diaphragm is selected according to the demand downstream pressure.

1.2 Working of Pressure Regulators

Initially the valve of regulator is held open by intelligently tightening the working spring by screw. High inlet pressure passes through the valve and enters in the regulator downstream chamber. This downstream chamber is connected with the sensing orifice, through which downstream pressure reaches to damping chambers. Damping chamber is connected with rolling diaphragm, which moves the main shaft upward and downward against the spring compression force. As downstream pressure increases, the force on the rolling diaphragm increases, in direct opposition to the spring force.

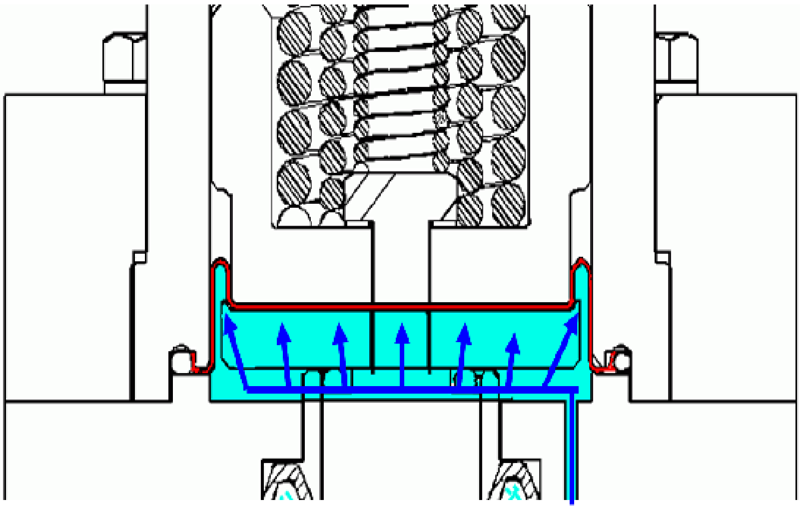

Figure 1.3 Pressure in damping chamber against the load spring force on diaphragm plate

When downstream pressure exceeds the spring force, the rolling diaphragm overpowers the spring loading. This compresses the spring and forces up the main shaft.

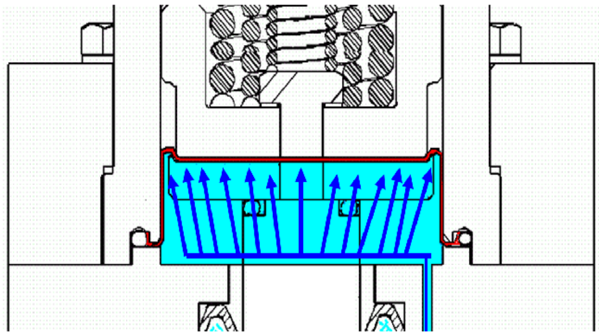

Figure 1.4 Lifting of diaphragm plate with increasing of controlled pressure

The valve, as part of the main shaft, closes against the main internal orifice, preventing additional pressure downstream. It will remain closed as long as downstream pressure exceeds the set points, as determined by the set screw controlling the force on the springs.

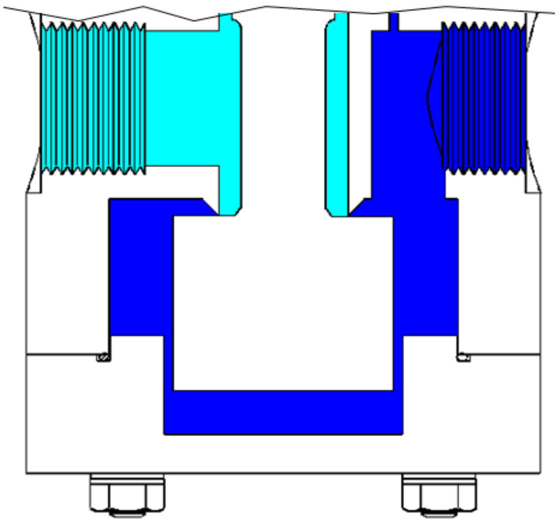

Figure 1.5 Closing of valve due to over pressure in downstream chamber

When the downstream pressure falls below the demand pressure then the pressure in the damping chamber and so the force on the diaphragm plate decreases as a result the valve begins to re-open as the springs again force the main shaft to move down.

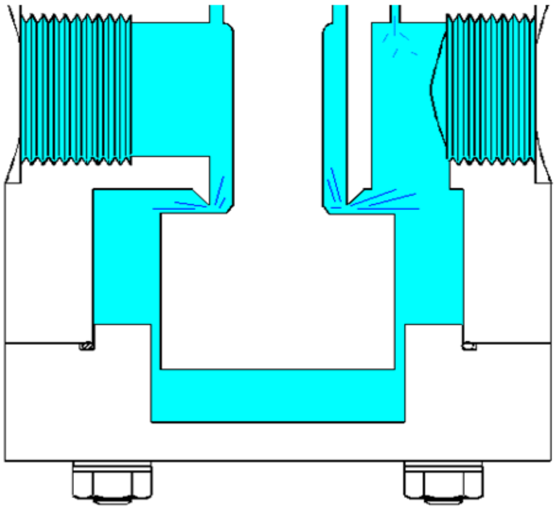

Figure 1.6 Valve opening due to decrement in required outlet pressure

The process of pressure increase and decrease in the damping chamber and in the downstream continues and as a result the main shaft and valve body move in upward and downward direction. In most application, a properly set pressure regulator quickly finds a balance as long as inlet pressure is higher and relatively constant and downstream conditions are stable. The valve stays partially open, with the force of the downstream pressure against the rolling diaphragm and the force of the internally springs in a state of equilibrium. This equilibrium continues as a long as upstream pressure decreases to certain pressure with respect to downstream pressure.

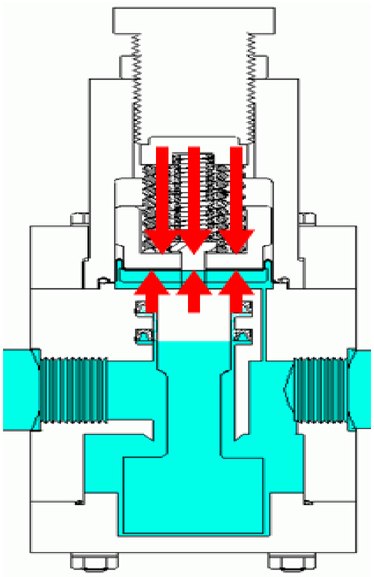

Figure 1.7 Balance of force in upward and downward direction

The actual magnitude of the decrease in controlled pressure require to open the valve is a function of the design parameters for the given regulator and is caused by the required change in spring compression. This is why it is occasionally referred to as spring effect. Adjusting the amount of initial compression will change the value of the pressure at which we will operate under any load condition. As a matter of fact, this is exactly how we adjust the set point pressure on our regulator. As we have seen, however, adjusting the spring compression does not change the amount of spring effect.

1.3 Application of Pressure Regulator

Various application of pressure regulator can be found in industrial as well as in commercial sites. Below some of its basic applications are given below.

1.3.1 Turbine system

In Turbine systems uniform pressure is needed throughout it operation. The main factor that affects the efficiency of any turbine system are the pressure losses through the control valves which is located between turbine and the boiler to control the mass flow rate in turbine system. Due to the desirability of maintaining the steam supply to a turbines as nearly as possible at a uniform pressure it is customary to generate steam at a pressure somewhat higher than the required by the turbine and to effect the necessary reduction by means of a pressure regulator. These pressure regulators should be sensitive to these rapid fluctuations in inlet pressure.

1.3.2 Gas piping network

In Gas piping network, it is necessary to ensure a supply of demand pressure with acceptable errors. Demand pressure level are controlled by gas pressure regulating station in which pressure regulators are responsible for maintaining a stable downstream pressure to the end user. These pressure regulators are designed in such a way that the downstream pressure oscillates with acceptable limits and it should not lead to instability. In this gas piping network, amplitude and frequency of downstream pressure are sensitive to upstream pressure and the size of downstream pressure.

1.3.3 CNG-Powered Engines

In CNG-Powered Engines, pressure regulator is the central part of whole system, which reduces the gas storage pressure to a level acceptable for injection into the intake pipe of respective cylinder. Mechanical pressure regulator has slow dynamic response for decreasing upstream pressure and variable downstream pressure demand. So for increasing performance of mechanical pressure regulators, sensors are added to it. This sensor system detects the downstream pressure demand and quickly finds a valve opening for variable demand pressure.

1.3.4 Aircraft Environmental control system

In Aircraft Environmental control system pressure regulator is critical component. Pressure regulator is installed in a pipe line in an air flow path where available inlet pressure to the valve may vary within a wide range. Core function of this pressure regulator is to regulate the air flow and maintain almost a constant pressure in pressure control circuits of pilot chamber. Depending on the air flow these pressure control circuits set the criteria for valve opening inside regulator.

1.3.5 Rocket Feed System

In Rocket Feed System**,** pressure regulator is used to feed the gas into the liquid propellant tank of rocket at a controlled pressure. Simple pressurised feed system consist of high-pressure gas tank, a gas starting valve, a pressure regulator, propellant tank, propellant valve and feed lines. When the gas start valve is open, high pressure gas flows from the high-pressure gas tank to the pressure regulator which converts this high pressure gas to constant and low downstream pressure. A reduced pressure is transmitted through feed lines to propellant tank for its control pressurization.

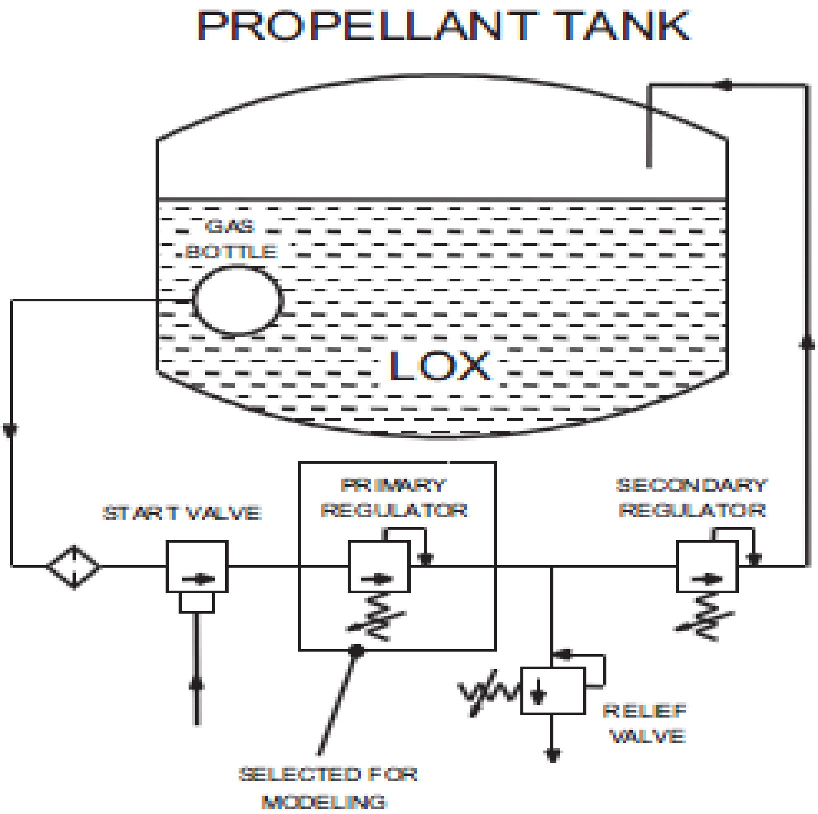

Figure 1.8 Rocket feed system

Besides above major application some other uses of pressure regulator are in oil and mining industry, in air compressor system, in distribution of water and natural gas to houses and factories, in sea exploring with oxygen cylinder, in fire protection system of high rise buildings and in various other industrial and commercial applications.

1.4 Research Objectives

The objectives of this research endeavor are:

- Development of non-linear mathematical model for the simulation of pressure regulator.
- Analysis of pressure regulator for required outlet pressure and corresponding mass flow rate as a function of valve opening and inlet pressure.
- Development of closed form solution of flow equations with some assumptions.

- Comparisons of mass flow rate and valve opening with closed form solution and through system of non-linear equations.
- RANS simulation of pressure regulator for visualizing pressure drop inside regulator.
- Comparison of RANS simulation and simulation of non-linear mathematical model.
- Our main objective is to find the design parameters for our particular type of regulator. The important design parameters of pressure regulator are control spring stiffness, diaphragm area, return spring stiffness, sensing orifice area, inlet and outlet diameter, discharge coefficient, valve opening and load on control spring for desired outlet pressure.
- Corresponding to above design parameters values, we make a mathematical model of pressure regulator in which inlet pressure is changing from 150bar to 60bar and we require 15bar pressure at outlet port of pressure regulator. Mass flow rate equation for different chambers of pressure regulator and the dynamic equation of moving shaft will be developed for above inlet pressure. Dynamic equation of pressure change and temperature change for inner flow volumes of pressure regulator will be derived based on the simplification of continuity equation and energy equation. Based on the design parameters and mathematical model we will simulate pressure regulator numerically and analyze the mass flow rate and valve opening as a function of time and inlet pressure.
- For gaining flow characteristics inside pressure regulator we will develop the computational model for CFD analysis of pressure regulator. This will consist of both 2D axis symmetry model and 3D model of pressure regulator for CFD simulation of flow visualization inside pressure regulator for steady and unsteady conditions. We will perform CFD analysis for finding pressure, velocity and temperature distribution for different valve opening and inlet pressure. A curve of valve opening and mass flow rate will be obtained with respect to different inlet pressure. This will provide potential for geometry improvement and reduce experimental cost.

- This research also includes the development of analytical solution of flow equations based on some assumptions. Outlet pressure as a function of time will be then compared with the numerical solutions.

1.5 Methodology

Using simplified form of continuity and energy equations, a non-linear mathematical model is developed for finding pressure and temperature change in different flow volumes of pressure regulator. This system of non-linear and coupled equations is numerically simulated with MATLAB®. Closed form solution of non-linear pressure equation is obtained by making it linear differential equation with some assumptions. 3D and 2D CAD geometry of pressure regulator are developed and meshed in GAMBIT®. Mesh file is imported in FLUENT® and RANS simulation is carried out for finding the pressure drop inside regulator corresponding to different inlet pressure. A detailed conceptual methodology is pictorially depicted below

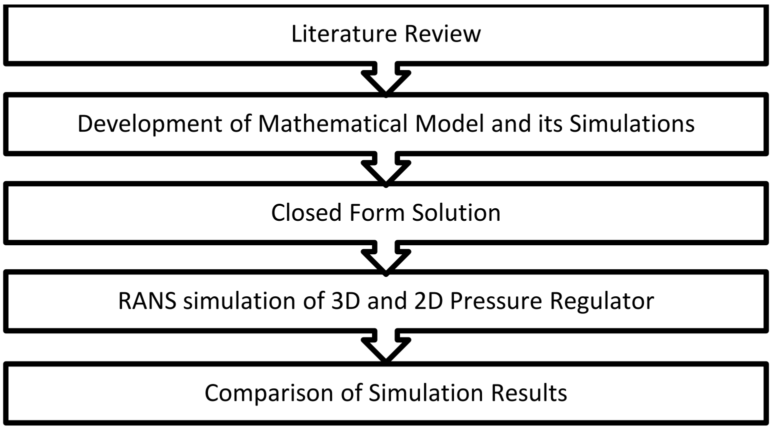

Fig 1.9 Methodology Flow Chart

1.6 Organization of Thesis

This thesis is composed of 8 chapters. The outline of each chapter is discussed below.

Chapter 1: Introduction

In chapter 1 brief introduction to pressure regulator is presented. Overall working of pressure regulator and all its components are briefly discussed. Applications of pressure regulator in various industrial works are also explained.

Chapter 2: Literature Review

A brief summary of literature review is presented in chapter 2. It consists of fundamental principles of pressure regulator its mathematical modeling and its stability study. Analysis of pressure regulator with CFD is also presented in chapter 2.

Chapter 3: Development of Mathematical Model

A non-linear mathematical model is developed based on continuity and energy equations which measure the pressure and temperature in each flow volumes of pressure regulator. Equation of moving shaft is also developed in this chapter for the analysis of valve opening and mass flow rate calculations.

Chapter 4: Numerical Computation of Governing Equations

In this chapter computational form of mathematical model are presented. Flow equations for each control volumes of pressure regulator are discritize with finite differencing method. Computational form of moving shaft equation is also presented.

Chapter 5: Simulation Results and Discussion

In this chapter simulation of pressure regulator is presented. Results of outlet pressure, temperature, mass flow rate and valve opening are presented for each flow volume of pressure regulator.

Chapter 6: Analytical solution of flow model for pressure regulator

Based on some assumptions, closed form solution of pressure equation is presented in this chapter. Comparison of results is also discussed.

Chapter 7: CFD analysis of pressure regulator

In this chapter CFD analysis of 3D and 2D pressure regulator is presented based on different inlet pressure and valve opening. Results of outlet pressure and mass flow rate of pressure regulator are also compared with that of mathematical models.

Chapter 8: Conclusion and Future work

Overall thesis conclusion is presented in this chapter and future research on pressure regulator is also presented for its better performance.

CHAPTER 2

Literature Overview

2.1 Fundamentals of Pressure Regulator

Floyd D. Jury [1] briefly explained the working of gas pressure regulator and basic principle of gas flow from the regulator. He systematically explained the three main essential elements of pressure regulator and their working. Physics of pressure change inside regulator is also discussed. He briefly describes the spring and diaphragm effect for demand pressure with examples. Self operated regular, pilot operated regulator and service regulator without velocity boost are also explained.

EMERSON[2] technical reference section includes articles covering regulator theory, valve sizing, over pressure protection and other topics relating to regulator. Selection criteria of different types of regulator are provided according to demand pressure and design requirement. Principles of direct operated regulator and self-operated regulator are studied with advantages and disadvantages. General sizing guidelines for designing pressure regulator are provided. Physics of valve sizing calculation both for liquid services and gas services are explained for users. Temperature drop consideration and reduced freezing problem are also briefly described. Conversion tables and different informative charts are also provided at the end. Kevin Shaw [3] briefly explained the natural gas pressure regulator and summarizes different types of regulator advantages and disadvantages. He also measured the flow rate with respect to outlet pressure for boost and droop analysis.

2.2 Modeling of Gas Pressure Regulator

Limited research is available in modeling complex flow inside pressure regulator. For many years, the trial and error method were used for designing and modifying pressure regulator. Miles O. Dustin [4] studied the simulation of a spring-loaded, direct-acting, single –stage gas pressure regulator which was used in solar Brayton cycle space power generator. He examined the effect of design parameters on stability that includes transient response and steady-state accuracy. He found that stability increases with increasing spring rate but regulating ability of regulator is decreased. He investigated that nonlinear spring can provide good stability at all supply pressures with minimum steady- state offset. Dependency of outlet volume on stabilizing effect was also investigated. DragoljubVujic [5] presented the non-linear dynamic model of a gas pressure regulator. His model shows the self-exciting oscillations of systems with certain amplitude and frequency without the presence of outside disturbance. He investigated the effect of each design parameters for self-exciting oscillating and found methods to correct them. He proposed that a linear model is sufficient for evaluation of stability and transient response if flow through valve is laminar, dry friction is negligible and the motion of valve and diaphragm is not constrained.

Jiang Yanping and ShenChibing [6] presented the dynamic model of pressure reducing valve. They studied the dynamic processes of valve for pressurizing, startup and for different operating conditions by numerical simulations and experimental investigation. They concluded that increasing the area of damping hole or decreasing the volume of damping cavity can not only reduce redressing time of the pressure regulating valve, but also reduce overshoot and increasing the stiffness of the main spring can reduce the redressing time of the pressure regulating valve. Sunil S. & UllekhPandey [7] developed the linear dynamic mathematical model for cryogenic pressure regulator. They tested the model with the experimental test of cryogenic pressure regulator which was developed by Liquid Propulsion Systems Centre (LPSC) of Indian Space Research Organization. They measured the effect of cryogenic temperature in the regulated pressure taking into account of spring load variation, design changes and also fluid property.

A.R. Shahani, H. Esmaili [8] studied the dynamic equation of pressure and temperature with the assumption of adiabatic process happening in high pressure regulator. They simulated this model using numerical tools and tested the result experimentally. They found that as outlet volume increases the stability of outlet pressure increases and as spring load increases, outlet pressure increases proportionally. According to them control spring stiffness and diaphragm area are two sensitive parameters that effect too much to downstream pressure of regulator. They suggested that for the better control of outlet pressure of regulator these two parameters should be designed and manufactured carefully. Kakulka et al [9] studied the pressure regulator with conical valve to control the downstream pressure. He investigated the dynamic effect of valve opening with changing upstream and downstream volumes. Nabi et al [10] obtained the dynamic model for newly designed regulator. He simulated the model by Runge Kutta method and measured the regulator behavior for different design. He performed an experiment for the physical test of this regulator and compared with the result of dynamic model.

2.3 Stability Study of Pressure Regulator

Various authors studied the variation in downstream pressure for the analysis of stability criteria of regulator. NaciZafer, Greg R. Luecke [11] developed the comprehensive dynamic model of self-regulating high pressure gas regulator and use the linear model to analyze the stability of system. They simulated this linear model using root locus technique with variation of various design parameters and found the most influential system parameters. They concluded that damping coefficient, the diaphragm area, and upper and lower volumes are most important design parameters that affect the stability. They found improvement in stability with the decrease in flow path between regulator body and lower pressure chamber. Liptak [12] suggested that stability of the system increases by using larger downstream pipes, more restrictive flow from orifice to lower chamber and straight pipes both in upstream and downstream. He provided an equation for the offset of the regulating pressure with varying flow. He concluded that decrease in offset pressure decreases the stability of the regulator in term of noise and oscillatory downstream pressure.

E1 golli Rami, Bezian Jean-Jacques [13] provided mathematical models and experimental analysis for a common pilot controlled regulator. They carried experimental as well as numerical simulation for finding the regulator performance and found that operating conditions that increase stability. Their numerical and experimental results were in good agreement with respect to each other. They concluded that oscillation in downstream pressure increases for small volumes and higher upstream pressure. Their study showed that opening of valve and driving pressure have less effect on oscillation of downstream pressure. They also showed that length of sensing lines from downstream chamber to damping chambers of regulator has only little influences on the oscillation of downstream pressure.

2.4 CFD Study of Pressure Regulator

With the advancement of Computational Fluid Dynamics (CFD) techniques, lots of authors are able to see the complex flow pattern inside of pressure control valve. CFD techniques are now becoming popular for the analysis of transient, compressible and turbulent flow. Both steady state analysis and unsteady analysis of different design of pressure regulator are also investigated by different authors. CFD predict the result close to the experimental test. Binod Kumar Saha [14] numerically analyzed the flow forces on different interfaces of the moving shaft of regulator. ANSYS® FLUENT were used for simulating the transient, compressible and turbulent flow inside the pressure regulator and near the valve opening. He developed the special User Defined Function (UDF) for varying inlet pressure and reducing the valve opening by delta amount for transient analysis of pressure regulator. Flow convergence was checked at each time step using UDF and calculation was allowed to move to next time step only after meeting the required criteria for convergence. HaraldOrtwig, Prof. Dr.-Ing [15] worked on mechatronical pressure controller for CNG- Engines. They carried both experimental analysis and numerical simulation for observing flow behavior inside newly design mechatronical pressure regulator of CNG vehicle. They carried CFD simulation for analysis of shock and vortices formation near the valve opening and derived potential for the improvement in geometry with the help of CFD results. They concluded that flow forces are dependent on pressure differential but they are not dependent on mass flow rate. They observed that steady state flow forces are almost independent of valve opening. They examined that by increasing the pressure ratio, jet contraction revert to lowest valve opening area whereas intensity and vortex formation in the valve opening were reduced. He favored shard-edge transition for sealing efficiency and industrial production requirement.

AditiOza, SudiptoGhosh [16] performed CFD modeling of Globe valve for high pressure oxygen environment. They discussed different types of control valve with their applications. They simplified globe valve with axis symmetric numerical model for finding the flow characteristics with different turbulence models. They concluded that turbulent kinetic energy increases as the plug retracted beyond the plane of seat. The k-ω turbulence model gave higher value of velocity and turbulent kinetic energy than the k-ε model. They concluded that k-ε model converges slower than k-ω model and found that k-ω model does not utilize all wall functions and therefore needs a fine meshing around valve opening. G. Tamizharasi and S Kathiresan [17] carried CFD analysis of 3D butterfly valve for compressible flow with symmetric disc under different degree of valve opening. They concluded that smaller opening angle provide less pressure loss and the total pressure variation and the intensity of turbulence increase at downstream with large valve opening angle. X. Du and S. Gao [18] studied the effect of pressure loss near valve in steam turbine system under different operating conditions for optimizing valve design. They used three turbulence models: one equation Spalart- Allmaras model, the two equations standard k-ε model and realizable k-ε models. They found that standard k-ε model predict the best flow pattern. The results were used for more improvement of valve design for turbine system.

Jeremy Shipman, Ashvin Hosangadi [19] carried steady and unsteady simulation for the analysis of gas pressure regulator for rocket feed system. They used multi-element framework (contained in CRUNCH CFD) for simulating control valve system which provide flexibility in solving the structural and functional complexities associated with the high pressure feed system. They compared the numerical result and experimental data at NASA Stennis space center and found the comparison satisfactory. They also presented flow physics study for instability analysis.

Young JoonAn, Byeong Jin Kim and Byeong Rog Shin [20] studied the control valve used in LNG marine system. They numerically simulated the 3-D flow across valve by using CFD –ACE code for the analysis of anti-cavitation. They investigated complex flow fields across valve including pressure drop, cavitation effect and variation of flow coefficient. Their advance design valve showed a rectified velocity and pressure distribution with no cavitation at the whole valve areas comparing to conventional valve. Chang-Hoon Shin [21] investigated the characteristics of transient flow in a pressure regulator. Their main focus was to analyses the special characteristic of transient flow such as adverse pressure gradient effect and its propagation, surge wave phenomena, and drastic changes of pressure and temperature during the closure of pressure control valve. He carried steady state analysis with 50% valve opening and found the internal flow characteristics such as density distribution, Mach number and temperature distribution. For unsteady analysis they divided the regulator in different sections and found the pressure and mass flow rate at each section as a function of time. He concluded that maximum pressure drop occurred from the rear of pressure regulator connecting pipe with the time delay in the opposite directions. He suggested that installation of large buffer or pressure controller at the rear of the pressure regulator connecting pipe can suppress abnormal increase of transient pressure.

From the study of literature review, it is clear that lots of complex physical phenomena occurring inside pressure regulator such as compressibility, choking, turbulence, fluid structure interaction flow expansion with re-circulation and flow separation. There is dirt of published literature which discusses the design parameter of pressure regulator corresponding to particular outlet pressure. Also there is no research paper available which briefly discuss the dynamic simulation of high differential pressure regulator. Here pressure, temperature and mass flow rate for each flow volumes of pressure regulator are found as function of time and inlet pressure. Valve opening due to force balancing for high pressure differential regulator is also found as a function of time. From literature review we found no research in which simulation of pressure regulator with mathematical model is compared with CFD flow simulation and also by analytical results. For this reason CFD analysis are carried out based on above design parameters for finding the complex flow behavior inside pressure regulator and curve of pressure drop, mass flow rate and temperature drop are found form inlet of pressure regulator to outlet of pressure regulator. No literature study are also found corresponding to analytical solution of flow equation in pressure regulator, for this purpose we also study the ways of finding analytical solution of flow equation based on some assumption. Analytical solution of pressure drop inside pressure regulator is developed as function of time and results are compared with that of numerical computation of flow equations.

CHAPTER 3

DEVELOPMENT OF MATHEMATICAL MODEL

3.1 Development of Mass Flow Equation

For deriving the mass flow rate equation of the air in different ducts of regulator, we make certain assumptions. We are assuming that adiabatic process is occurring in the pressure regulator. The intermolecular forces in the gas are neglected and it obeys the perfect gas law, so the ideal gas equation can be used. This assumption may not be true if there occurs very large temperature changes in the flow or gas temperature is very high. We are also ignoring the gravitational effects on the flow because this is true for gas flow. Also because density of the fluid is not high near the regulator walls, so the effect of viscosity is also negligible. Finally we are assuming that gas is flowing in one direction at a certain time and it is continuous.

General energy equation from compressed air reservoir to regulator ducts with isentropic process and with above assumptions can be written as

$$H_1 + \frac{{v_1}^2}{2} = H_2 + \frac{{v_2}^2}{2} \qquad 3.10$$

Where H is the enthalpy of gas defined as

$$H = C_p T$$

And as velocity of air in reservoir is 0 therefore we can have a relation for temperature

$$\frac{T_{in}}{T_0} = \left(1 + \frac{v^2}{2\, C_p\, T} \right) \qquad 3.12$$

As flow is also considered as an isentropic flow, relationship between temperature and pressure is given by

$$\frac{T_{in}}{T_0} = (\frac{P_{in}}{P_0})^{(\gamma/\gamma-1)} \qquad 3.13$$

Air mass flow rate entering and leaving the regulators duct is given by

$$\dot{m} = \rho A V \qquad 3.14$$

And as $v = Ma$

Where $a = \sqrt{\gamma RT}$ and $R = C_p - C_v$ so the relationship between mass flow rate and Mach number is given by

$$\dot{m} = \rho AM\sqrt{\gamma RT} \qquad 3.15$$

By putting the value of equation $v = Ma$ in equation 3.2 we have

$$\frac{T_{in}}{T_0} = \left(1 + \frac{M^2\gamma R}{2\,C_p}\right) \qquad 3.16$$

By using equation 3.5 we have

$$\frac{T_{in}}{T_0} = \left(1 + \frac{M^{2(}\gamma-1)}{2}\right) \qquad 3.17$$

$$\frac{P_{in}}{P_0} = \left(1 + \frac{M^{2(}\gamma-1)}{2}\right)^{(\frac{\gamma}{\gamma-1})} \qquad 3.18$$

Now by replacing ρ in equation 3.5 as $\rho = \frac{P}{RT}$ we have

$$\dot{m} = P_0 AM\gamma/\sqrt{\gamma RT} \qquad 3.19$$

Rewriting above equation in terms of temperature ratio and Mach number

$$\dot{m}\sqrt{\gamma R}/A = P_0(\frac{T_{in}}{T_0})^{(\frac{\gamma}{\gamma-1})}M\gamma/\sqrt{T_{in}} \qquad 3.20$$

Rearranging above equation we have

$$\dot{m}\sqrt{\gamma R}/A = P_{in}(\frac{T_{in}}{T_0})^{(\frac{\gamma}{\gamma-1})}\sqrt{T_{in}}M\gamma/\sqrt{T_{in}T_0} \qquad 3.21$$

Above equation can be written as

$$\dot{m}\sqrt{\gamma RT_{in}}/AP_{in} = (\frac{T_{in}}{T_0})^{-\left(\frac{\gamma}{\gamma-1}\right)+1/2}M\gamma \qquad 3.22$$

By using equation 3.17 in 3.22 we have

$$\dot{m}\sqrt{\gamma RT_{in}}/AP_{in} = \left(1 + \frac{M^{2(}\gamma-1)}{2}\right)^{-(\frac{\gamma+1}{2(\gamma-1)})} \quad M\gamma \qquad 3.23$$

The above equation can be written in form of pressure ratio by using equation 3.18

$$\frac{\dot{m}\sqrt{\gamma RT_{in}}}{AP_{in}} = M\gamma((\frac{P_0}{P_{in}})^{(-\frac{\gamma}{\gamma-1})})^{-((\gamma+1)/2(\gamma-1))} = M\gamma(\frac{P_0}{P_{in}})^{(\gamma+1)/2(\gamma)} \qquad 3.24$$

Replacing the value of M from equation 3.18 in equation 3.24 we have

$$\frac{\dot{m}\sqrt{\gamma RT_{in}}}{AP_{in}} = \gamma(\frac{P_0}{P_{in}})^{(\gamma+1)/2(\gamma)}[\{(\frac{P_0}{P_{in}})^{(-\gamma)/(\gamma-1)} - 1\}2/(\gamma - 1)]^{1/2} \qquad 3.25$$

So the mass flow rate of air in entrance ducts of regulator, after final simplification is finally given by

$$\dot{m} = A\sqrt{\frac{2\gamma}{(\gamma-1)RT_{in}}}P_{in}\sqrt{[(\frac{P_0}{P_{in}})^{\frac{2}{\gamma}} - (\frac{P_0}{P_{in}})^{\frac{\gamma+1}{\gamma}}]} \qquad 3.26$$

If we define the flow function Ψ then following equation which was first use by Venant and Wantzel [22] in 1839 to describe the free discharge from vessel is given by

$$\dot{m} = A\,\Psi\,P_{in}\sqrt{\frac{2}{RT_{in}}} \qquad 3.27$$

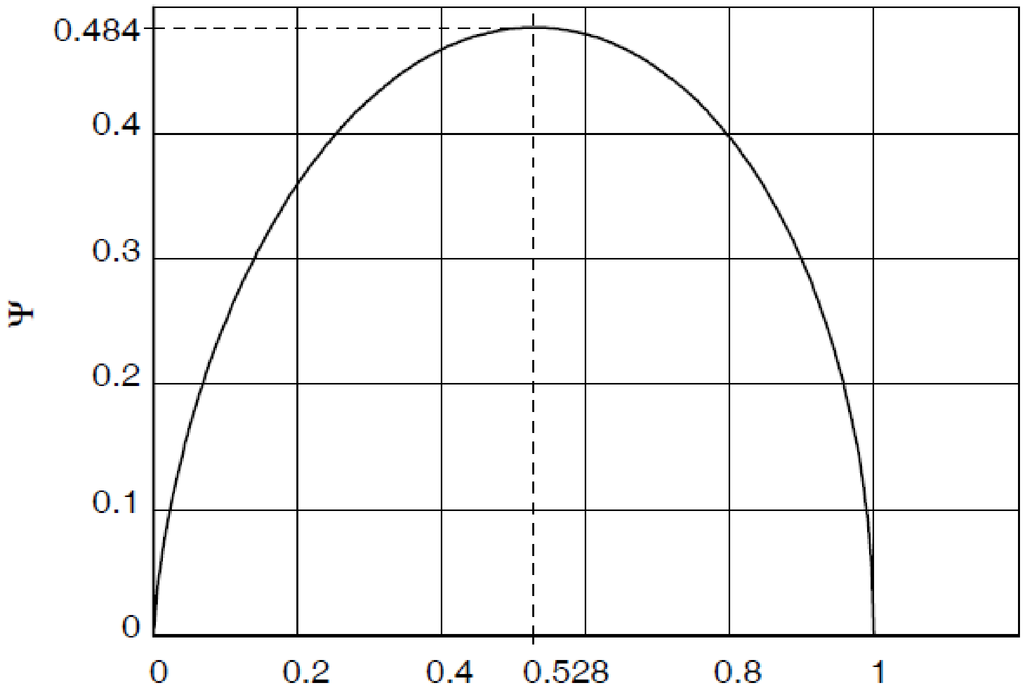

Pressure ratio $\frac{P_0}{P_{in}}$

Figure 3.1 Function ***Ψ*** for air with ***γ***=1.4, maximum value indicated by dashed line

Where the flow function Ψ is defined by

$$\Psi = \sqrt{\frac{\gamma}{\gamma-1}[(\frac{P_0}{P_{in}})^{\frac{2}{\gamma}} - (\frac{P_0}{P_{in}})^{\frac{\gamma+1}{\gamma}}]}$$

The flow function is plotted against constant inlet pressure and varying outlet pressure. The maximum of flow function is

$$\Psi_{max} = 0.484$$

For a pressure ratio $\frac{P_0}{P_{in}} = (\frac{2}{\gamma+1})^{\frac{\gamma}{\gamma-1}}$ or

$P_0 = 0.528P_{in}$ for air.

The pressure ratio 0.528 is called the critical pressure ratio because at this pressure differential the air velocity reaches a sonic velocity in the ducts. Further increase of this pressure differential does not increase the velocity or mass flow rate. If flow ratio is less than or equal to the critical pressure ratio, the flow model is called choked flow

$$\Psi = \sqrt{\frac{\gamma}{\gamma-1}[(\frac{P_0}{P_{in}})^{\frac{2}{\gamma}} - \left(\frac{P_0}{P_{in}}\right)^{\frac{\gamma+1}{\gamma}}\right]} \frac{P_0}{P_{in}} > 0.528 \qquad for\ subsonic\ flow$$

$$\Psi = (\frac{2}{\gamma+1})^{\frac{\gamma}{\gamma-1}}\sqrt{\frac{\gamma}{\gamma+1}}\frac{P_0}{P_{in}} < 0.528 \qquad for\ chocked\ flow$$

For describing the flow through thin, sharp edge orifices where flow contraction and losses occur due to geometry of entrance ducts discharge coefficient is introduced in the mass flow rate equation as

$$\dot{m} = A\ C_d\ \Psi\ \ P_{in}\sqrt{\frac{2}{RT_{in}}}$$

$C_d$depends on numbers of parameters, it contains the effect of reduction of mass flow rate due to friction and heat losses as well as effect of jet contraction.C_d Also depends on pressure ratio for compressible fluid. Perry [23] studied the flow through a thin, sharp edged orifice at Reynolds numbers above 100,000 and found decrease in pressure ratio from 0.84 at pressure ratio of 0.1 to 0.6 at pressure ratio of 1. Pugy et al. (2004) provided the mathematical model for discharge coefficient with respect to pressure ratio

$$C_d = 0.8414 - 0.1002(\frac{P_0}{P_{in}}) + 0.8415(\frac{P_0}{P_{in}})^2 - 3.9(\frac{P_0}{P_{in}})^3 + 4.6001(\frac{P_0}{P_{in}})^4 - 1.6827(\frac{P_0}{P_{in}})^5 \quad 3.28$$

Stenning (1954) [24] shows experimentally that this kind of dependency also exists for slide-valve orifices, i.e. metering orifices in spool valves. For a compressible flow Benedict [25] calculated the value of the discharge coefficient from the knowledge for incompressible flow. Anderson [26] gives a range of coefficients for several types of orifices. The use of cylindrical orifices for measurement purposes is studied by Ward-Smith [27] and Reid and Stewart [28]. Brower et al [29] derived a theoretical expression for mass flow through an orifice. Flesiher [30] shows that the discharge coefficient also heavily depends on the geometry of the orifice

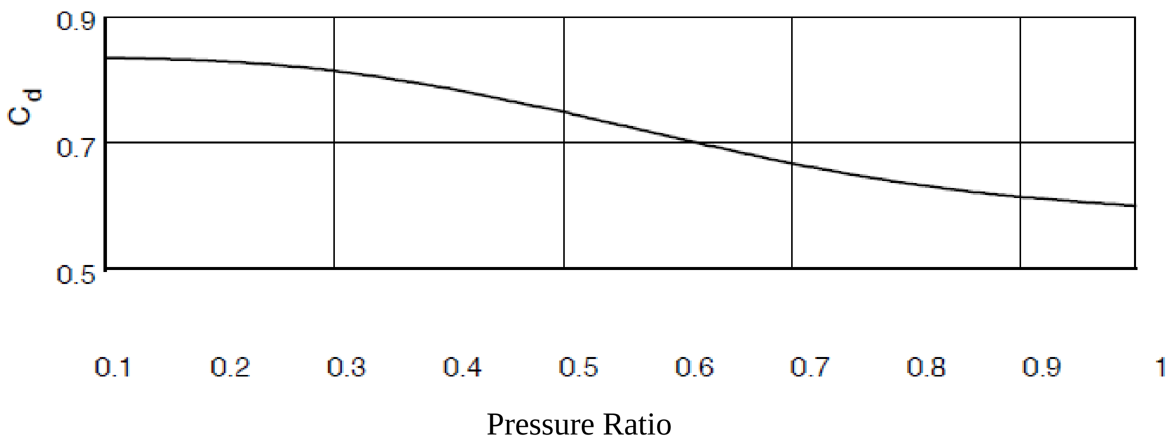

Figure 3.2 Discharge coefficient $\boldsymbol{C_d}$ according to Perrey and equation 3.28

Similarly mass flow rate equation $\dot{m}_1$ from volume V_{in} to V_1, Mass flow rate $\dot{m}_s$ from V_1 to Vout and mass flow rate $\dot{m}_{dam}$ from V_{out} to V_{dam} can also be written

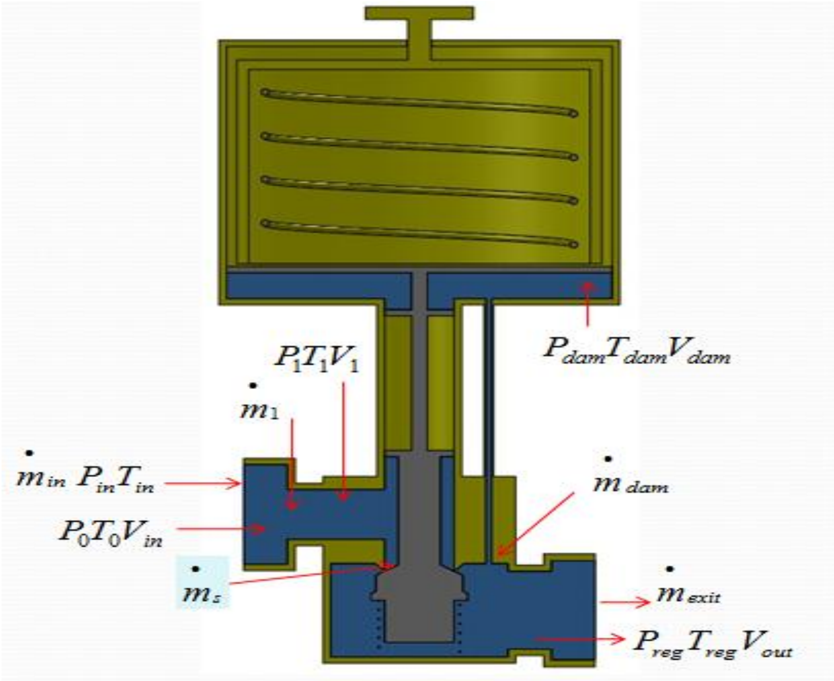

Figure 3.3 Regulator Volumes and corresponding mass flow rate, pressure &temperature

3.2 Development of Dynamic Equation of Pressure in Regulator Ducts

For the derivation of dynamic equation of pressure change in regulator we disintegrate regulator into different volume and then for each volume we find the pressure and temperature change with respect to time and inlet pressure. We are assuming that gas behaves ideally and ideal gas equation can be used in the modeling process. We are also assuming that adiabatic and reversible process is occurring in the regulator volumes so we can use the relation

$$\frac{P}{\rho^{\gamma}} = constant \qquad 3.29$$

Where P is the pressure, ρ is the density of the air in the regulator ducts and γ is the specific heat ratio. By using the definition of density we have from equation 3.29

$$P(\frac{V}{M})^{\gamma} = constant \qquad 3.30$$

Where V is the volume of regulator duct and M is the mass of air in the duct

Differentiating with respect to time the above equation become

$$d\dot{P}(\frac{V}{M})^{\gamma} + \gamma P(\frac{1}{M})^{\gamma}V^{\gamma-1}d\dot{V} - \gamma PV^{\gamma}M^{-\gamma-1}d\dot{M} = 0 \qquad 3.31$$

Or

$$(\frac{V}{M})^{\gamma}\frac{dP}{dt}+\gamma P(\frac{1}{M})^{\gamma}V^{\gamma-1}\frac{dV}{dt}-\gamma PV^{\gamma}M^{-\gamma-1}\frac{dM}{dt}=0 \qquad 3.32$$

Or

$$(\frac{V}{M})^{\gamma}\frac{dP}{dt}=+\gamma PV^{\gamma}M^{-\gamma-1}\frac{dM}{dt}-\gamma P(\frac{1}{M})^{\gamma}V^{\gamma-1}\frac{dV}{dt} \qquad 3.33$$

Cancelling $(\frac{V}{M})^{\gamma}$ from 3.33 we have

$$\frac{dP}{dt}=\gamma PM^{-1}\frac{dM}{dt}-\gamma PV^{-1}\frac{dV}{dt} \qquad 3.34$$

Using ideal gas law $P=\ \rho\ R\ T$ and replacing $\rho=M/V$ we have

$P=\ M\ R\ T/V$ Equation 2.34 becomes

where R is gas constant and T is the temperature of air in the regulator duct

$$\frac{dP}{dt}=\frac{\gamma RT}{V}\frac{dM}{dt}-\frac{\gamma P}{V}\frac{dV}{dt} \qquad 3.35$$

Here $\frac{dM}{dt}=\ \dot{M}_{\mathrm{in}}-\dot{M}_{\mathrm{out}}+\dot{M}_{\mathrm{s}}$ 3.36

$\dot{M}_{\mathrm{in}}$ is the mass flow rate at inlet of regulator duct

$\dot{M}_{\mathrm{out}}$ is mass flow rate at outlet of regulator duct

$\dot{M}_{\mathrm{s}}$ is the mass flow rate through damping orifice. This will be zero except for outlet volume

$\frac{dV}{dt}$ is the rate of volume change of regulator duct with respect to time. If volume is fixed then this quantity will be zero. It depends on the valve opening x of regulator. If shaft moves upward then outlet volume increase and we take $\frac{dV}{dt}$ as positive and if shaft moves downward then outlet volume decrease and we take $\frac{dV}{dt}$ as negative. So $\frac{dV}{dt}$ can be written as

$$\frac{dV}{dt}=A\,\dot{x} \qquad 3.37$$

where *A* is the corresponding area to valve opening so we can write 3.35 as

$$\frac{dP}{dt}=\frac{\gamma RT}{V}(\dot{M}\mathrm{in}\ -\ \dot{M}\mathrm{out}\ +\ \dot{M}s\,)-\frac{\gamma PA}{V}\dot{x} \qquad 3.35$$

If we Temperature in the regulator duct is not constant then 3.35 can also be modified as

$$\frac{dP}{dt} = \frac{\gamma R}{V}(T_{in}\dot{M}\text{in} \; - \; T_{out}\dot{M}\text{out} \; + \; T_s\dot{M}s\,) - \frac{\gamma PA}{V}\dot{x}$$

Now corresponding to Figure 3.3, Equation 3.35 can be written for different duct of regulator

For inlet volume V_{in} dynamic equation of pressure will be

$$\frac{dP_0}{dt} = \frac{\gamma R}{Vin}(T_{in}\dot{M}\text{in} \; - T_0\dot{M}_1) \qquad 3.36$$

Because there is no orifice in inlet volume so $\dot{M}$will be zero and also because inlet volume is not changing so

$$\dot{x} = 0$$

For volume V_1 dynamic equation of pressure will be

$$\frac{dP_1}{dt} = \frac{\gamma R}{V1}\left(T_0\dot{M}1 \; - T_1\dot{M}s\right) - \frac{\gamma P_1 A_1}{V1}\dot{x} \qquad 3.37$$

For volume V_{out} dynamic equation of pressure will be

$$\frac{dP_{reg}}{dt} = \frac{\gamma R}{Vout}\left(T_1\dot{M}s \; - T_{reg}\dot{M}exit + \; T_{reg}\dot{M}dam\,\right) - \frac{\gamma P_{reg}A_s}{Vout}\dot{x} \qquad 3.38$$

For damping volume V_{dam}, dynamic equation of pressure is

$$\frac{dP_{dam}}{dt} = \frac{\gamma R}{Vdam}\left(-T_{dam}\dot{M}dam\,\right) - \frac{\gamma P_{dam}A_{slphon}}{Vdam}\dot{x} \qquad 3.39$$

3.3 Development of Dynamic Equation of Temperature in Regulator Ducts

As in the pressure regulator, pressure drops suddenly due to restriction in flow, temperature also changes in different volumes of regulator. So it is necessary that changing temperature value will be taken when modeling the pressure in regulator duct. From first law of thermodynamics and considering the air density change in regulator ducts we can write the sum of all energies added to ducts of pressure regulator by the energy equation as described by J.F. Carneiro[31], L. Guzzella & C.H. Onder[32] and A.J.Kotwicki[33]

$$\frac{d}{dt}E + \frac{d}{dt}W = \frac{d}{dt}Q + \dot{H}_{in} - \dot{H}_{out} \quad 3.40$$

where E is the total energy of the air in the regulator ducts. As we are assuming that no substantial changes in potential or kinetic energy in the flow occur, hence here E is only represent the total internal energy U.

W is the rate of change in the work.

Q is the heat transfer inside and outside of regulator. We are assuming that no heat transfer occur in our case.

$\dot{H}_{in}$is the inlet enthalpy of air mass in regulator duct and $\dot{H}_{out}$ is the outlet enthalpy of air mass from corresponding regulator duct.

Equation 2.43 with the above mentioned assumption become

$$\frac{d}{dt}U = -\frac{d}{dt}W + \dot{m}_{in}h_{in} - \dot{m}_{out}h_{out} \quad 3.41$$

where h_{in} and h_{out} are the specific enthalpy of air. From caloric relation we have

$$U = mC_vT_{out} \quad 3.42$$

$$h_{in} = C_pT_{in} = (C_v + R)\,T_{in} \quad 3.43$$

$$h_{out} = C_pT_{out} = (C_v + R)\,T_{out} \quad 3.44$$

where C_p and C_v are specific heat ratios at constant pressure and constant volume, respectively. R is the specific gas constant. So using equation 3.42, 3.43 and 3.44 equation3.41 becomes

$$\frac{d}{dt}(mC_vT_{out}) = -\frac{d}{dt}W + \dot{m}_{in}(C_v + R)T_{in} - \dot{m}_{out}(C_v + R)T_{out} \qquad 3.45$$

Differentiating left hand side of 3.45 as

$$\frac{d}{dt}(mC_vT_{out}) = C_v\dot{T}_{out}m + C_vT_{out}\dot{m}_{in} - C_vT_{out}\dot{m}_{out} \qquad 3.46$$

Also work done by the regulator diaphragm is the product of pressure inside the regulator and change in the volume of the regulator ducts. It is given by

$$\frac{d}{dt}W = P_{out}\dot{V}_{out} \qquad 3.47$$

Using equation 3.46 and 3.47 we have

$$\begin{aligned} &C_v\dot{T}_{out}m + C_vT_{out}\dot{m}_{in} - C_vT_{out}\dot{m}_{out} \\ &\qquad = -P_{out}\dot{V}_{out} + \dot{m}_{in}(C_v + R)T_{in} - \dot{m}_{out}(C_v + R)T_{out} \end{aligned} \qquad 3.48$$

Simplifying above equation we have

$$C_v\dot{T}_{out}m + C_vT_{out}\dot{m}_{in} = -P_{out}\dot{V}_{out} + \dot{m}_{in}(C_v + R)T_{in} - \dot{m}_{out}RT_{out} \quad 3.49$$

Simplifying

$$C_v\dot{T}_{out}m = \dot{m}_{in}(C_v + R)T_{in} - C_vT_{out}\dot{m}_{in} - \dot{m}_{out}RT_{out} - P_{out}\dot{V}_{out} \qquad 3.50$$

Replacing the terms with specific heat at constant volume by specific heat ratio

$$\frac{C_v+R}{C_v} = \gamma$$

So equation 2.50 becomes

$$C_v\dot{T}_{out}m = \dot{m}_{in}C_v\gamma T_{in} - C_vT_{out}\dot{m}_{in} - \dot{m}_{out}RT_{out} - P_{out}\dot{V}_{out} \qquad 3.51$$

Taking common $\dot{m}_{in}$ and simplifying

$$C_v\dot{T}_{out}m \ = C_vT_{out}(\gamma\frac{T_{in}}{T_{out}} - 1)\dot{m}_{in} - \dot{m}_{out}RT_{out} - P_{out}\dot{V}_{out} \qquad 3.52$$

Dividing by $C_v m$ We have

$$\dot{T}_{out} = \frac{T_{out}}{m}\left(\gamma\frac{T_{in}}{T_{out}} - 1\right)\dot{m}_{in} - \dot{m}_{out}R\frac{T_{out}}{C_v m} - \frac{P_{out}}{C_v m}\dot{V}_{out} \qquad 3.53$$

Replacing $C_v = \frac{R}{\gamma-1}$, mass $m = \frac{PV}{RT}$ and $\dot{V}_{out} = A\dot{x}$ in equation 3.53

$$\dot{T}_{out} = \frac{RT_{out}{}^2}{V_{out}P_{out}}\left[\left(\gamma\frac{T_{in}}{T_{out}} - 1\right)\dot{m}_{in} - (\gamma - 1)\dot{m}_{out}\right] - \frac{(\gamma-1)T_{out}}{V_{out}}A\dot{x} \qquad 3.54$$

where A is the cross section area of entrance duct and x is the valve opening.

Equation 3.54 is the final form of dynamic equation of temperature in regulator duct. This equation is changed with respect to the different volumes of regulator which are given below

For volume V_{in} dynamic equation of temperature is

$$\dot{T}_0 = \frac{RT_o{}^2}{V_0P_0}\left[\left(\gamma\frac{T_{in}}{T_o} - 1\right)\dot{m}_{in} - (\gamma - 1)\dot{m}_1\right] \qquad 3.55$$

Here $\dot{x}$ is zero because volume V_{in} is constant

For volume $\mathbf{V_1}$ dynamic equation of temperature is

$$\dot{T}_1 = \frac{RT_1{}^2}{V_1P_1}\left[\left(\gamma\frac{T_0}{T_1} - 1\right)\dot{m}_1 - (\gamma - 1)\dot{m}_s\right] - \frac{(\gamma-1)T_1}{V_1}A_1\dot{x} \qquad 3.56$$

where $A_1$is the area of entrance duct from volume V_{in} to V_1

For Volume V_{reg} dynamic equation of temperature is

$$\dot{T}_{reg} = \frac{RT_{reg}{}^2}{V_{out}P_{reg}}\left[\left(\gamma\frac{T_1}{T_{reg}} - 1\right)\dot{m}_s - (\gamma - 1)\dot{m}_{exit}\right] - \frac{(\gamma-1)T_{reg}}{V_{out}}A_s\dot{x} \qquad 3.57$$

Where A_s is the area corresponding to valve opening x

For volume V_{dam} dynamic equation of temperature is

$$\dot{T}_{dam} = \frac{RT_{dam}{}^2}{V_{dam}P_{dam}} \left[\left(\gamma \frac{T_{reg}}{T_{dam}} - 1\right) \dot{m}_{dam}\right] - \frac{(\gamma-1)T_{dam}}{V_{dam}} A_{dam}\dot{x} \qquad 3.58$$

where A_{dam} is the area of damping orifice

3.4 Equation of Moving Shaft

Shaft of the pressure regulator moves upward and downward to maintain a nearly constant pressure at outlet of regulator. This shaft moves under the influence of force balance. This force balance is provided by control spring as loading element, pressure force on diaphragm plate and return spring on valve body. We are assuming that positive forces act upward and positive motion is assumed in the direction that open the valve that is in downward direction. This force balancing is shown in figure 3.4

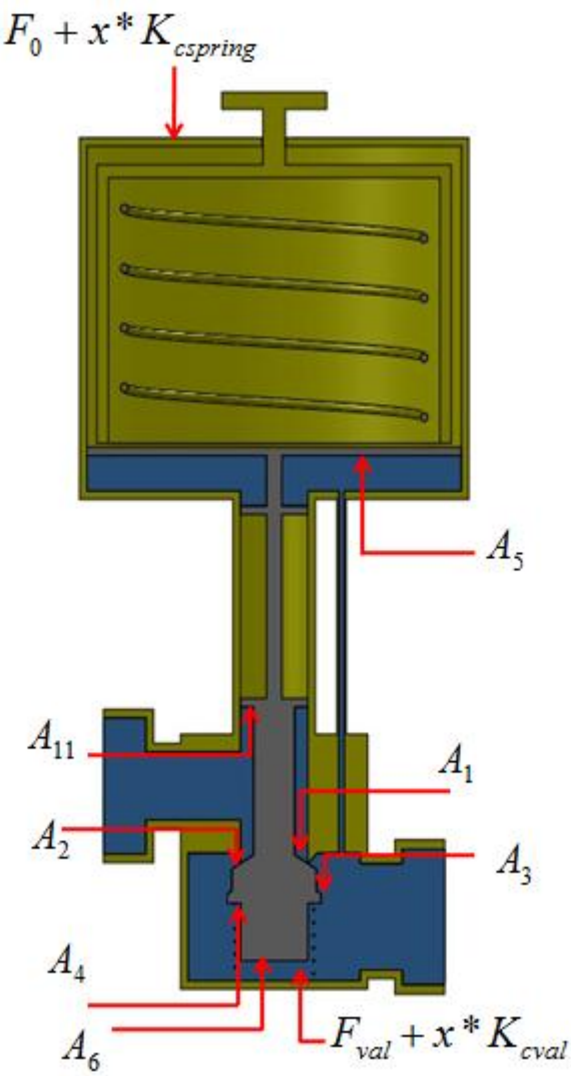

Figure 3.4 Force balancing on moving shaft due to spring force and pressure force

Here all areas are affected by pressure force corresponding to their pressure interaction on their surfaces. Here A5, area of diaphragm is the most influential area in creating the pressure force opposite to spring load force

If x is the valve opening and $\ddot{x}$ is the acceleration of moving shaft, then from Newton 2nd law of motion for one degree of freedom and differential equation of free damped motion of spring we have from fig 2.4 after force balancing

$$m\ddot{x} = F$$

Here force F on upward and downward direction of moving shaft is balanced as

$$F = A_{11}P_{in} - A_1P_{in} - A_2P_{reg} - A_3P_{reg} + A_4P_{reg} + A_5P_{reg} + A_6P_{reg} - F_0 - F_{valve} - F_c sign(\dot{x}) - (K_{cspring} + K_{cvalve})x$$

So by Newton 2nd law of motion, equation of moving shaft finally become

$$m\ddot{x} + F_c sign(\dot{x}) + (K_{cspring} + K_{cvalve})x = A_{11}P_{in} - A_1P_{in} - A_2P_{reg} - A_3P_{reg} + A_4P_{reg} + A_5P_{reg} + A_6P_{reg} - F_0 - F_{valve} \qquad 3.59$$

where

$K_{cspring}$ and k_{cvlave} are the control spring and return spring rates. M is the mass of moving shaft and P_{in} is the inlet pressure. P_{reg} is the regulated pressure or controlled pressure.F_0 is the control spring pre load or initial force set on spring. F_{valve} is the return spring pre compression. F_c is dry friction between shaft seal and regulator. It is also called lubricated or coulomb friction.

Sign($\dot{x}$) is the signum function it provide friction force in upward direction when valve shaft moves downward and provide friction force in downward direction when valve shaft moves upward as shown in figure

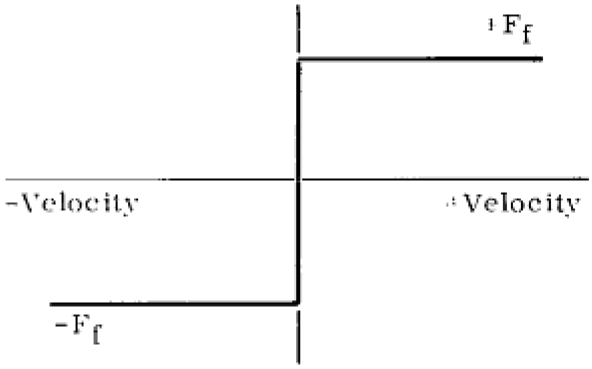

Figure 3.5 Coulomb friction

These parameters of shaft are very important and sensitive as they provide the design parameter for a controlled pressure regulator. Control spring rate and diaphragm area are most sensitive parameter. Friction between moving shaft and regulator chambers are very difficult to estimate they are found experimentally.

CHAPTER 4

NUMERICAL COMPUTATION OF GOVERNING EQUATIONS

4.1 Mathematical Model for Each Flow Volume

Complete mathematical model of pressure regulator is developed in chapter 3. We compute this mathematical model for each flow volumes of pressure regulator. Mass flow rates for different inlet pressure on each regulator entrance flow volume are found with respect to time and valve opening. The overall mathematical model of pressure regulator for each flow volumes are given below

For inlet volume V_{in} equation of mass flow rates, dynamic equation of pressure and temperature are finally given by

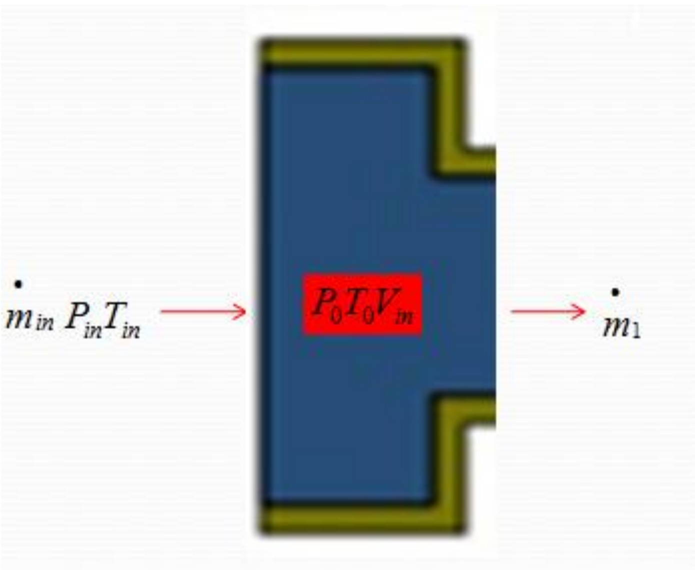

Figure 4.1 Flow volume V_{in} and corresponding pressure and temperature

$$\dot{m}_{in} = A\,\Psi\,P_{in}\sqrt{\frac{2}{RT_{in}}} \qquad 4.01$$

where

$$\Psi = \sqrt{\frac{\gamma}{\gamma-1}\left[\left(\frac{P_0}{P_{in}}\right)^{\frac{2}{\gamma}} - \left(\frac{P_0}{P_{in}}\right)^{\frac{\gamma+1}{\gamma}}\right]} \quad \frac{P_0}{P_{in}} > 0.528 \qquad for\ subsonic\ flow$$

$$\Psi = (\frac{2}{\gamma+1})^{\frac{\gamma}{\gamma-1}} \sqrt{\frac{\gamma}{\gamma+1}\frac{P_0}{P_{in}}} < 0.528 \qquad for\ chocked\ flow$$

Here $\dot{m}_{in}$ is the mass flow rate from compressed air cylinder to regulator entrance duct.

P_{in} and T_{in} are the inlet pressure and temperature from compressed air cylinder to inlet port of regulator. Initial pressure of compressed air cylinder is taken as 150bar and initial temperature of it is taken as 300k.

$$\frac{dP_0}{dt} = \frac{\gamma R}{V_{in}}(T_{in}\dot{m}_{in} - T_0\dot{m}_1) \qquad 4.02$$

$$\frac{dT_0}{dt} = \frac{RT_o{}^2}{V_{in}P_0}\left[\left(\gamma\frac{T_{in}}{T_o} - 1\right)\dot{m}_{in} - (\gamma-1)\dot{m}_1\right] \qquad 4.03$$

And mass flow rate equation from inlet volume V_{in} to out to volume V_1

$$\dot{m}_1 = A\,\Psi\,P_0\sqrt{\frac{2}{RT_0}} \qquad 4.04$$

And here

$$\Psi = \sqrt{\frac{\gamma}{\gamma-1}\left[(\frac{P_1}{P_0})^{\frac{2}{\gamma}} - \left(\frac{P_1}{P_0}\right)^{\frac{\gamma+1}{\gamma}}\right]}\frac{P_1}{P_0} > 0.528 \qquad for\ subsonic\ flow$$

$$\Psi = (\frac{2}{\gamma+1})^{\frac{\gamma}{\gamma-1}} \sqrt{\frac{\gamma}{\gamma+1}\frac{P_1}{P_0}} < 0.528 \qquad for\ chocked\ flow$$

A is the cross section area of volume $V_1$and γ is the specific heat ratio for air

For flow volume V_1 equation of mass flow rates, dynamic equation of pressure and temperature are given by

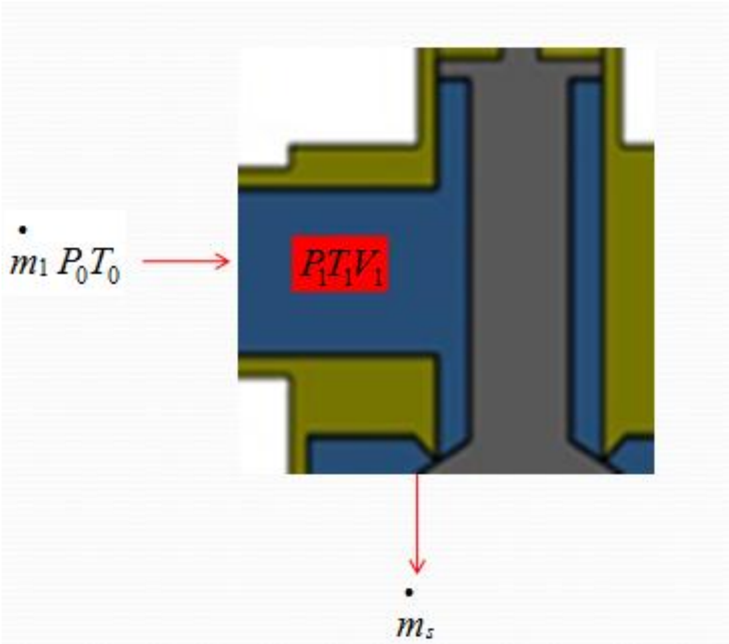

Figure 4.2 Flow volume V_1 and its corresponding pressure and temperature $P_1$and T_1

Here P_0 and T_0 are pressure and temperature of inlet volume V_{in} and $\dot{m}_1$ is the mass flow rate from volume V_{in} to $V_1$and is given in equation 3.04 and $\dot{m}_s$ is the mass flow rate from valve opening to outlet volume of regulator. $\dot{m}_s$is the most critical mass flow rate to calculate and is given by

$$\dot{m}_s = A_s\ \Psi\ P_1\sqrt{\frac{2}{RT_1}} \qquad 4.05$$

Where $\Psi = \sqrt{\frac{\gamma}{\gamma-1}[(\frac{P_{reg}}{P_1})^{\frac{2}{\gamma}} - \left(\frac{P_{reg}}{P_1}\right)^{\frac{\gamma+1}{\gamma}}\Big]}\ \frac{P_{reg}}{P_1} > 0.528 \qquad for\ subsonic\ flow$

$$\Psi = (\frac{2}{\gamma+1})^{\frac{\gamma}{\gamma-1}}\sqrt{\frac{\gamma}{\gamma+1}}\ \frac{P_{reg}}{P_1} < 0.528 \qquad for\ chocked\ flow$$

Where P_{reg} is the regulated pressure in outlet volume and A_s is the cross section corresponding to valve opening

Dynamic Equation of pressure and temperature in volume V_1 are given by

$$\frac{dP_1}{dt} = \frac{\gamma R}{V1}(T_0\dot{m}_1 \; - T_1\dot{m}_s) - \frac{\gamma P_1 A_1}{V1}\dot{x} \tag{4.06}$$

$$\frac{dT_1}{dt} = \frac{RT_1{}^2}{V_1 P_1}\left[\left(\gamma\frac{T_0}{T_1} - 1\right)\dot{m}_1 - (\gamma - 1)\dot{m}_s\right] - \frac{(\gamma-1)T_1}{V_1}A_1\dot{x} \tag{4.07}$$

Sign of $\dot{x}$ will be positive when volume V_1 increases as a result of shaft movement in downward direction and negative when shaft move upward in decreasing the volume V_1

For volume V_{out} equation of mass flow rates, dynamic equation of pressure P_{reg} and temperature T_{reg} are given by

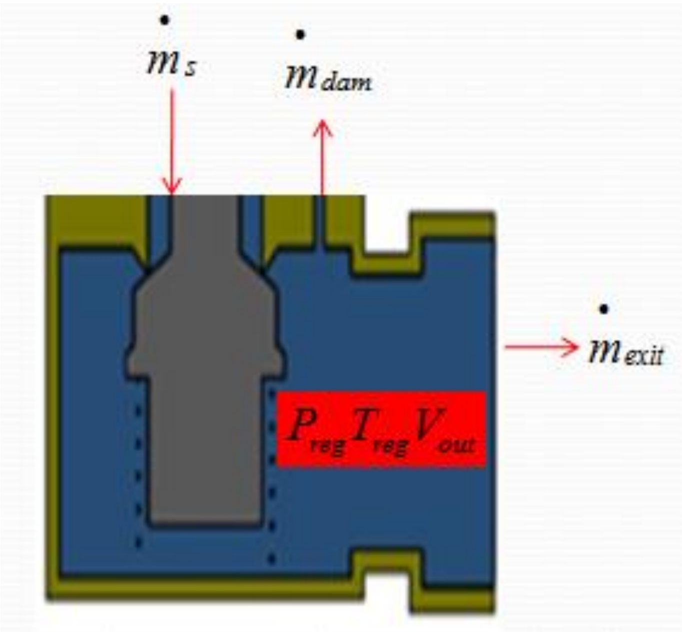

Figure 4.3 Flow volume V_{out} and corresponding pressure and temperature

Here $\dot{m}_{exit}$ is the exit mass flow rate of air to system attached to outlet port of pressure regulator or to free atmosphere and $\dot{m}_{dam}$ is damping mass flow rate from outlet volume to damping chamber and are given by

$$\dot{m}_{exit} = A_{exit}\,\Psi\,P_{reg}\sqrt{\frac{2}{RT_{reg}}} \tag{4.08}$$

Where T_{reg} is the regulated temperature in outlet volume and

$$\Psi = \sqrt{\frac{\gamma}{\gamma-1}[(\frac{P_{atm}}{P_{reg}})^{\frac{2}{\gamma}} - \left(\frac{P_{atm}}{P_{reg}}\right)^{\frac{\gamma+1}{\gamma}}\Big]} \frac{P_{atm}}{P_{reg}} > 0.528 \;\; for\ subsonic\ flow$$

$$\Psi = (\frac{2}{\gamma+1})^{\frac{\gamma}{\gamma-1}} \sqrt{\frac{\gamma}{\gamma+1}} \frac{P_{atm}}{P_{reg}} < 0.528 \qquad for\ chocked\ flow$$

here P_{atm} is the atmospheric pressure

$\dot{m}_{dam}$ is given by Poiseuille's equation (Baline et al [34])

$$\dot{m}_{dam} = \frac{\pi d^4}{128\varphi LRT} P_{dam}\left(P_{dam} - P_{reg}\right) + \frac{\gamma P_{dam}}{V_{dam}} A_{diaphragm} \qquad 4.09$$

Where $P_{dam}$the pressure in damping chamber, L is the length of damping orifice and φ is the dynamic viscosity of air. For air dynamic viscosity is 1.78*10^{-5} kg/ms. $A_{diaphragm}$ is the area of diaphragm.

Dynamic equation of pressure and temperature in volume V_{out} are given by

$$\frac{dP_{reg}}{dt} = \frac{\gamma R}{Vout}\left(T_1 \dot{m}_s - T_{reg}\dot{m}_{exit} + T_{reg}\dot{m}_{dam}\right) - \frac{\gamma P_{reg} A_s}{Vout}\dot{x} \qquad 4.10$$

$$\frac{dT_{reg}}{dt} = \frac{RT_{reg}{}^2}{V_{out}P_{reg}} \left[\left(\gamma \frac{T_1}{T_{reg}} - 1\right)\dot{m}_s - (\gamma - 1)\dot{m}_{exit}\right] - \frac{(\gamma-1)T_{reg}}{V_{out}} A_s \dot{x} \qquad 4.11$$

For damping volume V_{dam} we have dynamic equation of pressure and temperature as

$$\frac{dP_{dam}}{dt} = \frac{\gamma R}{V_{dam}}(-T_{dam}\dot{m}_{dam}) - \frac{\gamma P_{dam} A_{slphon}}{V_{dam}}\dot{x} \qquad 4.12$$

$$\frac{dT_{dam}}{dt} = \frac{RT_{dam}{}^2}{V_{dam}P_{dam}} \left[\left(\gamma \frac{T_{reg}}{T_{dam}} - 1\right)\dot{m}_{dam}\right] - \frac{(\gamma-1)T_{dam}}{V_{dam}} A_{dam}\dot{x} \qquad 4.13$$

From the analysis of the above mathematical model we concluded that a simulation of system of non-linear coupled equations is required therefore a numerical simulation of mathematical model is necessary for the analysis of pressure regulator. For each flow volume of pressure regulator we need initial values of pressure and temperature. We are also taking a compressed air cylinder of 150bar pressure which is attached to the inlet port of regulator.

Initial pressure for each volume of pressure regulator are taken as the atmospheric pressure which are given below

V_{in}	Pressure P_0=1.01bar
	Temperature T_0=300k
V_1	Pressure P_1=1.01bar
	Temperature T_1=300k
V_{out}	Pressure P_{reg}=1.01bar
	Temperature T_{reg}=300k
V_{dam}	Pressure P_{dam}=1.01bar
	Temperature T_{dam}=300k

Initial temperature for each volume of pressure regulator is taken as 300k and in some cases it can be taken 280k or 290k. We have to measure the pressure and temperature for whole simulation time as a function of time. From the initial information of pressure and temperature in each flow volume we compute the initial mass flow rates entrance for each flow volume of pressure regulator. Initial valve opening is set as 2.5mm by providing a load force in the control spring. For finding the pressure and temperature for the next time step we use finite difference scheme. By using finite differencing scheme we discretize the dynamic equation of pressure and temperature for each flow volume

4.2 Discretization of Dynamic Equation of Pressure and Temperature

By using the forward time differencing scheme for pressure and temperature as

$$\frac{dP_0}{dt} = \frac{P_0(\,t + \Delta t) - P_0(\,t)}{\Delta t}$$

And

$$\frac{dT_0}{dt} = \frac{T_0(\,t + \Delta t) - T_0(\,t)}{\Delta t}$$

Introducing finite differencing in dynamic equation of pressure and temperature in each flow volume we have

For flow volume V_0

$$\frac{P_0(\,t + \Delta t) - P_0(\,t)}{\Delta t} = \frac{\gamma R}{V_{in}}(T_{in}(\,t) * \dot{m}_{in}(\mathrm{t}) - T_0(\,t) * \dot{m}_1(t)\,) \qquad 4.14$$

Simplifying 4.14 we have

$$P_0(\,t + \Delta t) = \left[\frac{\gamma R}{V_{in}}(T_{in}(\,t) * \dot{m}_{in}(\mathrm{t}) - T_0(\,t) * \dot{m}_1(\,t)\,)\right] * \Delta t + P_0(\,t) \qquad 4.15$$

Finite difference equation of temperature in volume V_{in}

$$\frac{T_0(\,t + \Delta t) - T_0(\,t)}{\Delta t} = \frac{R{T_o}^2(\,t)}{V_{in}P_0(t)}\left[\left(\gamma\frac{T_{in}(t)}{T_o(t)} - 1\right)\dot{m}_{in}(\mathrm{t}) - (\gamma - 1)\dot{m}_1(t)\right] \qquad 4.16$$

Simplifying 4.16, we have

$$T_0(\,t + \Delta t) = \left[\frac{R{T_o}^2(\,t)}{V_{in}P_0(t)}\left[\left(\gamma\frac{T_{in}(t)}{T_o(t)} - 1\right)\dot{m}_{in}(\mathrm{t}) - (\gamma - 1)\dot{m}_1(t)\right]\right] * \Delta t + T_0(\,t) \qquad 4.17$$

Finite difference equation of pressure in volume V_1

$$\frac{P_1(t+\Delta t)-P_1(t)}{\Delta t}=\frac{\gamma R}{V1}(T_0(t)*\dot{m}_1(t)-T_1(t)*\dot{m}_s(t))-\frac{\gamma P_1 A_1}{V1}\dot{x}(t) \qquad 4.18$$

Simplifying 4.18, we have

$$P_1(t+\Delta t)=\left[\frac{\gamma R}{V1}\left(T_0(t)*\dot{m}_1(t)-T_1(t)*\dot{m}_s(t)\right)-\frac{\gamma P_1(t)A_1}{V1}\dot{x}(t)\right]*\Delta t+P_1(t) \qquad 4.19$$

Finite difference equation of temperature in volume V_1

$$\frac{T_1(t+\Delta t)-T_1(t)}{\Delta t}=\frac{RT_1{}^2(t)}{V_1P_1(t)}\left[\left(\gamma\frac{T_0(t)}{T_1(t)}-1\right)\dot{m}_1(t)-(\gamma-1)\dot{m}_s(t)\right]-\frac{(\gamma-1)T_{1(t)}}{V_1}A_1\dot{x}(t)$$

4.20

Simplifying equation 4.20, we have

$$T_1(t+\Delta t)=\left[\frac{RT_1{}^2(t)}{V_1P_1(t)}\left[\left(\gamma\frac{T_0(t)}{T_1(t)}-1\right)\dot{m}_1(t)-(\gamma-1)\dot{m}_s(t)\right]-\frac{(\gamma-1)T_{1(t)}}{V_1}A_1\dot{x}(t)\right]*\Delta t+T_1(t) \qquad 4.21$$

Finite difference equation of pressure in volume V_{out}

$$\frac{P_{reg}(t+\Delta t)-P_{reg}(t)}{\Delta t} = \frac{\gamma R}{V_{out}}\Big(T_1(t)\dot{m}_s(t) - T_{reg}(t)\dot{m}_{exit}(t) + T_{reg}(t)\dot{m}_{dam}(t)\Big) - \frac{\gamma P_{reg}(t)A_s}{V_{out}}\dot{x}(t) \qquad 4.22$$

Simplifying equation 4.22, we have

$$P_{reg}(t+\Delta t) = \left[\frac{\gamma R}{V_{out}}\Big(T_1(t)\dot{m}_s(t) - T_{reg}(t)\dot{m}_{exit}(t) + T_{reg}(t)\dot{m}_{dam}(t)\Big) - \frac{\gamma P_{reg}(t)A_s}{V_{out}}\dot{x}(t)\right] * \Delta t + P_{reg}(t) \qquad 4.23$$

Finite difference equation of temperature in volume V_{out}

$$\frac{T_{reg}(t+\Delta t)-T_{reg}(t)}{\Delta t} = \frac{R{T_{reg}}^2(t)}{V_{out}P_{reg}(t)}\left[\left(\gamma\frac{T_1(t)}{T_{reg}(t)}-1\right)\dot{m}_s(t) - (\gamma-1)\dot{m}_{exit}(t)\right] - \frac{(\gamma-1)T_{reg}(t)}{V_{out}}A_s\dot{x}(t) \qquad 4.24$$

Simplifying equation 4.24, we have

$$T_{reg}(t+\Delta t) = \left[\frac{R{T_{reg}}^2(t)}{V_{out}P_{reg}(t)}\left[\left(\gamma\frac{T_1(t)}{T_{reg}(t)}-1\right)\dot{m}_s(t) - (\gamma-1)\dot{m}_{exit}(t)\right] - \frac{(\gamma-1)T_{reg}(t)}{V_{out}}A_s\dot{x}(t)\right] * \Delta t + T_{reg}(t) \qquad 4.25$$

Finite difference equation of pressure in volume V_{dam}

$$\frac{P_{dam}(t+\Delta t)-P_{dam}(t)}{\Delta t}=\frac{\gamma R}{V_{dam}}\left(-T_{dam}(t)\dot{m}_{dam}(t)\right)-\frac{\gamma P_{dam}(t)A_{slphon}}{V_{dam}}\dot{x}(t) \qquad 4.26$$

Simplifying equation 4.26, we have

$$P_{dam}(t+\Delta t)=\left[\frac{\gamma R}{V_{dam}}\left(-T_{dam}(t)\dot{m}_{dam}(t)\right)-\frac{\gamma P_{dam}(t)A_{slphon}}{V_{dam}}\dot{x}(t)\right] \qquad 4.27$$

Finite difference equation of temperature in volume V_{dam}

$$\frac{T_{dam}(t+\Delta t)-T_{dam}(t)}{\Delta t}=\frac{RT_{dam}{}^{2}(t)}{V_{dam}P_{dam}(t)}\left[\left(\gamma\frac{T_{reg}(t)}{T_{dam}(t)}-1\right)\dot{m}_{dam}(t)\right]-\frac{(\gamma-1)T_{dam}(t)}{V_{dam}} \qquad 4.28$$

Simplifying equation 3.28, we have

$$T_{dam}(t+\Delta t)=\left[\frac{RT_{dam}{}^{2}(t)}{V_{dam}P_{dam}(t)}\left[\left(\gamma\frac{T_{reg}(t)}{T_{dam}(t)}-1\right)\dot{m}_{dam}(t)\right]-\frac{(\gamma-1)T_{dam}(t)}{V_{dam}}A_{dam}\dot{x}(t)\right]*\Delta t+T_{dam}(t) \qquad 4.29$$

4.3 Computational Form of Moving Shaft Equation

Equation of moving shaft of pressure regulator is developed in chapter 3 and is reproduced here from equation 3.59

$$m\ddot{x} + F_c sign(\dot{x}) + \left(K_{cspring} + K_{cvalve}\right)x = A_{11}P_{in} - A_1 P_{in} - A_2 P_{reg} - A_3 P_{reg} + A_4 P_{reg} + A_5 P_{reg} + A_6 P_{reg} - F_0 - F_{valve} \quad 4.30$$

With initial conditions

$$\dot{x}(0) = \ 2.5mm$$

$$\ddot{x}(0) = \ 0$$

where x is the valve opening and other parameters are given in chapter 3

Equation 4.30 is second order differential equation and values of pressure in all volume of pressure regulator are required with the two spring constants.

Equation 4.30 is solved numerically in Matlab® by Runge Kutta (ode45) method as it is an initial value problem. The equation is deformed into two equations by substitution

$$x(1) = x$$

$$x(2) = \dot{x}$$

And

$$dx(1) = \ x(2)$$

4.31

$$dx(2) = \left[A_{11} * P_{in}(t) - A_{1*}P_{in}(t) - A_2 P_{reg}(t) - A_3 P_{reg}(t) + A_4 P_{reg}(t) + A_5 P_{reg}(t) + A_6 P_{reg}(t) - F_0 - F_{valve} - F_c sign(x(2)) - \left(K_{cspring} + K_{cvalve}\right)x(1)\right]/m$$

4.32

4.4 Friction Modeling

The value of friction force used in equation 4.32 is very difficult to compute. However there exists some model of friction that can be helpful for the determination of friction force between shaft body and regulator internal body [35,36]. Although the place where this friction occur is full of lubrication to reduce the friction but due to very fast movement of shaft for opening the required area of valve, this friction is still a very important factor and it should be handled very carefully.

Friction phenomena can be divided into two components. The first is the static friction which keeps the bodies at rest. Static friction has to overcome to start the relative motion between two bodies [37]. The second which manifests itself during motion is called the dynamic friction. It is further divided into two components i.e., Coulomb and Viscous friction.

Coulomb friction is the minimum value of friction that happen when the body moves, it depend on the bodies in contact. The discontinuities in the system due to static friction are very difficult to model and simulate on the computer. Static friction models consider friction to be a static function of the system's velocity. In fig 4.4 coulomb friction force is shown against the velocity. Karnop [38] friction model is the most popular static friction models which was developed in 1985 to handle the discontinuity due to static friction and to provide a friction models that can be simulated on the computer and is given by

$$F = f_c sgn(\dot{x}) \qquad \text{when } \dot{x} \neq 0$$

$$F = f_p \qquad \text{when } \dot{x} = 0 \; \& f_p < f_s$$

$$F = f_s sgn(f_p) \qquad \text{when } \dot{x} = 0 \& f_p > f_s$$

Where f , f_c , f_p and f_s are friction force, coulomb friction force, applied force and static friction force respectively.

Viscous friction is a linear function of velocity and is attributed to lubricants. When a body starts from zero velocity, i.e. breaks away from static friction, the transition between static friction and dynamic friction is called Stribeck effect [37]. Stribeck effect is generally described as a composite of two different processes: the static process when an object is stationary (no sliding is involved) and likely to move under certain applied force, and the dynamic process when sliding is involved.

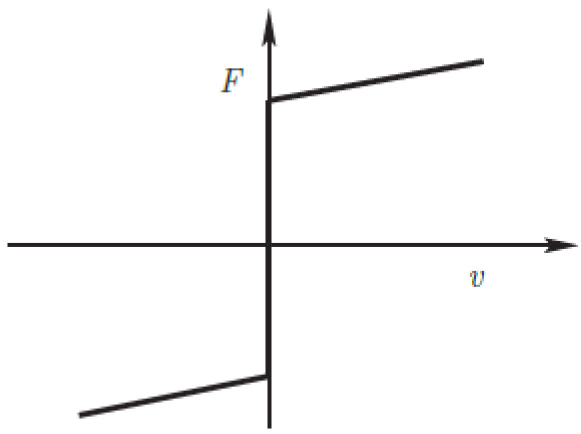

Figure 4.4 Coulomb frictions against velocity

The deficiency in static model that they are problematic in simulation of dynamic system for this reason dynamic model such as Dahl model [39,40], the Bouc-Wen model [41] and the LuGre model [42] etc. More detailed analysis on LuGre model can be found in [43] and [44].

CHAPTER 5

SIMULATION RESULTS AND DISCUSSION

5.1 Problem Formulation

On the inlet part of regulator a compressed air cylinder with pressure 150bar is attached. Our system, which is attached to the outlet part of regulator require a constant supply of 15bar pressure for 19 seconds until a pressure in compressed air cylinder reaches to 60bar. We have to find all design parameter of regulator for the above requirement. Mass flow rate and valve opening are also required as a function of time.

Based on the mathematical model a code in MATLAB® is developed for the simulation of the overall system. For simulation purpose, pressure of compressed air cylinder is decreased linearly. The decrement rate of -4.73684bar/sec is taken. For this linear decrement following equation is used in our simulation

$$P_{in} = P + \frac{dP}{dt} * t \qquad 5.01$$

P_{in} is the supply of pressure from compressed air cylinder reservoir to regulator at any time t

P is initial pressure in compressed air cylinder which is 150bar

$\frac{dP}{dt}$ is the decrement rate of pressure in cylinder which is -4.73684bar/sec

Time step for flow simulation is taken as 0.001sec.

Problem formulation is illustrated with the following figure

Figure 5.1 Overview of problem description

5.2 Design Parameters used for Flow Simulation

For the requirement of constant supply of 15bar pressure, following design parameters values are used in flow simulation. These design parameters can be adjusted according to other requirement

Design parameter	Symbol	Value
Mass of moving shaft	M1	0.124 kg
Mass of control spring	M2	0.24 kg
Mass of Return spring	M3	0.015 kg
Control spring pre load	F0	60.7 N
Control spring constant rate	K1	16200 N/m
Inlet and outlet area of regulator	A	4.06e-3m^2
Gas constant of air	R	286.7J/kg-K
Specific heat ratio	γ	1.396
Return Spring load	Fval	9.6 N
Return spring constant rate	K2	5400 N/m
Outlet volume	Vout	1.356e-4 m^3
Coulomb friction force	Fc	10N
Viscosity of dry air	ζ	1.78e-5 kg/ms
Discharge Coefficient	Cd	0.9 &1

Simulation results have been derived for two cases in first case we increase the inlet pressure of reserviour from 60 bar to 150 bar at the rate of 4.7384 bar/sec and note the outlet pressure of regulator. Simulation results such as pressure, temperature, mass flow rate and valve opening for each flow volume of pressure regulator are computed. In second case of simulation, pressure in the reservior or compressed air cylinder is reduced from 150bar to 60bar at the rate of 4.7384 bar/sec and overall regulator performance are checked corresponding to outlet pressure. For second case we also simulated the result for a pre determine temperture distribution for each flow volume of pressure regulator. For each flow volume pressure, mass flow rate and valve opening are also computed.Simulation results of both the cases are shown below.

5.3 Case1: Inlet Pressure is increasing from 60bar to 150bar

5.3.1 Simulation of valve Opening as a Function of Time

Load or contol spring compression on pressure regulator are initally set in such a way that a initial valve clearance of regulator is 2.5mm. When the inlet valve of regulator is open then high pressure fluids begin to flow from reservior to different volume of regulator. Pressure in each volume of regulator begins to increase. The pressure in outlet volume is continiously checked in damping chamber through damping orifce. As the pressure in the outlet volume of regulator reaches above 15bar, pressure creates a force on the diapharm plate against the load force of spring which was set for a 15bar pressure at the outlet. As a result the main shaft of regulator moves upward and suddenly valve clearance reaches it minimum opening position. After that the moving shaft of regulator oscillates up and down and providing that area of flow for which a pressure of near 15bar maintain in outlet volume of regulator. This situation is shown in following Figure 5.2

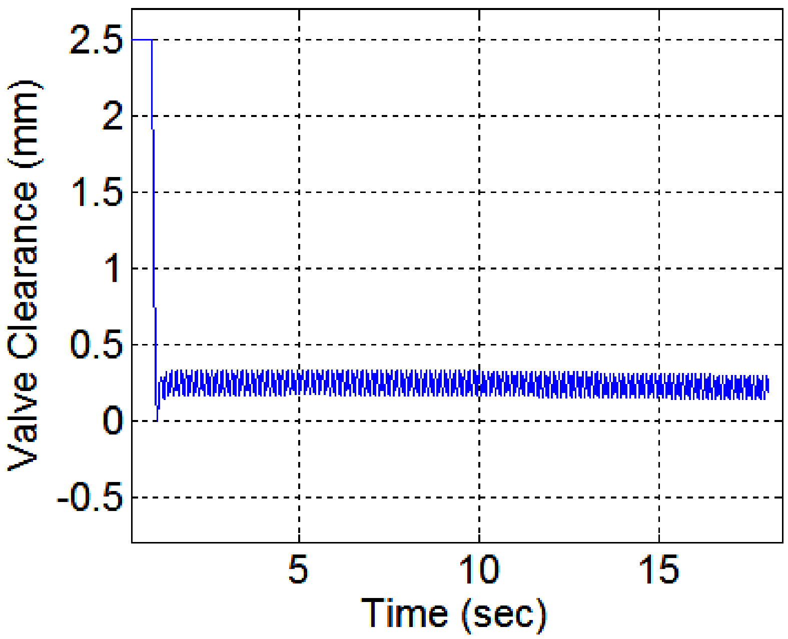

Figure 5.2 Valve clearance (opening) as a function of time

Here near about 0.8 second outlet reaches to 15bar and valve opening reduces to its minimum level after that a steady state osicllation happen near about 0.25mm opening as shown in Figure5.3. The magnitude of oscillation is round about 0.1mm which can be negligible.

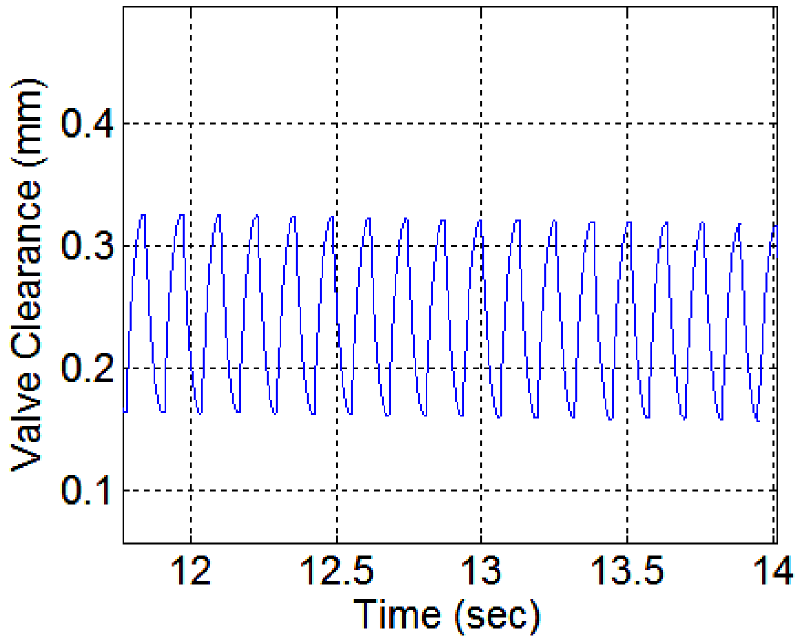

Figure 5.3 Valve osciallation near about 0.25mm

5.3.2 Simulation of Outlet Pressure with Inlet Pressure

Initial pressure at outlet was 1bar, near about 0.8 seconds outlet pressure reaches to 15bar (fig 5.4) and then a minor oscillationin oultlet pressure is seen for whole simulation time (fig 5.5).

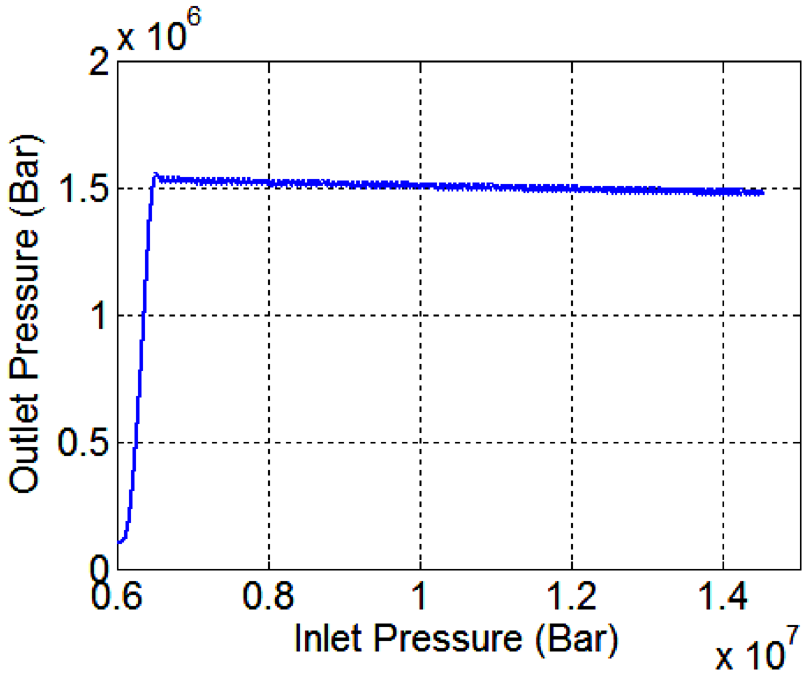

Figure 5.4 Outlet pressure of regulator as a function of time

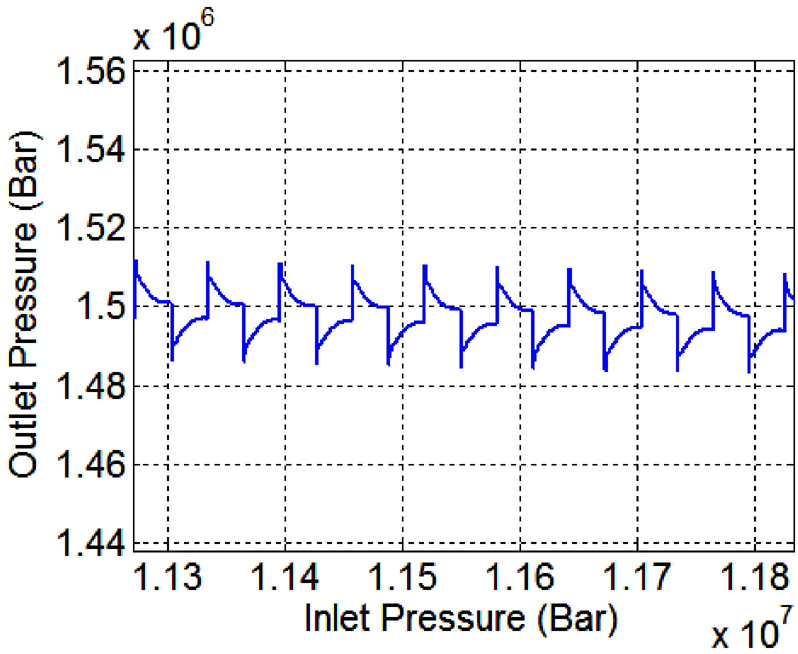

Figure 5.5 Outlet pressure oscillation near 15bar pressure

5.3.3 Mass Flow Rate $\dot{m}_{in}$ from Cylinder to Regulator Inlet

Initial pressure in inlet volume of regulator was 1 bar and initial pressure of compressed air cylinder was 60bar. Due to high pressure difference and large regulator inlet area a high mass flow rate is seen nearly about 0.8 second (fig 5.6). After that this pressure difference reduces and low mass flow rate (nearly about 0.5kg/s) is seen for whole simulation time (fig 5.7).

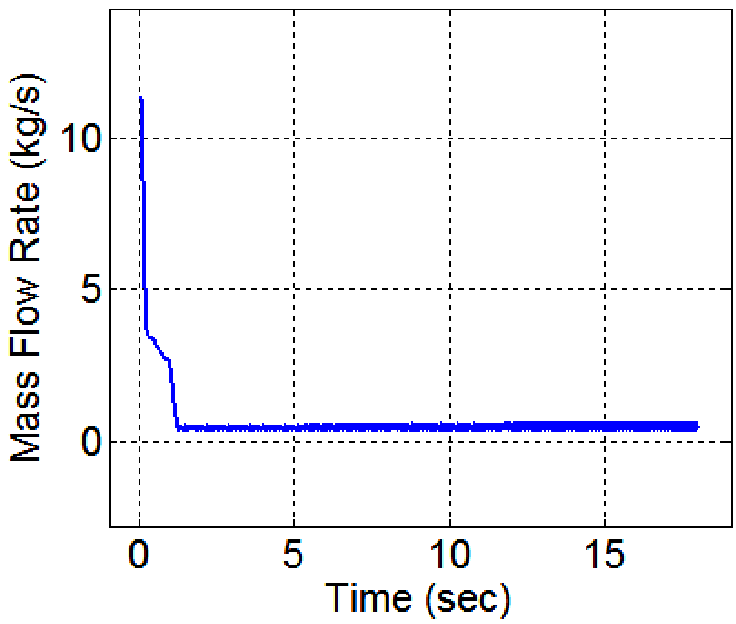

Figure 5.6 Inlet mass flow rate for a supply inlet pressure from 60bar to 150bar

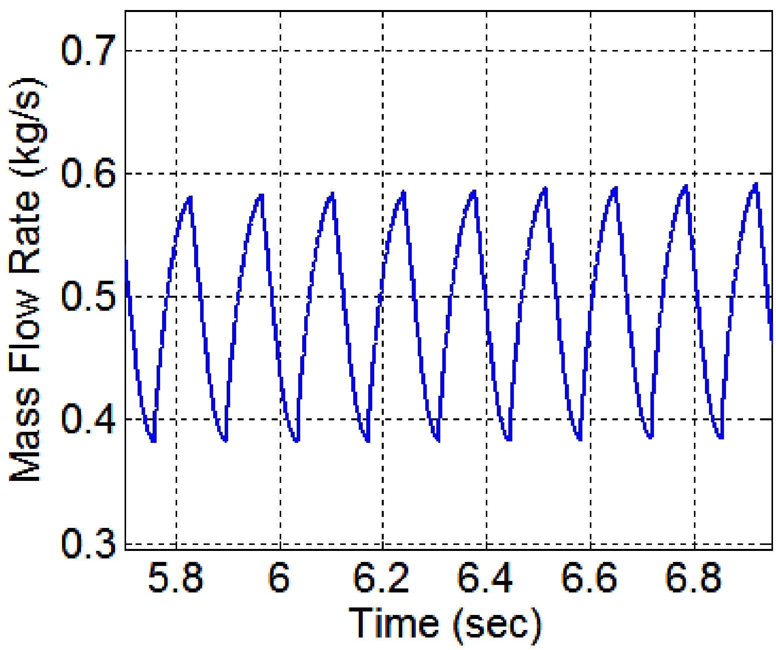

Figure 5.7 Inlet mass flow rate oscillation near about 0.5kg/sec

5.3.4 Simulation of Pressure and Temperature for Volume V_{in}

Initial temperature of inlet volume was 290k due to sudden increase of pressure, temperature of inlet volume also increases (fig 5.8) and as the pressure differential of compressed air cylinder and inlet volume decreases (fig 5.9) the temperature begins to drop and reaches near about 320k.

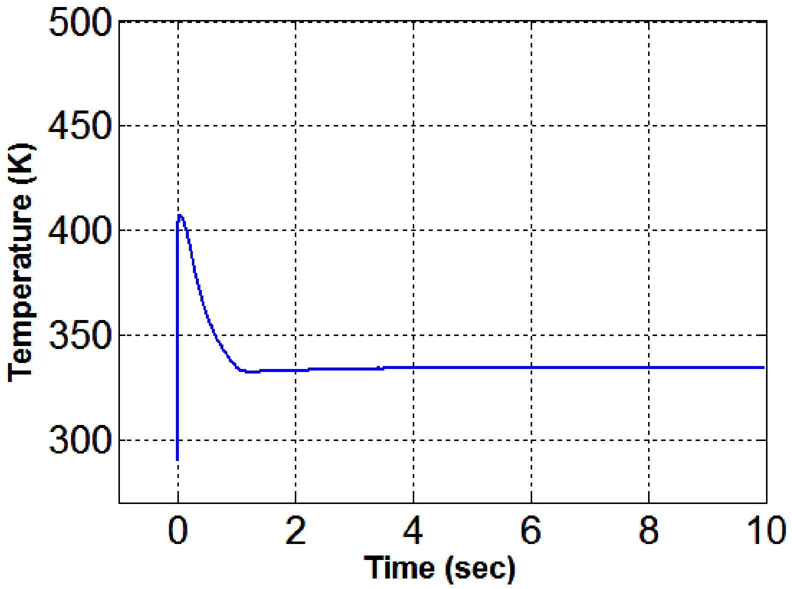

Figure 5.8 Temperature simulation for inlet volume of regulator

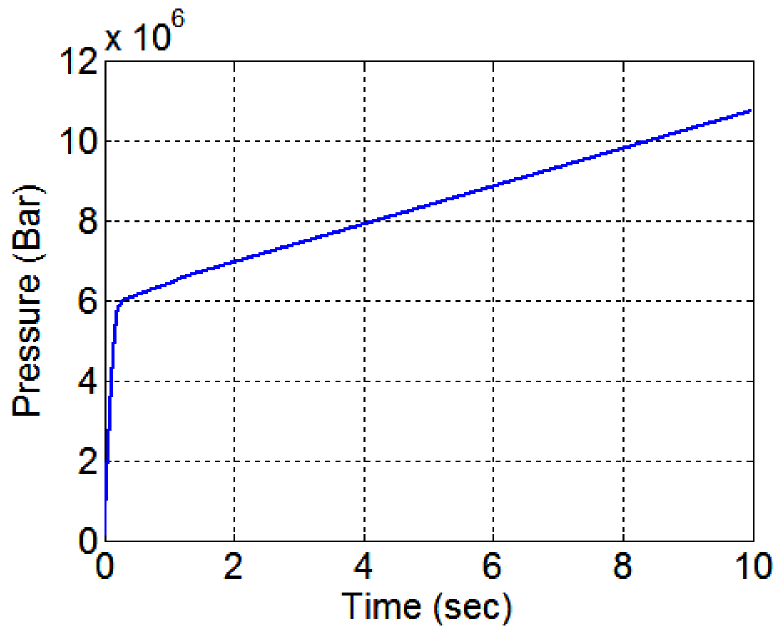

Figure 5.9 Sudden increase of pressure in inlet volume due to large inlet area of regulator

5.3.5 Mass Flow Rate ($\dot{m}_1$) from Inlet Volume V_{in} to Volume V_1

As the inlet pressure increase, the pressure in the Volume V1 also increases so a high mass flow rate is seen initially and then due to reduction of pressure differential in inlet volume and volume V1 mass flow rate decreases suddenly (fig 5.10) and then this mass flow rate oscillate (fig 5.11) near about 0.32 kg/s .

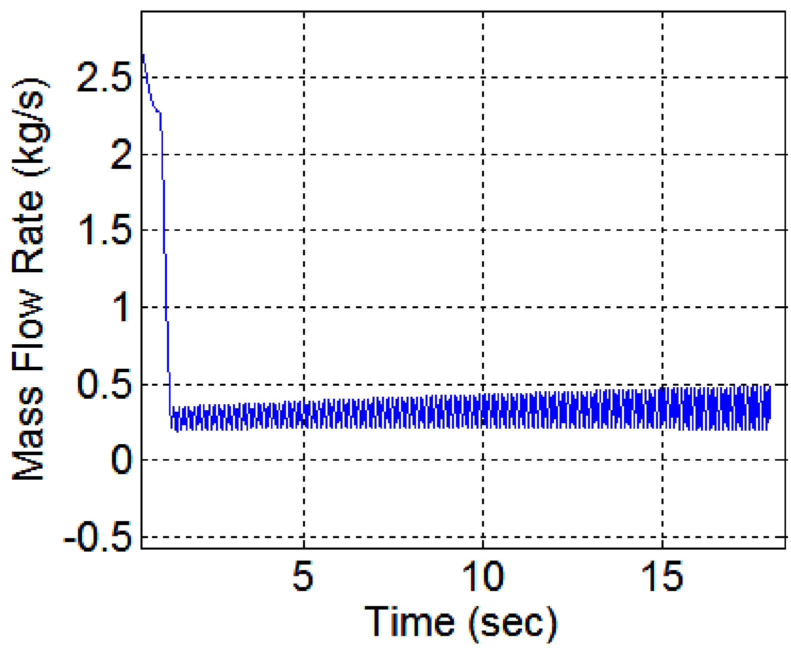

Figure 5.10 Mass flow rate as a function of time

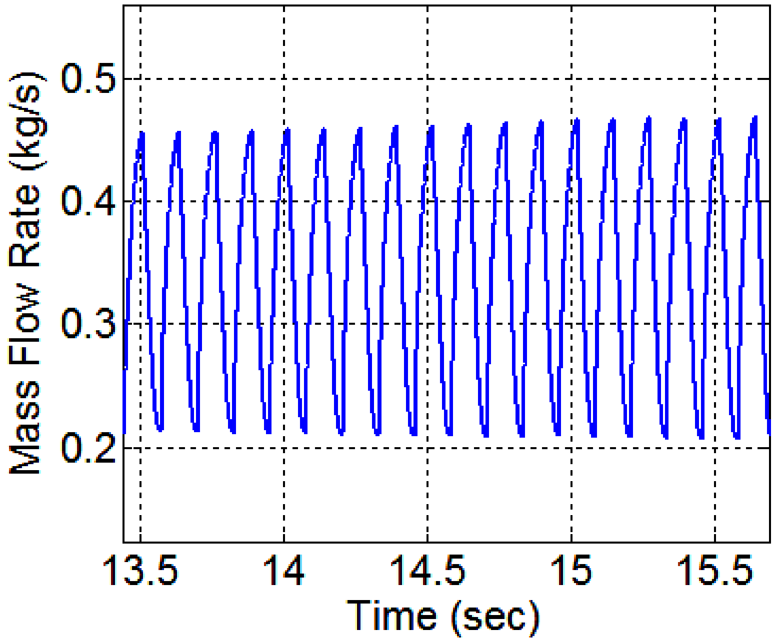

Figure 5.11 Mass flow rate oscillation near 0.36kg/s

5.3.6 Simulation of Pressure and Temperature for Volume V_1

Initial temperature of volume V1 was 290k, due to sudden increase of pressure in volume V1(fig 5.13) due to high pressure flow form inlet volume, temperature rises in volume V1 initially, then by the passage of time the pressure differential reduces between these two volumes and temperature begins to slow down as shown in fig 5.12

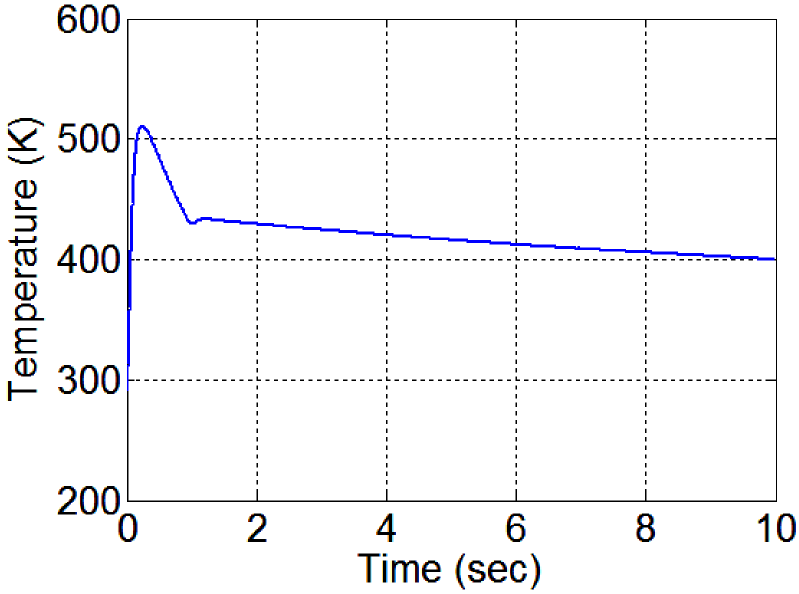

Figure 5.12 Temperature as a function of time in volume V1

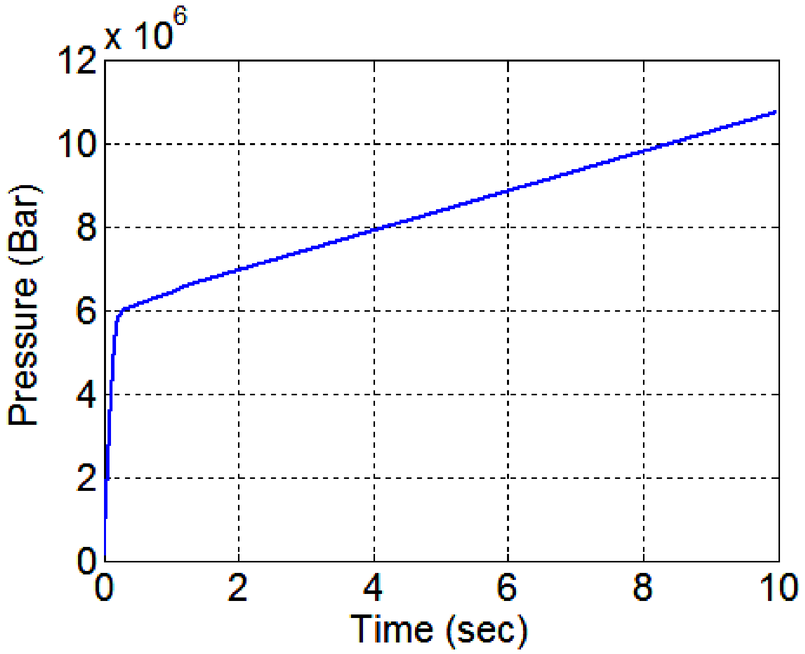

Figure 5.13 Pressure increment in volume V1 as a function of time

5.3.7 Mass Flow Rate ($\dot{m}_s$) from Volume V_1 to VolumeV_{out}

Initial valve clearance was 2.5mm due to which high mass flow rate is seen initially form volume V1 to volume Vout. As the pressure in volume Vout reaches 15bar, the valve opening reduces and a sudden decrement in mass flow rate can be seen in fig 5.14. After that mass flow rate value oscillate near about 0.24kg/sec for maintaining nearly 15bar at outlet as shown in fig 5.15

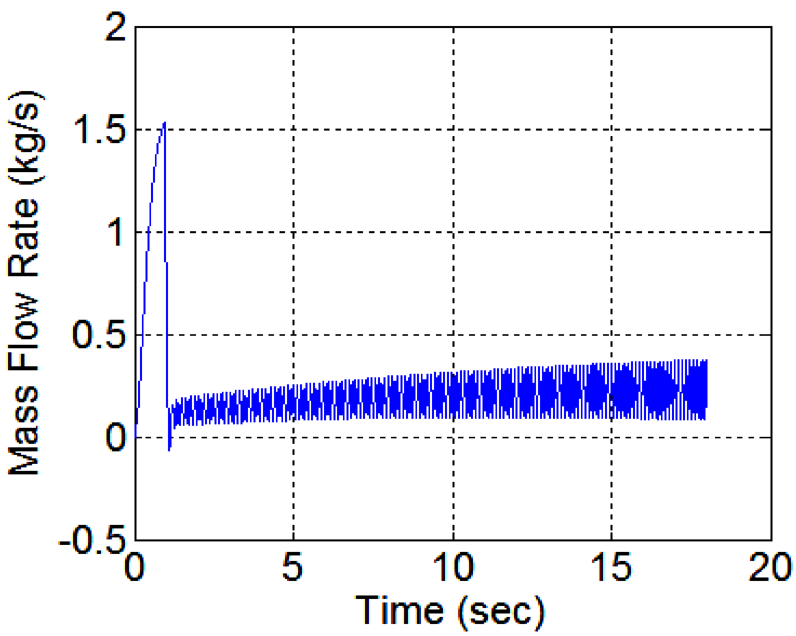

Figure 5.14 Mass flow rate near valve opening as a function of time

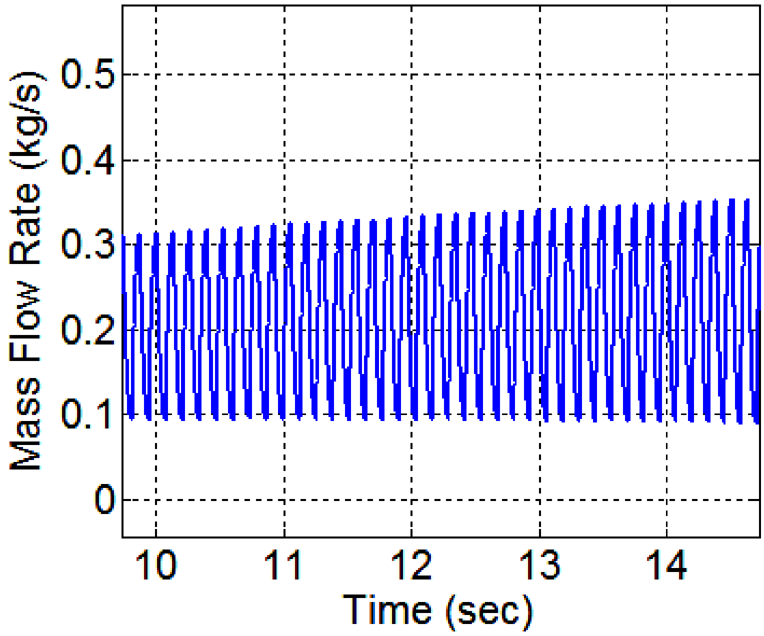

Figure 5.15 Mass flow rate oscillation near about 0.24kg/s

5.3.8 Simulation of Pressure and Temperature for Volume V_{out}

Initial temperature of volume Vout was 290k as the pressure suddenly increases from 1bar to 15 bar, temperature also increases. Due to compressibility effect in this volume temperature does not decreases sharply but it decrease smoothly as shown in fig 5.16 and due to reduction of valve opening area a pressure of 15bar is controlled from sensing orifice as shown in figure 5.17

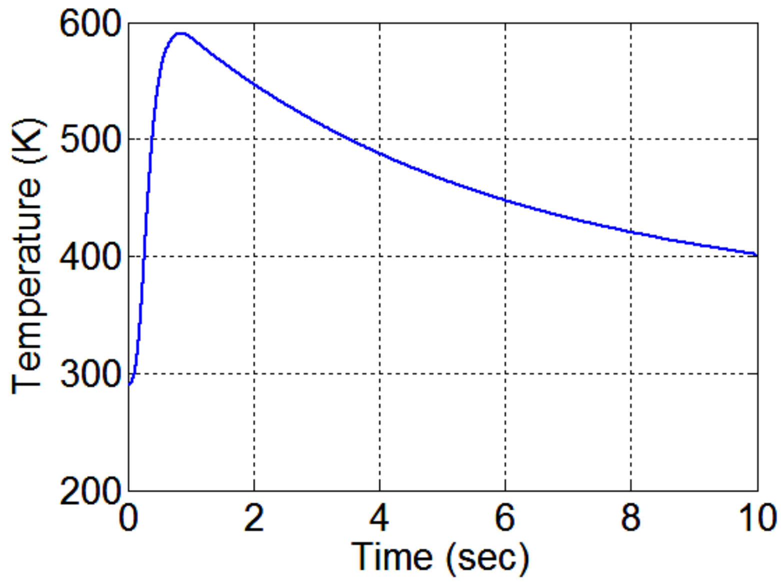

Figure 5.16 Temperature in outlet volume as a function of time

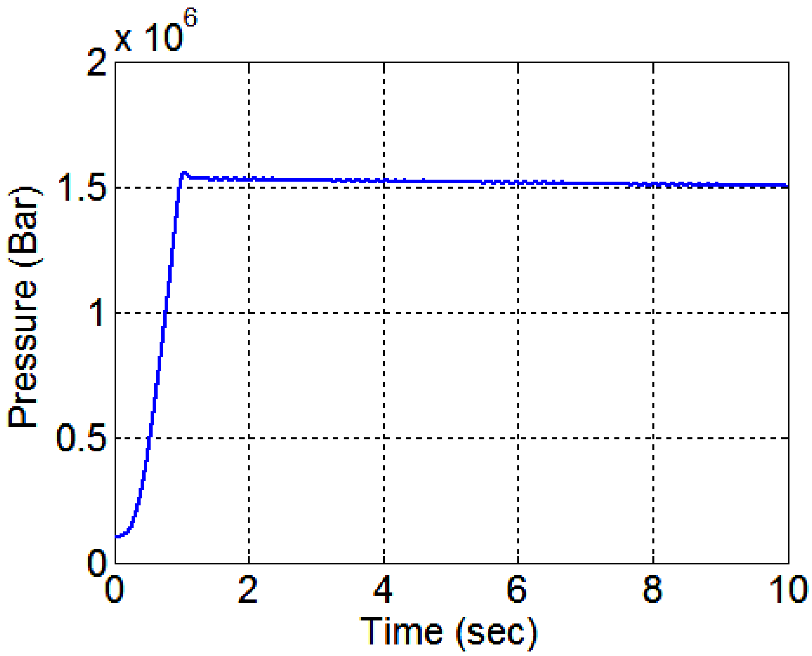

Figure 5.17Controlled pressue in outlet volume as a function of time

5.3.9 Mass Flow Rate ($\dot{m}_{dam}$) from Volume V_{out} to VolumeV_{dam}

Initial mass flow rate value here goes to negative due to large outlet area of regulator and very small area of sensing orifice. When the pressure begins to rise in volume Vout and reaches to a controlled pressure of 15bar then a net of 0 mass flow rate values is seen as shown in figure 5.18 and 5.19

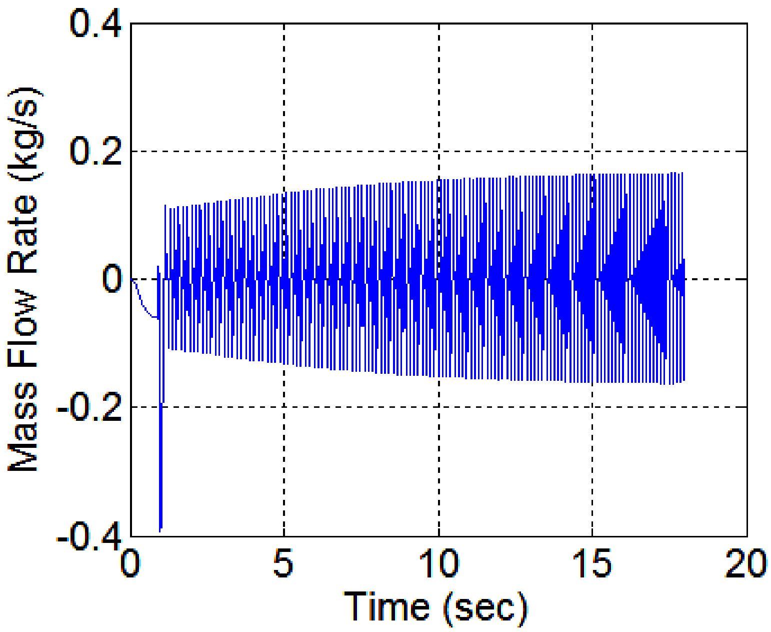

Figure 5.18 Mass flow rate in damping volume as a function of time

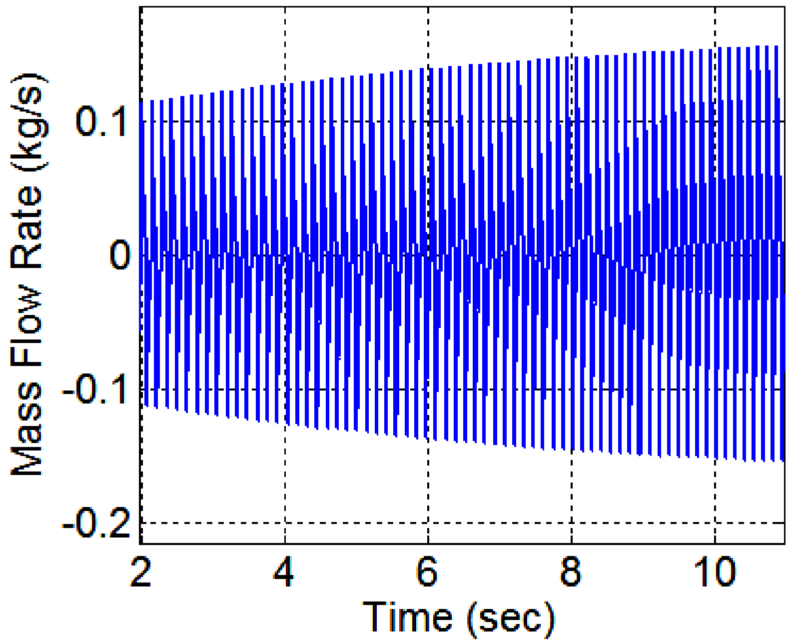

Figure 5.19 Nearly 0 mass flow rate due to same pressure in both volumes Vout and Vdam

Simulation of Pressure and Temperature for Volume V_{dam}:

Due to compressibility effect in damping chambers of pressure regulator a high temperature is seen and then due to balance of pressure between outlet volume and damping volume, this temperature decreases as shown in figure 5.20. As in through damping chamber the outlet pressure is controlled so the pressure in this volume will nearly be same as in the outlet volume as shown in figure 5.21

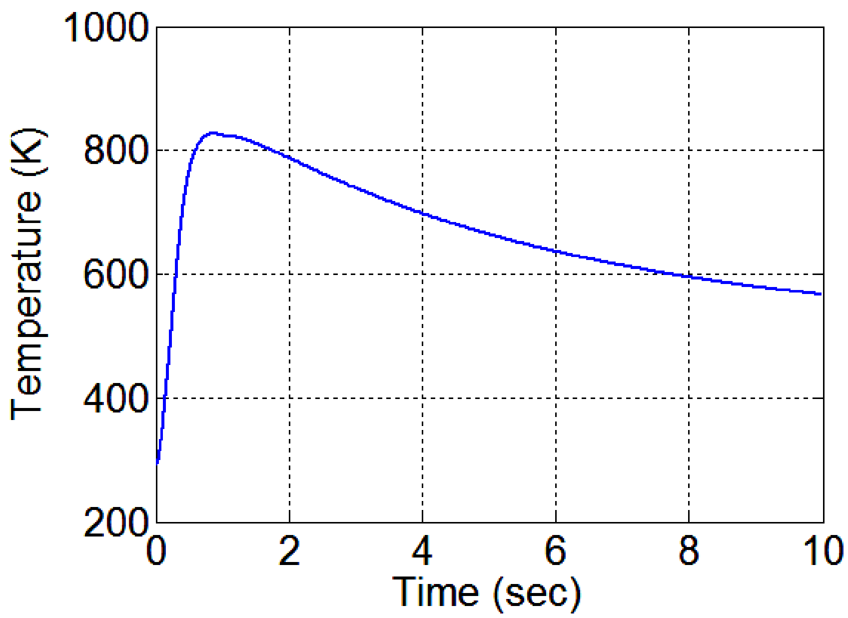

Figure 5.20 Temperature in damping chamber as a function of time

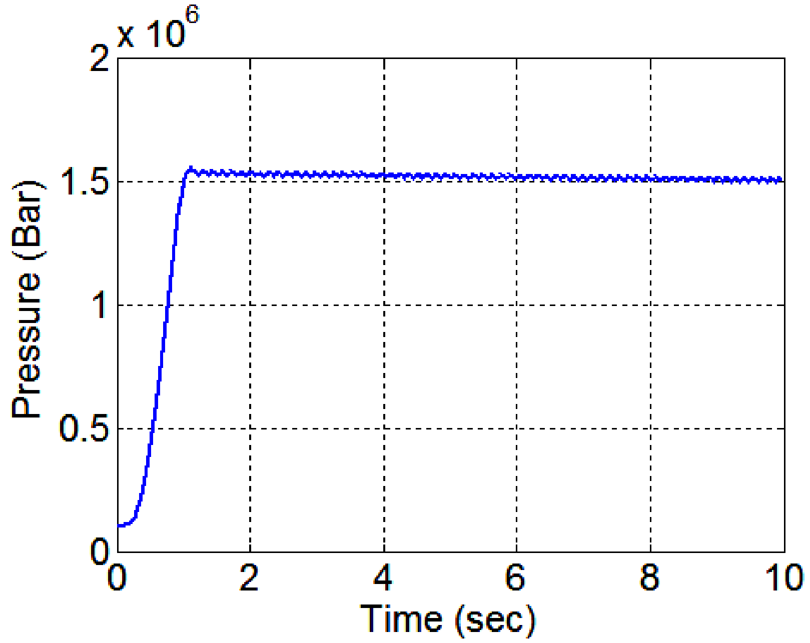

Figure 5.21 Pressure in damping volume as a function of time

5.4 Case2: Inlet Pressure is decreasing from 150bar to 60bar

For the second case we simulated the mathematical model of pressure regulator with decreasing pressure from 150bar to 60bar and with constant temperature for inlet and outlet volumes.

Initial valve clearance was 2.3mm, near about after 0.7sec pressure in the outlet volume reaches 15bar and and valve reaches its minimum opening, afterward as inlet pressure decreases valve begins to open (fig 5.22) according for maintaining a nearly 15bar pressure at outlet. During opening of vavle magnitude of oscillation was found near 0.01mm (fig 5.23)

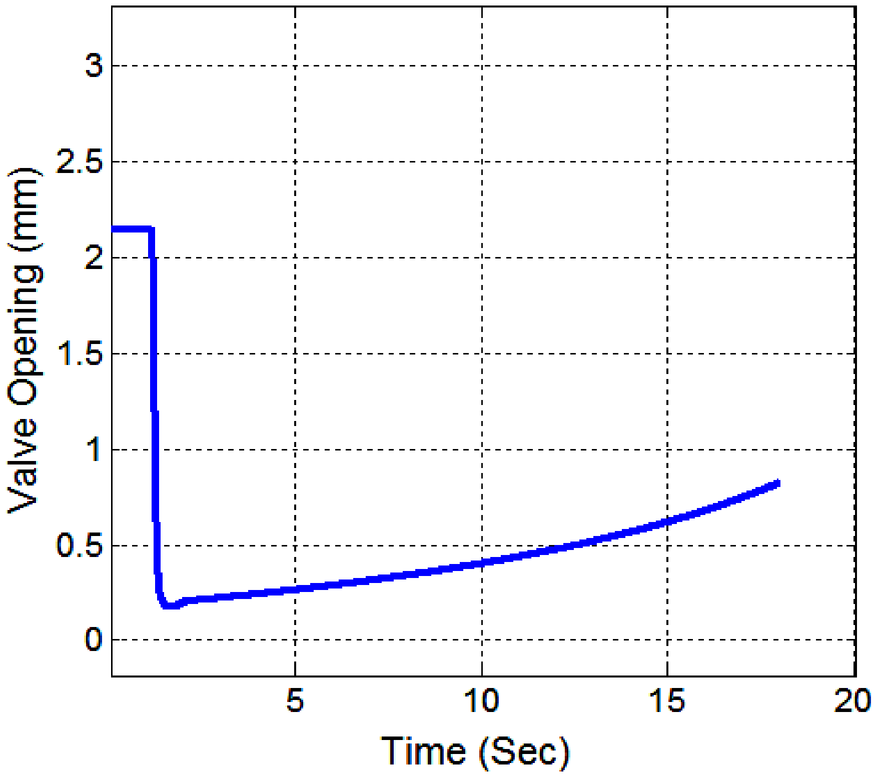

Figure 5.22 Valve opening as a function of time and decreasing inlet pressure

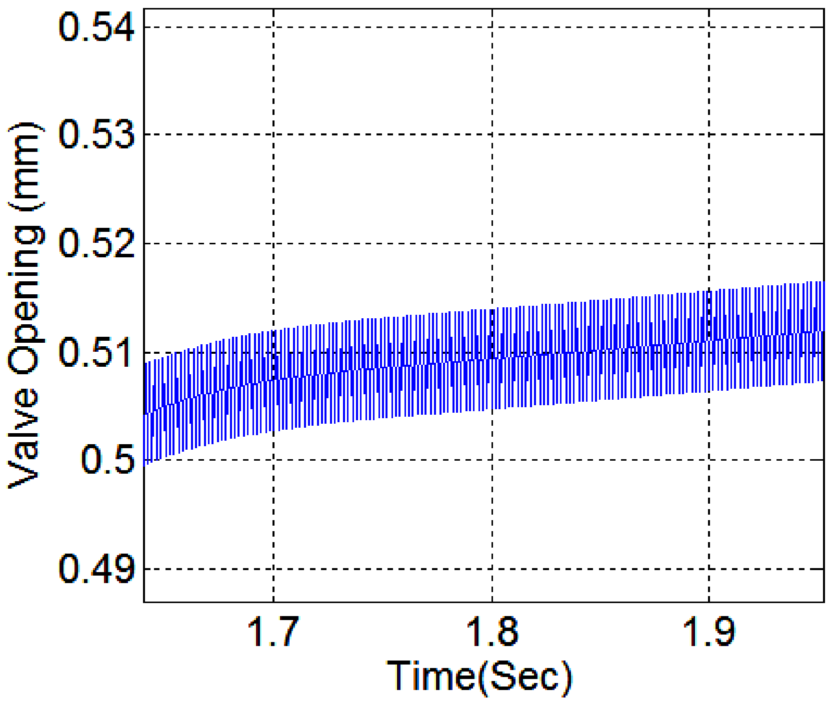

Figure 5.23 Valve opening oscillation as a function of time

5.4.1 Simulation of Outlet Pressure with Inlet Pressure

Initial pressure in outlet volume was 1bar near about 0.7 second, outlet pressure reaches to near 15bar with some oscillations of magnitude 0.5bar (fig 5.24 &fig 5.25)

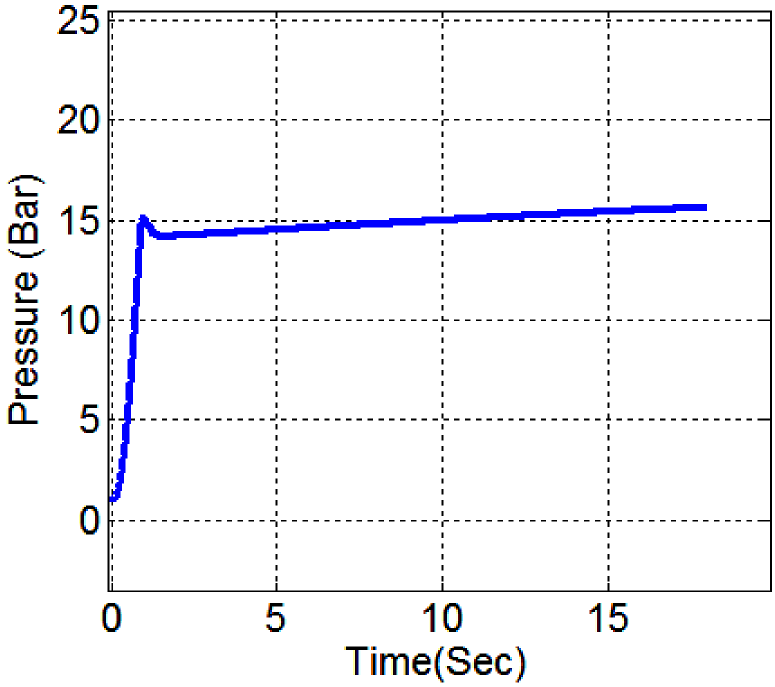

Figure 5.24 Pressure in outlet volume as a function of time

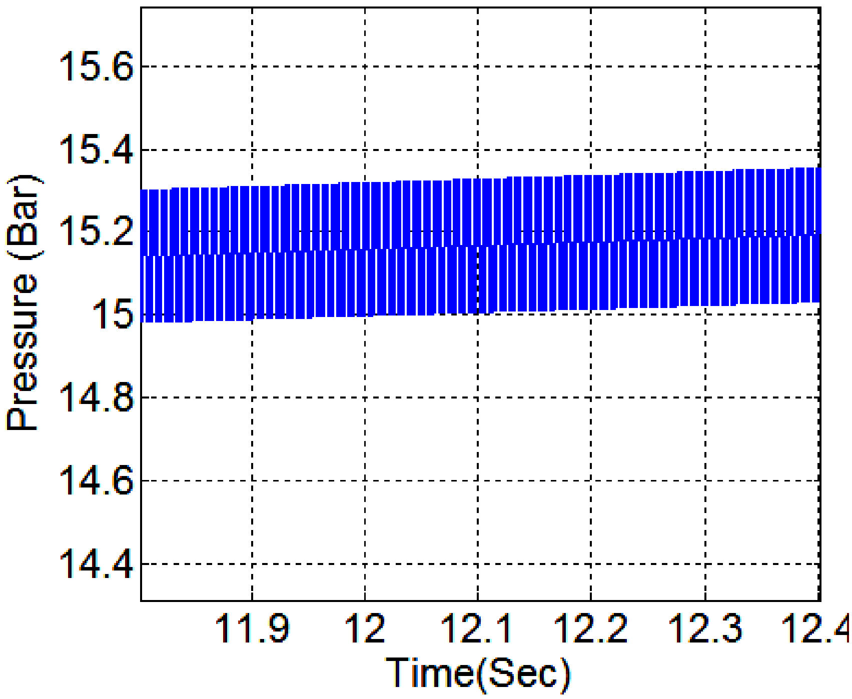

Figure 5.25 Outlet pressure oscillation near 15 bar pressure

5.4.2 Mass Flow Rate $\dot{m}_{in}$ from Cylinder to Regulator Inlet

Initial pressure in inlet volume of regulator was 1bar and reservoir pressure was 150bar. Due to this high pressure differential a high mass flow rate is seen initially. After some time this pressure differential decreases and steady state mass flow is obtained (fig 5.26). Oscillation in mass flow rate is shown in figure 5.27

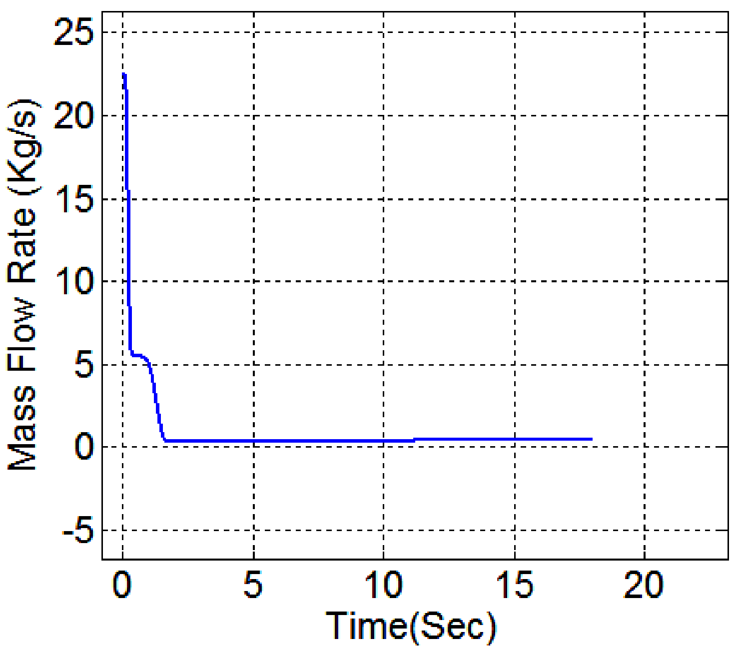

Figure 5.26 Inlet mass flow rate as a function of time

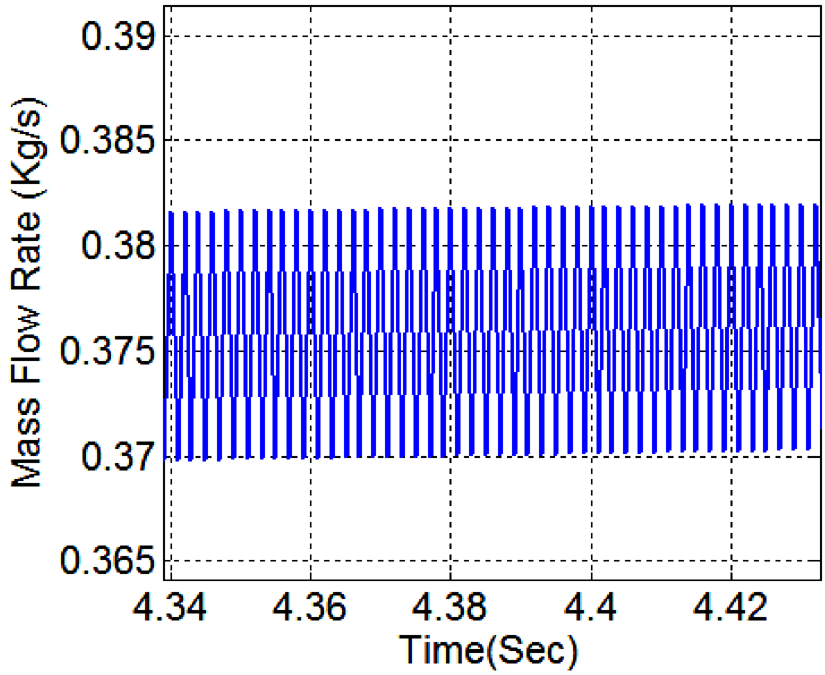

Figure 5.27 Mass flow rate oscillation in steady state condition

5.4.3 Mass Flow Rate ($\dot{m}_1$) from Inlet Volume V_{in} to Volume V_1

Initial pressure in volume V1 was 1bar. Due to high differential of pressure in volume Vin and volume V1, a high mass flow rate is observed here (fig 5.28). With the time this pressure differential decreases and steady state mass flow rate is seen with some oscillation in figure 5.29.

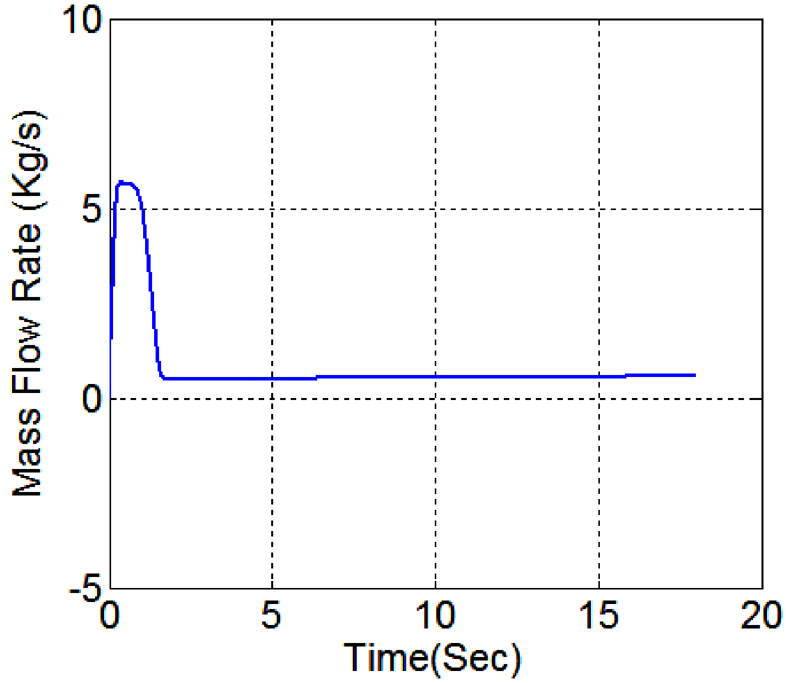

Figure 5.28 Mass flow rate as a function of time with decreasing inlet pressure

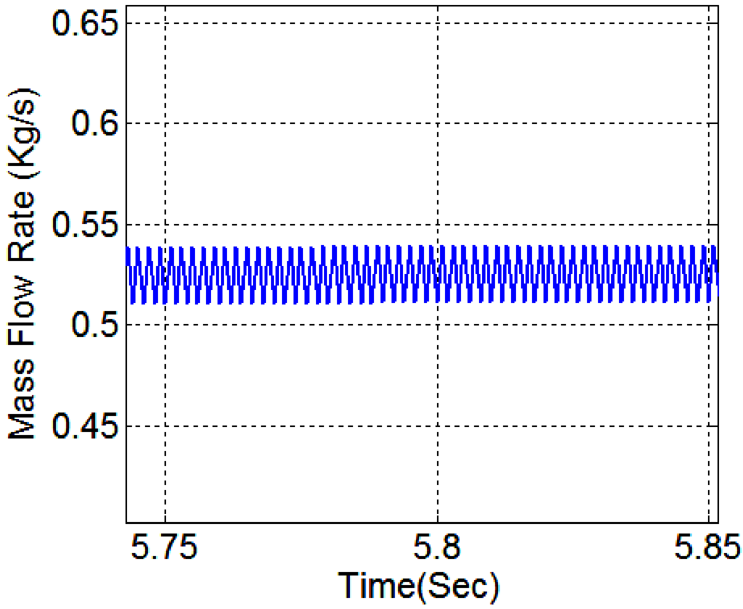

Figure 5.29 Mass flow rate oscillation near about 0.53 kg/sec

5.4.4 Mass Flow Rate ($\dot{m}_s$) from Volume V_1 to Volume V_{out}

Mass flow rate from the valve clearance was high initially due to 2.5mm valve opening. As outlet pressure reaches to 15bar, valve opening reaches to its minimum position with minimum mass flow rate value (fig 5.30) and then a smooth mass flow rate is observed with some oscillation (fig 5.31)

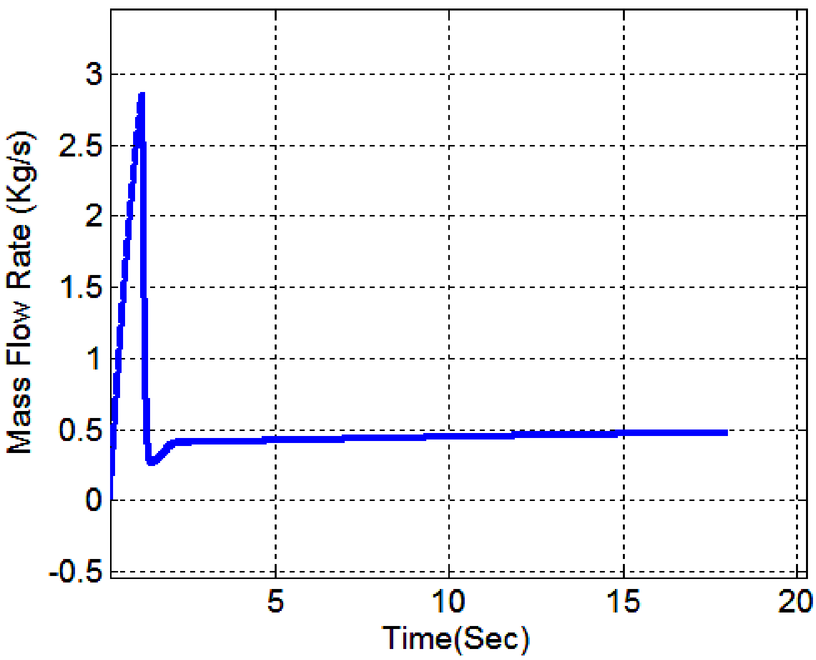

Figure 5.30 Mass flow rate from valve clearance as a function of time

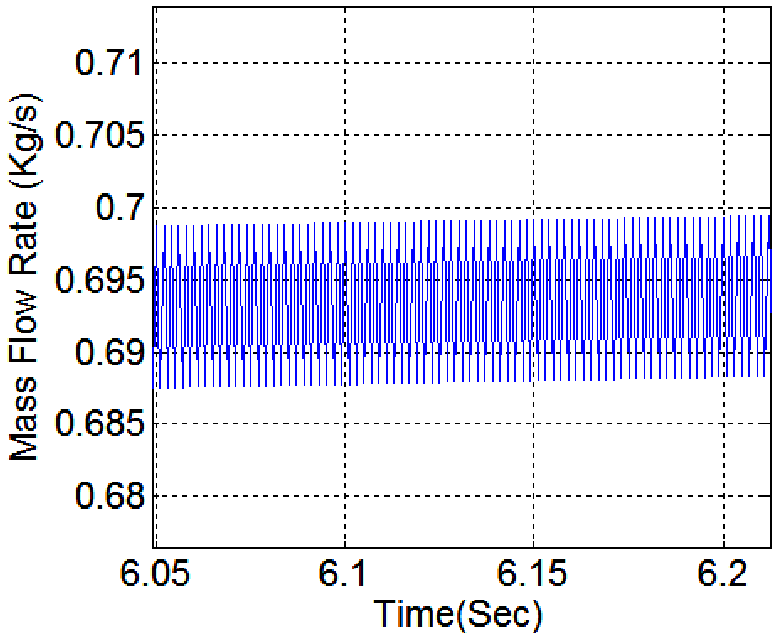

Figure 5.31 Mass flow rate oscillation near 0.695 kg/sec

5.4.5 Mass Flow Rate ($\dot{m}_{dam}$) from Volume V_{out} to Volume V_{dam}

A net of 0 mass flow rates is observed due to same pressure in volume Vout and volume Vdam as shown in figure 5.32

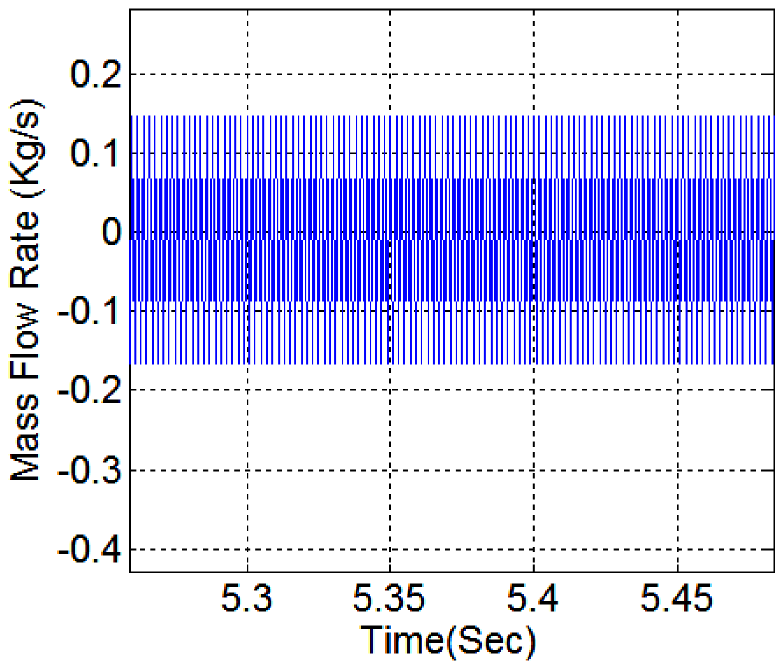

Figure 5.32 Mass flow rate oscillation near 0 kg/sec in steady state situation

5.4.6 Simulation of Pressure in Volume V_{in}

Initial pressure in inlet volume was 1 bar and in reservoir pressure was 150bar , due to large inlet cross section area of pressure regulator, pressure quickly accumulate in inlet volume and in volume V1. Afterward due to valve opening this pressure decreases linearly as shown in figure 5.33 and figure 5.34

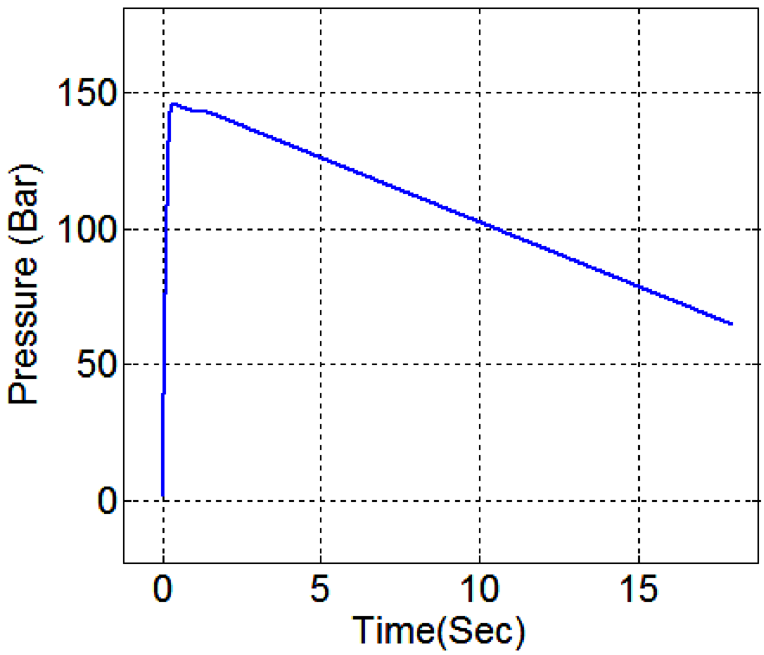

Figure 5.33 Simulation of pressure in inlet volume as a function of time

5.4.7 Simulation of Pressure for Volume V_1

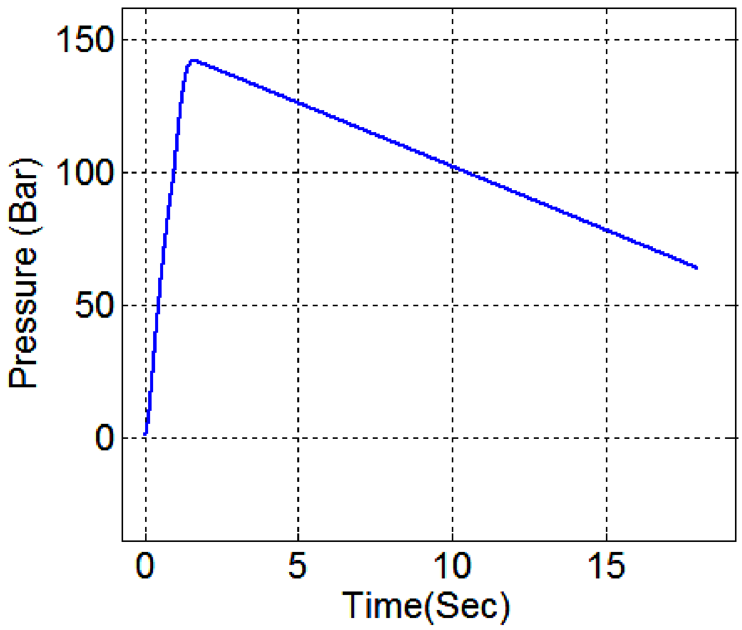

Figure 5.34 Pressure accumulation in volume V1 due to large inlet area

5.4.8 Simulation of Pressure for Volume V_{out}

Initial pressure in outlet volume was 1bar near about 0.7 second, outlet pressure reaches to near 15bar with some oscillations of magnitude 0.5bar (fig 5.36 &fig 5.37)

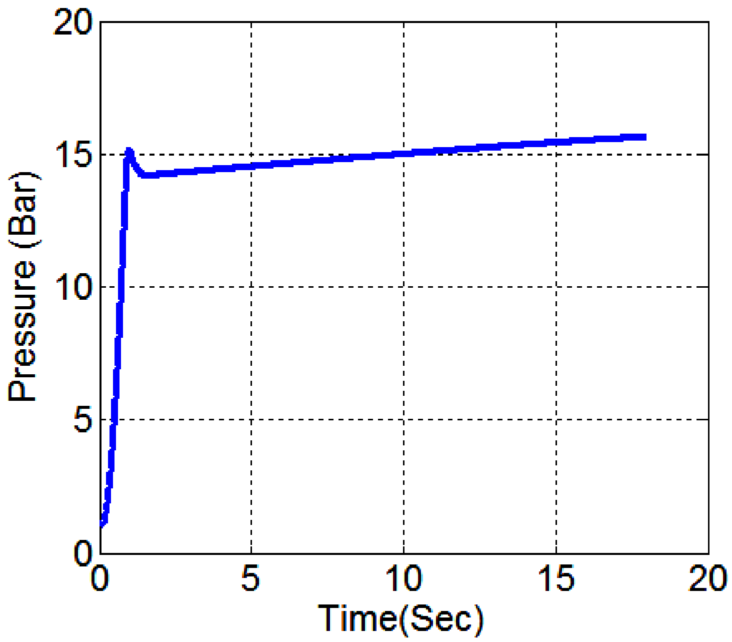

Figure 5.35 Simulation of outlet pressure with decrease of inlet pressure with respect to time

5.4.9 Simulation of Pressure for Volume V_{dam}

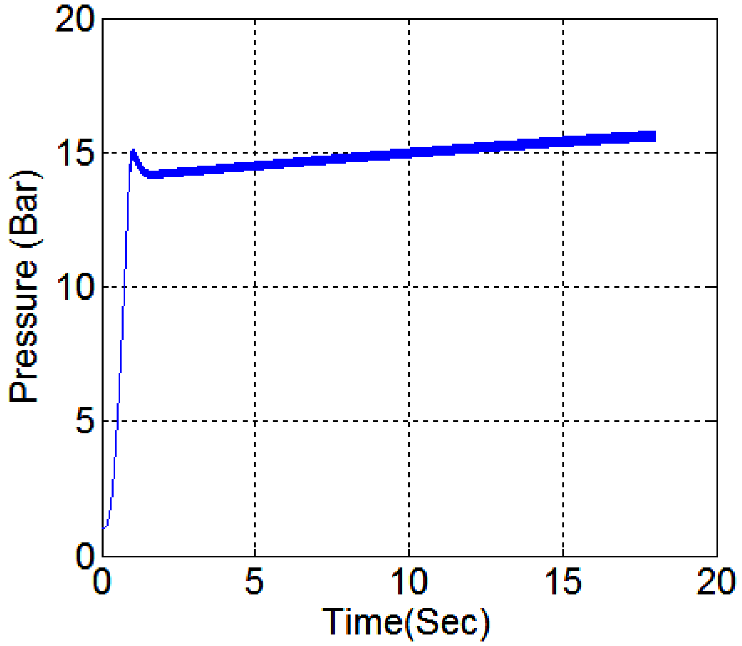

Figure 5.36 Pressure in damping chamber as a function of time

CHAPTER 6

Analytical Solution of flow model in Pressure Regulator

6.1 Development of Analytical Solution

For deriving analytical solution of pressure regulator, we made some assumptions. First we are dividing regulator in just two volumes. One volume is Vin which is the volume of regulator before valve opening and other is the volume after the valve opening. That outlet volume is named as regulated volume Vr as shown in figure.

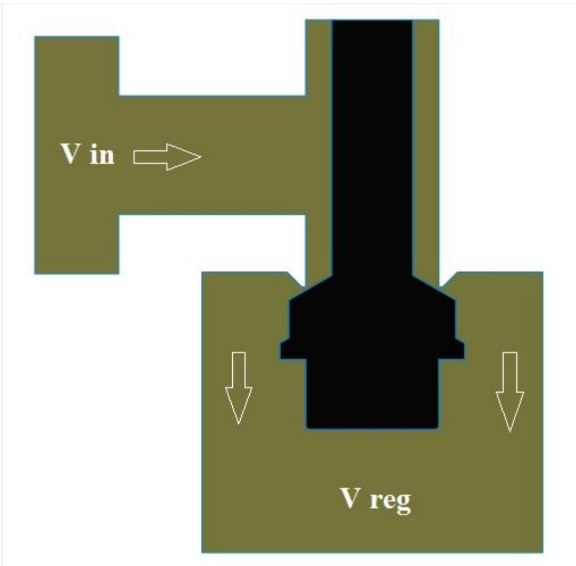

Figure 6.1 Only Two Flow Volumes

We are assuming a constant temperature in the above volumes.

$$\frac{dP_r}{dt} = \frac{\gamma R}{V_r}(T_{in}\dot{m}_s - T_{out}\dot{m}_e) - \frac{\gamma P_r A_s}{V_r}\dot{x}$$

Where V_r is outlet volume or regulated volume

If we assume the valve opening rate ($\dot{x}$) is very small then we can neglect the last term in dynamic equation of pressure change. And the continuity equation for main regulator flow can be written as

$$\frac{dP_r}{dt} = \frac{\gamma R}{V_r}(T_{in}\dot{m}_s - T_{out}\dot{m}_e) \qquad 6.01$$

$\dot{m}_s$is the mass flow rate from inlet volume to regulated volume and is given by

$$\dot{m}_s = A_s\,(\frac{2}{\gamma+1})^{\frac{\gamma}{\gamma-1}}\sqrt{\frac{\gamma}{\gamma+1}}P_{in}\sqrt{\frac{2}{RT_{in}}} \qquad 6.02$$

$\dot{m}_e$is the mass flow rate at exit of pressure regulator and is given by

$$\dot{m}_e = A_e\,(\frac{2}{\gamma+1})^{\frac{\gamma}{\gamma-1}}\sqrt{\frac{\gamma}{\gamma+1}}P_r\sqrt{\frac{2}{RT_{out}}} \qquad 6.03$$

Where A_s and A_e are the valve opening area and regulator exit area. Introducing 6.02 and 6.03 in equation 6.01 we have

$$\frac{dP_r}{dt} = \frac{\gamma R}{V_r}\left(T_{in}A_s\,(\frac{2}{\gamma+1})^{\frac{\gamma}{\gamma-1}}\sqrt{\frac{\gamma}{\gamma+1}}P_{in}\sqrt{\frac{2}{RT_{in}}} - T_{out}A_e\,(\frac{2}{\gamma+1})^{\frac{\gamma}{\gamma-1}}\sqrt{\frac{\gamma}{\gamma+1}}P_r\sqrt{\frac{2}{RT_{out}}}\right) \qquad 6.04$$

Here if we can valve opening area as function of time then we can solve equation 6.04 with assuming known temperature in both volumes

Here we will solve this problem by assuming first the constant mass flow rate and then finding the valve opening area using equation 6.02. Secondly we will assume that we know the mass flow rate as a function of time from some experimental source or by numerical computation.

Here we are first considering a constant mass flow rate problem. Let we have an average value of mass flow rate in an steady state situation. Let suppose that rate is

$$\dot{m}_s = 0.4178\,kg/s$$

Then from equation 6.02 we have valve opening area as

$$A_s(t) = 0.647/[\,(\frac{2}{\gamma+1})^{\frac{\gamma}{\gamma-1}}\sqrt{\frac{\gamma}{\gamma+1}}P_{in}(t)\sqrt{\frac{2}{RT_{in}}}\,] \qquad 6.05$$

Rearranging equation 6.04 we have

$$\frac{dP_r}{dt} + T_{out}A_e\ (\frac{2}{\gamma+1})^{\frac{\gamma}{\gamma-1}}\sqrt{\frac{\gamma}{\gamma+1}}\sqrt{\frac{2}{RT_{out}}} * P_r(t)$$
$$= \frac{\gamma R}{V_r}\left(T_{in}A_s\ (\frac{2}{\gamma+1})^{\frac{\gamma}{\gamma-1}}\sqrt{\frac{\gamma}{\gamma+1}}\sqrt{\frac{2}{RT_{in}}} \quad * P_{in}\right) \qquad 6.06$$

Which is the linear differential equation in P_r . Finding the integrating factor we have

$$I.F = e^{\int T_{out}A_e\ (\frac{2}{\gamma+1})^{\frac{\gamma}{\gamma-1}}\sqrt{\frac{\gamma}{\gamma+1}}\sqrt{\frac{2}{RT_{out}}}dt}$$

or

$$I.F = e^{T_{out}A_e\ t\ (\frac{2}{\gamma+1})^{\frac{\gamma}{\gamma-1}}\sqrt{\frac{\gamma}{\gamma+1}}\sqrt{\frac{2}{RT_{out}}}} \qquad 6.07$$

Multiplying equation 6.06 with integrating factor we have

$$\frac{d}{dt}\left(P_r * e^{T_{out}A_e\ t\ (\frac{2}{\gamma+1})^{\frac{\gamma}{\gamma-1}}\sqrt{\frac{\gamma}{\gamma+1}}\sqrt{\frac{2}{RT_{out}}}}\right)$$
$$= \frac{\gamma R}{V_r}\left(T_{in}A_s\ (\frac{2}{\gamma+1})^{\frac{\gamma}{\gamma-1}}\sqrt{\frac{\gamma}{\gamma+1}}\sqrt{\frac{2}{RT_{in}}} \quad * P_{in}\right)$$
$$* (e^{T_{out}A_e\ t\ (\frac{2}{\gamma+1})^{\frac{\gamma}{\gamma-1}}\sqrt{\frac{\gamma}{\gamma+1}}\sqrt{\frac{2}{RT_{out}}}})$$

6.08

Integrating 6.08 w.r.t to time and simplifying

$$P_r(t) * e^{T_{out}A_e\ t\ (\frac{2}{\gamma+1})^{\frac{\gamma}{\gamma-1}}\sqrt{\frac{\gamma}{\gamma+1}}\sqrt{\frac{2}{RT_{out}}}}$$
$$= \frac{\gamma R}{V_r}\left(T_{in}A_s\ (\frac{2}{\gamma+1})^{\frac{\gamma}{\gamma-1}}\sqrt{\frac{\gamma}{\gamma+1}}\sqrt{\frac{2}{RT_{in}}} \quad * P_{in}\right)$$
$$* \frac{e^{T_{out}A_e\ t\ (\frac{2}{\gamma+1})^{\frac{\gamma}{\gamma-1}}\sqrt{\frac{\gamma}{\gamma+1}}\sqrt{\frac{2}{RT_{out}}}}}{(e^{T_{out}A_e\ \ (\frac{2}{\gamma+1})^{\frac{\gamma}{\gamma-1}}\sqrt{\frac{\gamma}{\gamma+1}}\sqrt{\frac{2}{RT_{out}}}})} + C$$

6.09

Where C is the constant of integration. So regulating pressure is

$$P_r(t) = \frac{\gamma R}{V_r}\left(T_{in}A_s(t)\ (\frac{2}{\gamma+1})^{\frac{\gamma}{\gamma-1}} \sqrt{\frac{\gamma}{\gamma+1}} \sqrt{\frac{2}{RT_{in}}} \quad * P_{in}(t) \right)$$
$$* \frac{1}{(e^{T_{out}A_e \ \ (\frac{2}{\gamma+1})^{\frac{\gamma}{\gamma-1}} \sqrt{\frac{\gamma}{\gamma+1}}\sqrt{\frac{2}{RT_{out}}}})} + C$$
$$* e^{-T_{out}A_e \ \ t \ \ (\frac{2}{\gamma+1})^{\frac{\gamma}{\gamma-1}} \sqrt{\frac{\gamma}{\gamma+1}}\sqrt{\frac{2}{RT_{out}}}} \qquad 6.10$$

Where

$$C = P_r(0) - \frac{\gamma R}{V_r}\left(T_{in}A_s(0)\ (\frac{2}{\gamma+1})^{\frac{\gamma}{\gamma-1}} \sqrt{\frac{\gamma}{\gamma+1}} \sqrt{\frac{2}{RT_{in}}} \quad * P_{in}(0) \right) *$$
$$\frac{1}{(e^{T_{out}A_e \ \ (\frac{2}{\gamma+1})^{\frac{\gamma}{\gamma-1}} \sqrt{\frac{\gamma}{\gamma+1}}\sqrt{\frac{2}{RT_{out}}}})} \qquad 6.11$$

6.2 Comparison of Analytical and Numerical Model for Mass Flow Rate

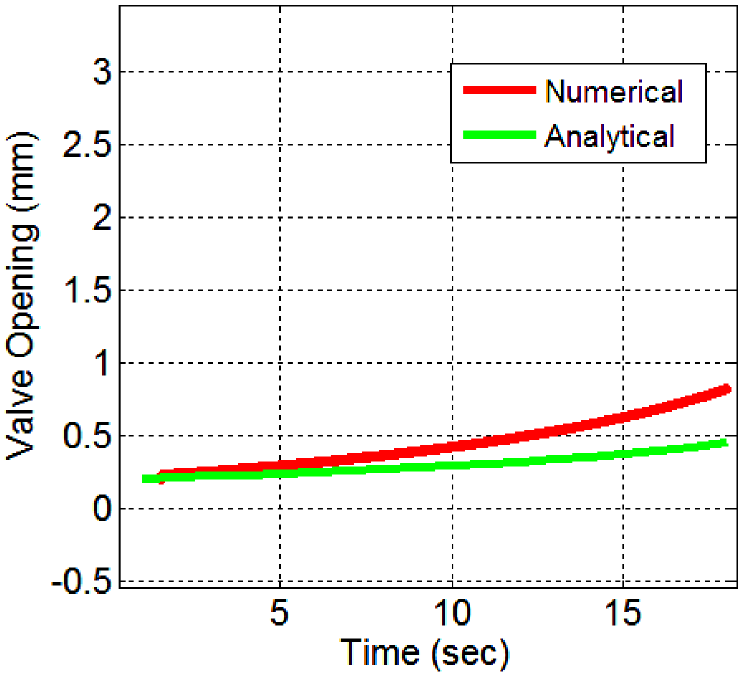

Figure 6.2 Comparison of valve opening

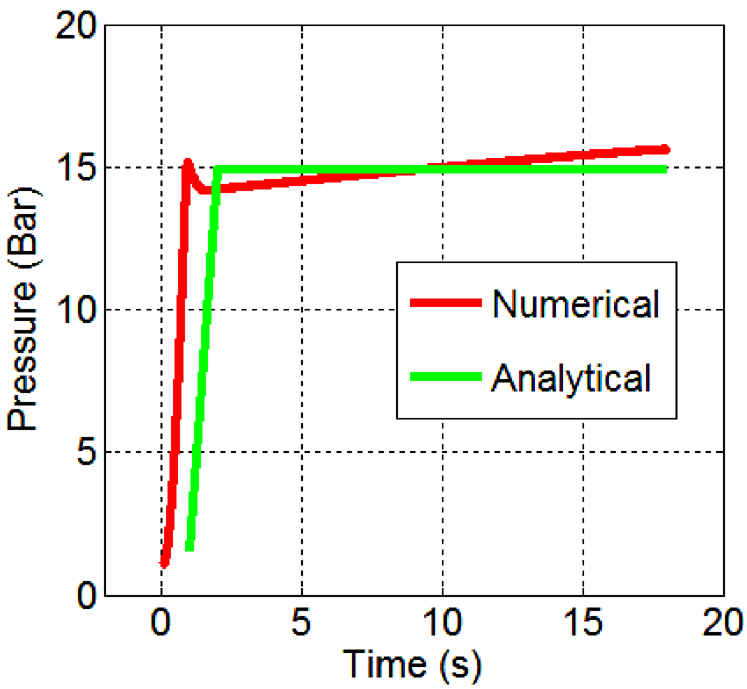

Figure 6.3 Comparison of Outlet Pressure

The constant mass flow rate in steady state condition can be used just for initial design parameters it does not simulate the minor oscillation in valve opening as well as in the outlet pressure variations. This is because when the constant mass flow rate assumption is taken then valve opening is only the function of inlet pressure and inlet temperature. In this way we are here ignoring the equation of moving shaft and finding valve opening from the mass flow rate equation.

CHAPTER 7

CFD Analysis of Pressure Regulator

In this chapter we perform computational fluid dynamics (CFD) simulation of pressure regulator for finding the flow behavior inside pressure regulator and particularly near the valve opening. We perform both steady and unsteady simulation with different inlet pressures and valve opening. Our main focus of CFD simulation of pressure regulator is to find valve opening curve and mass flow rate computations with respect to inlet pressure corresponding to 15bar outlet pressure. At the end of CFD simulation we compare our numerical computations with the CFD based analysis.

7.1 CFD Solution Method

The solution methods in Fluent are based on CFD models. CFD deals with numerical solution of the fluid flow, heat transfer and other similar phenomena like radiation. The objective of CFD in this thesis is to obtain the computer based prediction of the compressed air flow from the pressure regulator and analysis of overall pressure and temperature distribution in whole domain.

7.1.1 Steps of Solution

We used ANSYS Fluent 14 [45] as CFD software to simulate the fluid flow problem. Fluent uses Finite Volume Method to solve governing equations described below. There are three steps to solve any problem; Pre Processing, Processing Steps, and Post Processing Steps.

7.1.2 Pre Processing Steps

In this geometry and mesh of the problem domain is generated. With the help of design parameters values obtained in numerical computations, a 3D para solid body of pressure regulator is design in solid work software as shown in figure.

For the mesh generation commercial software package ANSYS ICEM CFD is used. In ICEM, para solid flow model of 3D pressure regulator which was designed in solid work is imported for mesh generation. ANSYS ICEM CFD provide advanced geometry acquisition, and mesh generation, and mesh optimization tools to meet the requirement for integrated mesh generation for today's sophisticated analysis. ANSYS ICEM CFD's mesh generation tools offer the capability to parametrically create meshes from geometry in numerous formats like multi block structured, unstructured hexahedral unstructured tetrahedral, Cartesian with H-grid refinement , hybrid meshes comprising hexahedral, tetrahedral, pyramidal and/or prismatic elements and quadrilateral and triangular surface meshes. Over all process of ICEM CFD as described in documentation of ANSYS ICEM CFD is described in the flow diagram. Flow model of pressure regulator in solid form in ANSYS ICEM is show in figure 7.2. Moving shaft of pressure regulator is also shown in figure 7.3. Moving shaft with valve is shown in figure 7.4

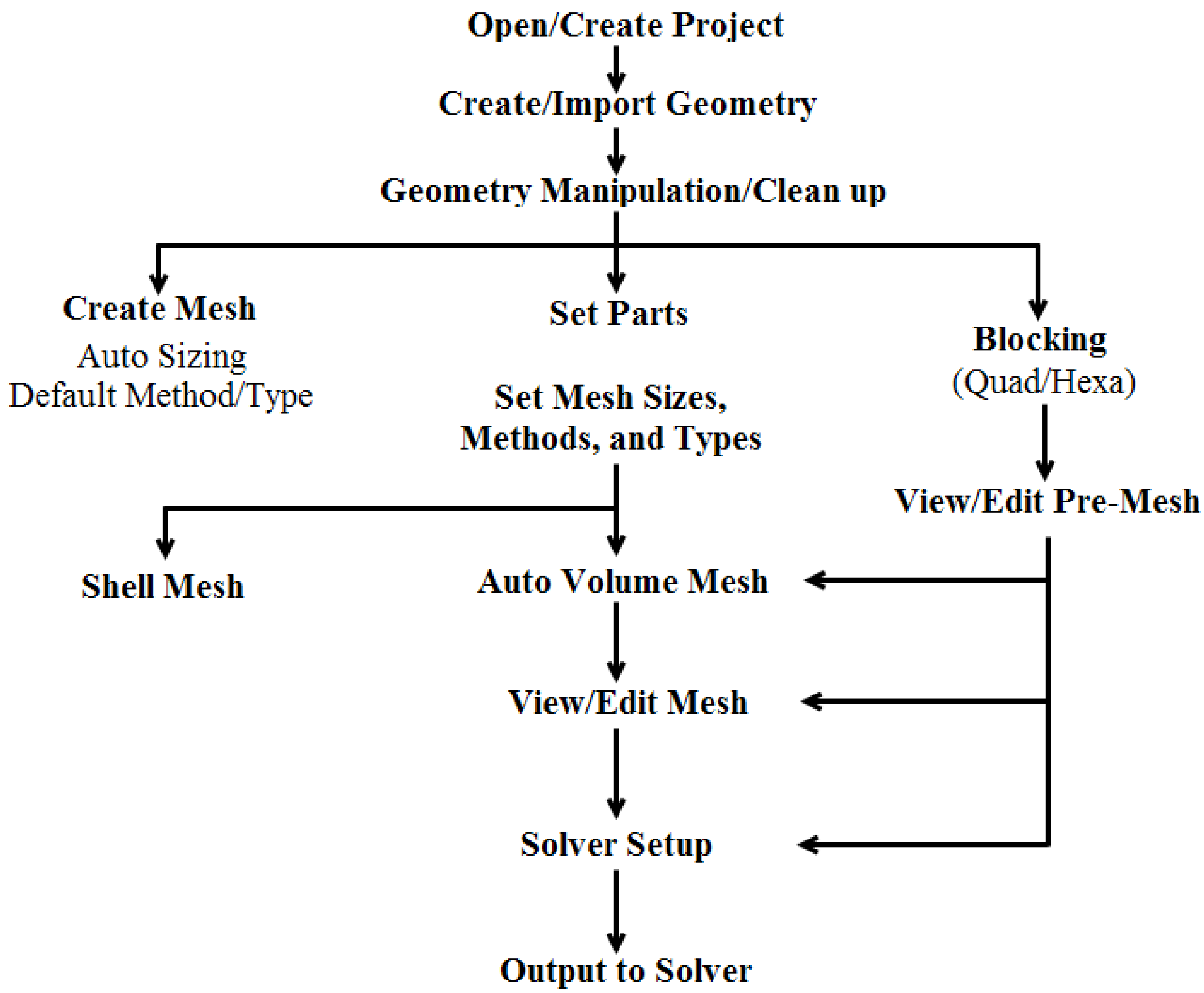

Figure 7.1 Problem solution steps in ANSYS ICEM CFD

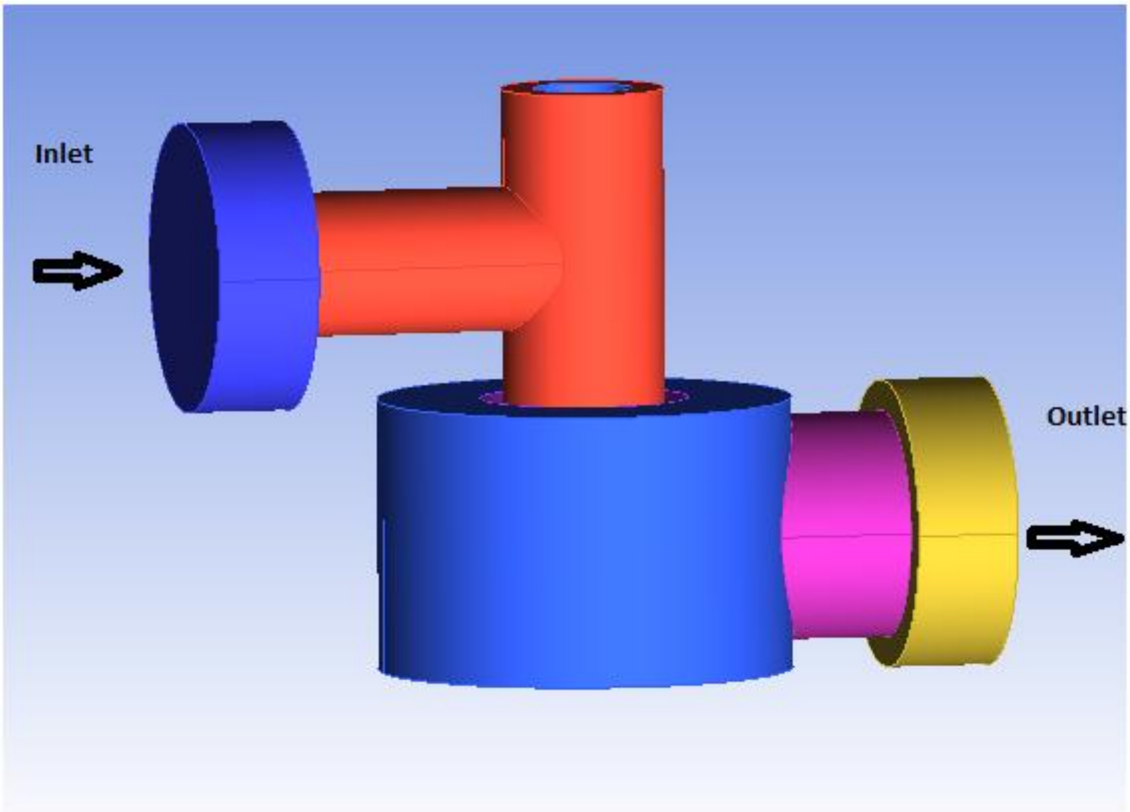

Figure 7.2 Complete 3D Flow volume of pressure regulator in ANSYS ICEM

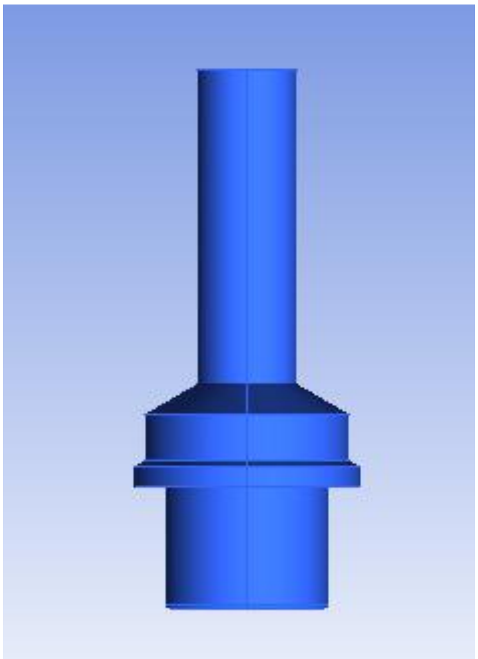

Figure 7.3 Moving shaft of pressure regulator

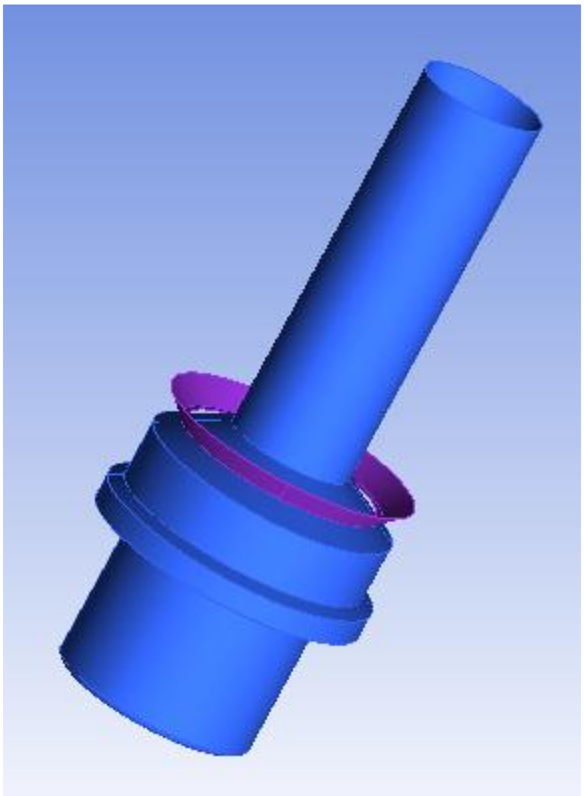

Figure 7.4 Moving shaft with valve clearance of 0.35mm

7.1.3 Meshing in ICEM

Meshing of the 3D pressure regulator is done in ICEM with tetrahedral/mixed element using Robust Octree mesh method. The Robust Octree generates a tetra mesh using a top-down meshing approach. An Octree mesher does not require an existing surface mesh because one is created by the Octree process. It allows you to run meshing operation in batch mode and enables a faster transition from the more refined elements to coarser elements instead of a more gradual transition when computing the mesh. This will reduce the number of elements in the overall mesh. An important useful option if the geometry to be captured is difficult to mesh with desired coarse mesh size then it allows the Octree process to fit to the geometry and flood fill with a finer mesh and then automatically coarsen it. As in our case we need a coarser mesh in valve opening area to capture the flow. Tetrahedral volume mesh of complete flow volume of regulator is shown in figure 7.5 and around the valve opening coarser mesh is shown in figure 7.6.

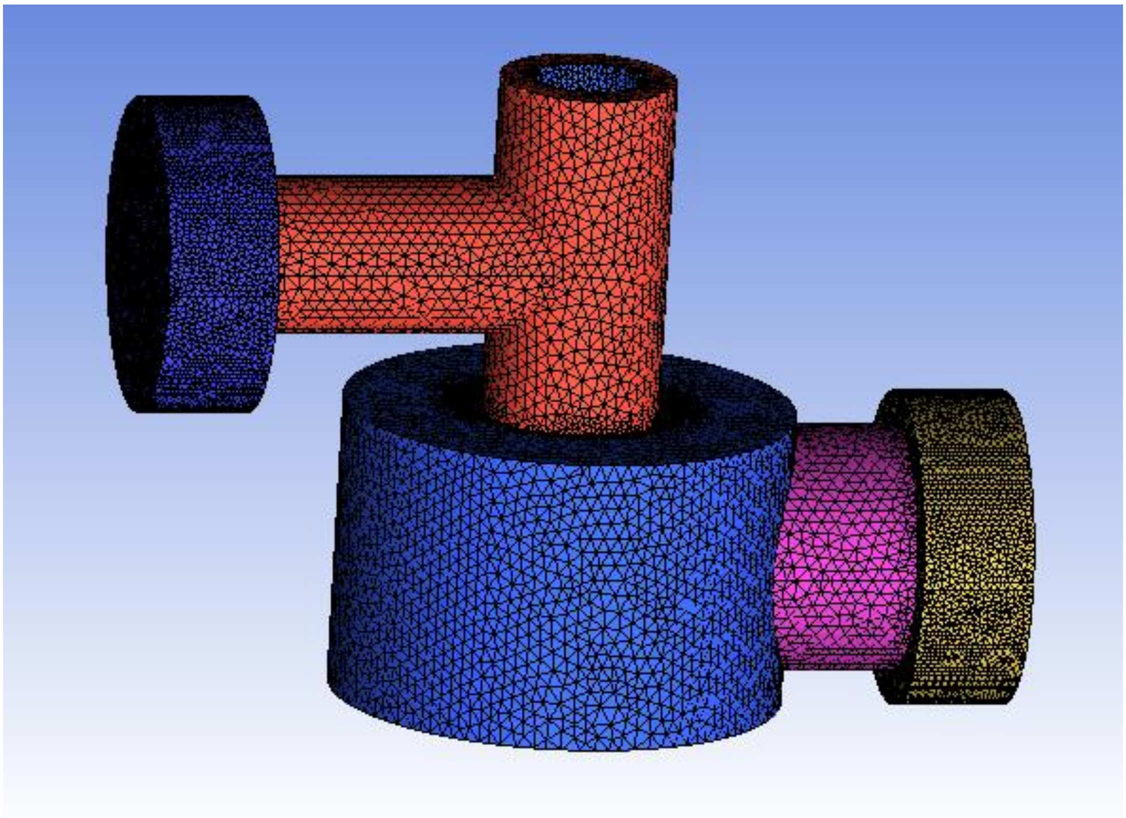

Figure 7.5 Tetrahedral volume mesh of flow volume

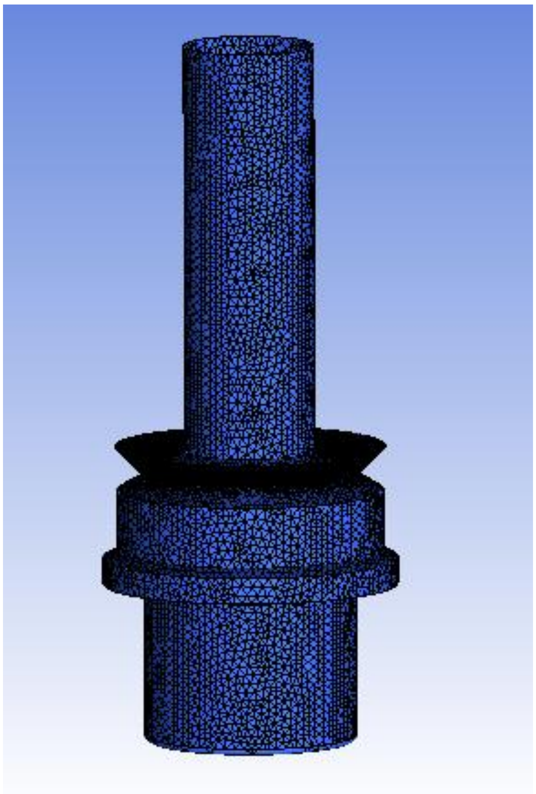

Figure 7.6 Meshing on moving shaft with coarser mesh near valve opening

7.1.4 Fluent Processing Steps

Once the mesh is generated, it is imported to FLUENT to solve for domain. Figure 7.7 shows the steps in the phase

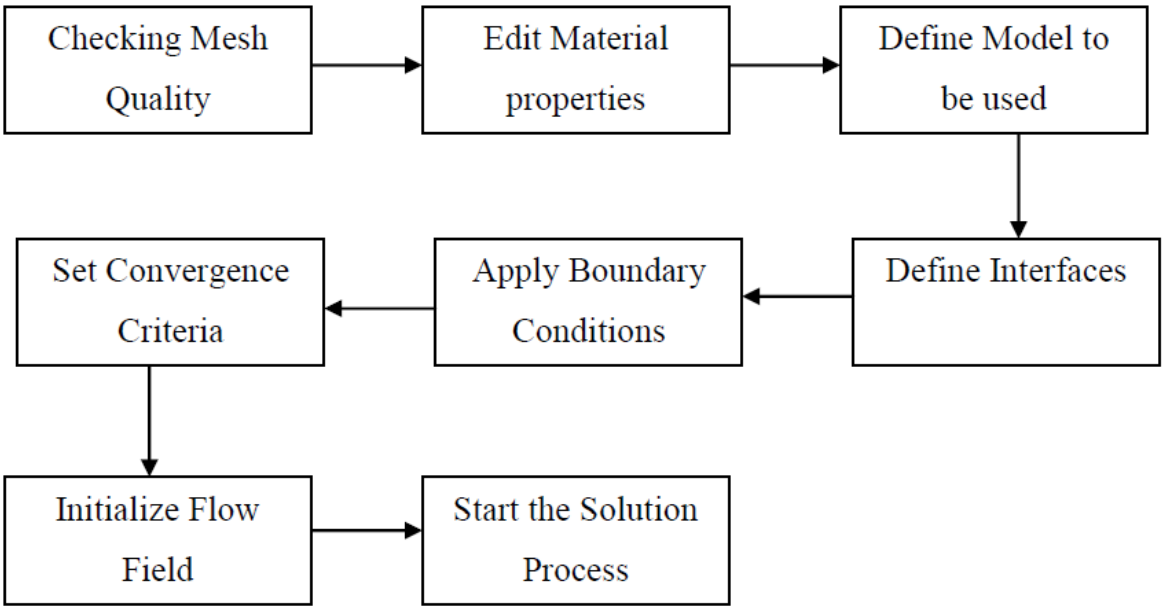

Figure 7.7 Fluent sequence in solving flow problem

7.1.5 Post Processing

Once the solution process is complete, case and data file is stored. Then we use post processing tools of fluent for analysis and interpretation of different results. Contour and graphs can also be well visualized using post processing tools.

7.2 Governing Equation

The numerical solution of fluid flow and heat transfer phenomena involves solutions of some coupled, non-linear partial differential equations known as Navier Stokes Equations. Fields variables involved in this governing equation are *u,v,w, T and P.* Where u,v and w are velocity components in x, y, and z direction respectively. T is the temperature and P is the pressure. All these variables are function of space dimensions x, y, z and time t.

7.2.1 Navier Stoke's Equations

Unsteady compressible Navier stokes equations consists of continuity equation, momentum equation and energy equation. Continuity equation is statement of mass conservation. Momentum equation is derived from newton second law and energy equation is derived from the fundamental principle of energy conservation.

7.2.2 Continuity Equation

$$\frac{\partial \rho}{\partial t} + \nabla.(\rho \bar{v}) = 0 \qquad 7.1$$

7.2.3 Momentum Equation:

$$\frac{\partial \rho \bar{v}}{\partial t} + \nabla.(\rho \bar{v}\bar{v}) = -\nabla p + \rho(v_l + v_t)\nabla^2 \bar{v} + \rho \bar{g} \qquad 7.2$$

The term v_l and v_t refer to molecular diffusivity (Kinematic viscosity) and turbulent diffusivity, respectively

7.2.4 Energy Equation

$$\frac{\partial T}{\partial t} + \bar{v}\nabla T = (\alpha + \alpha_t)\nabla^2 T + \nabla v \bar{\tau} \qquad 7.3$$

Here α and α_t refer to thermal diffusivity and corresponding turbulent diffusivity, respectively. The last term in the energy equation represents viscous dissipation which was duly considered to arise out of viscous stress τ. The turbulent viscosity term v_t is to be computed from an appropriate turbulence model. In this approach, the turbulent viscosity is computed using two different equations for parameters such as turbulent kinetic energy k and dissipation rate ε. For compressible flows, the mass conservation becomes a transport equation for density. An additional equation in the form of ideal gas law becomes transport equation for pressure. Here pressure appears as a source term in momentum equation. There is no separate equation for pressure. Therefore continuity equation combined with momentum equation to give equation for pressure known as pressure-velocity coupling.

7.3 Turbulence Modeling:

To obtain a numerical solution for turbulence, Reynolds decomposition is applied to N-S equation. This technique employed the decomposition of turbulent component into instantaneous (fluctuating).

7.3.1 Standard k-ε Model

The standard K-ε turbulence model was proposed by launder and splading in 1974 [46]. It is the most used turbulence model for predicting internal flows such as flow inside pressure regulator or nozzle. Standard K-ε model is based on transport equations for turbulent kinetic energy (K) and its rate of dissipationε. In this study, for closing the time-averaged momentum equation, a realizable K-ε model proposed by Shih et al [47] was chosen. As such, the model was found to work satisfactorily as observed by chattopadhyay et al [48]. The expression for the turbulent viscosity is given as

$$\nu_t = C_\mu \frac{k^2}{\epsilon} \qquad 7.4$$

Where C_μ is a constant

The turbulent diffusivity is related to molecular diffusivity in following manner

$$\mathrm{Pr}\frac{\nu_t}{\propto_t} = Pr_t \qquad 7.5$$

The value of turbulent prandtl number is Pr_t is chosen as 0.85

7.4 Working Fluid

Working fluid material is air in the compressible regime with varying density which has been modeled using ideal gas law. The viscosity has been modeled using Sutherlands viscosity for air which can be expressed with three coefficients as

$$\mu = \mu_0 \frac{T}{T_0}^{3/2} \frac{T_0 + S}{T + S} \qquad 7.6$$

Where μ_0 and T_0 are reference viscosity and temperature and S is Sutherland constant. A value of μ_0 =1.716*10-5kg/ms, T_0 =273.11k and S=110.56K are used.

7.5 Boundary Conditions

At inlet boundary, varying inlet pressure conditions are used with respect to valve opening. The inlet temperature is chosen to 300k. At inlet direction specification method is chosen at normal to boundary. Turbulent intensity of 8% and hydraulics diameter 16mm at inlet is chosen for turbulent specification method. No-slip boundary condition is assigned for all the walls. The valve wall was generally assumed to be at adiabatic condition. At outlet pressure is fixed to 15bar and temperature is fixed to 298k. At outlet direction specification method is chosen at normal to boundary. Turbulent intensity of 8% and back flow hydraulics diameter of 16mm at outlet is chosen for turbulent specification method.

7.6 SIMPLE Algorithm

For Solution method of pressure velocity coupling, SIMPLE scheme is chosen. The SIMPLE (Semi-Implicit Method for Pressure-Linked Equations) allows coupling the Navier-Stokes equations with an iterative procedure. This method has been discussed by Patankar and Spalding [49]. In this method, we initially guess the pressure field *P**. This *P** is the assumed pressure and using its value we solve the Navier Stoke's equation and find *u**, *v** and *w**. Now we use pressure correction equation and find values of corrected pressure *P'*. Then we calculate *P* by adding *P** and *P'*. Also find *u*, *v* and *w* from their assumed values using respective formulas. Solve the Discretization equation and find other unknowns such as temperature concentration, turbulence quantities etc. Treat the corrected pressure as assumed pressure *P*. Find starred velocities and the whole process repeated until a converged solution is obtained.

7.7 Solution Initialization

Problem is initialized using hybrid initialization method with 20 iterations. For some cases standard initialization is also chosen. Hybrid initialization is a collection of boundary interpolation methods, where variables, such as temperature, turbulence, species fractions, volume fractions, etc., are automatically patched based on domain averaged values or a particular interpolation recipe. It solves Laplace's equation to determine the velocity and pressure fields.

7.8 CFD Simulation Analysis and Discussions

For a valve opening of 0.35mm and inlet pressure of 103bar following results of CFD simulations are observed. Mass flow rate for this inlet is found to be 0.4036kg/s

First mesh display is shown with 730089 tetrahedral elements in fluent. Mesh is check in fluent and no negative volume is found. Inlet is shown in blue color while outlet is shown in red color. Dense mesh can be seen near the valve opening and on whole moving shaft in figure 7.9

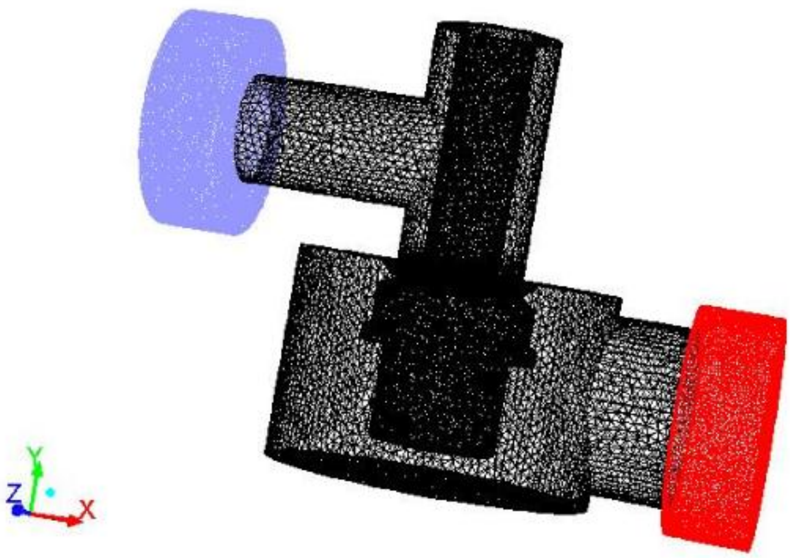

Figure 7.8 Tetrahedral mesh of flow volume of pressure regulator

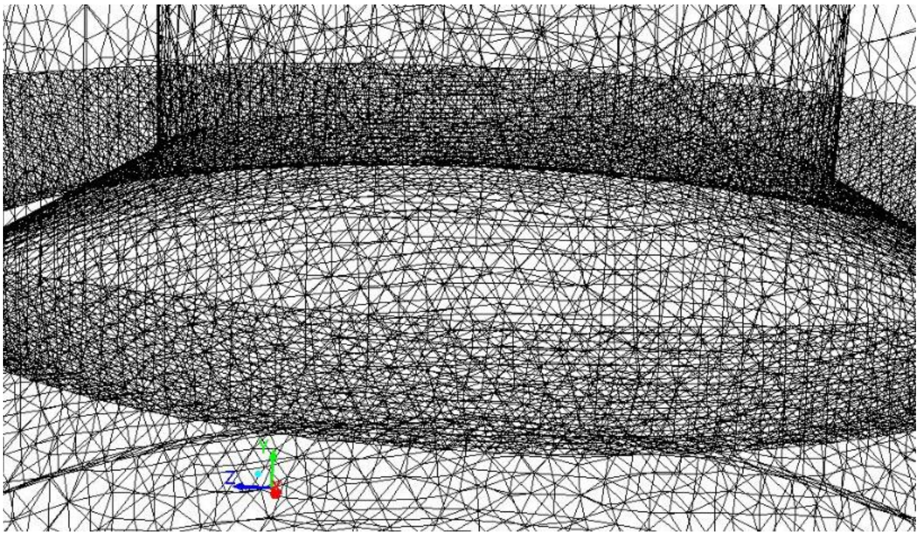

Figure 7.9 Dense mesh near valve opening

Overall pressure distribution in regulator is shown steady state condition in figure 7.9. Two major distinctions in pressure can be observed form the figure. In steady state conditions pressure of 103bar accumulate in all flow volume before the valve opening and a pressure of near 15bar surrounds all the outlet volume after the valve opening. Pressure drop with respect to position can be seen in figure 7.10

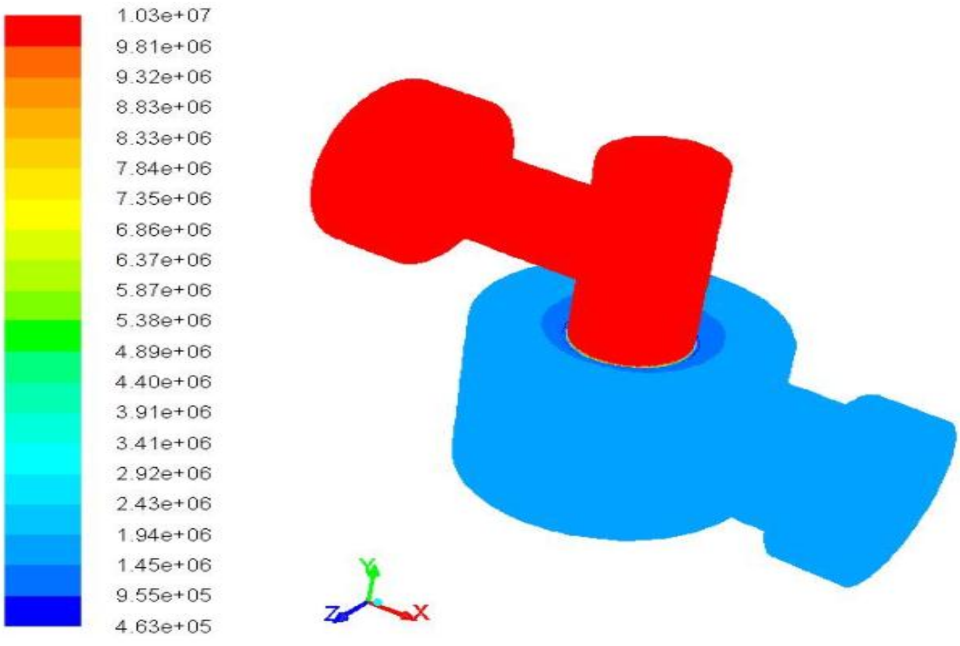

Figure 7.10 Static pressure distribution in pressure regulator

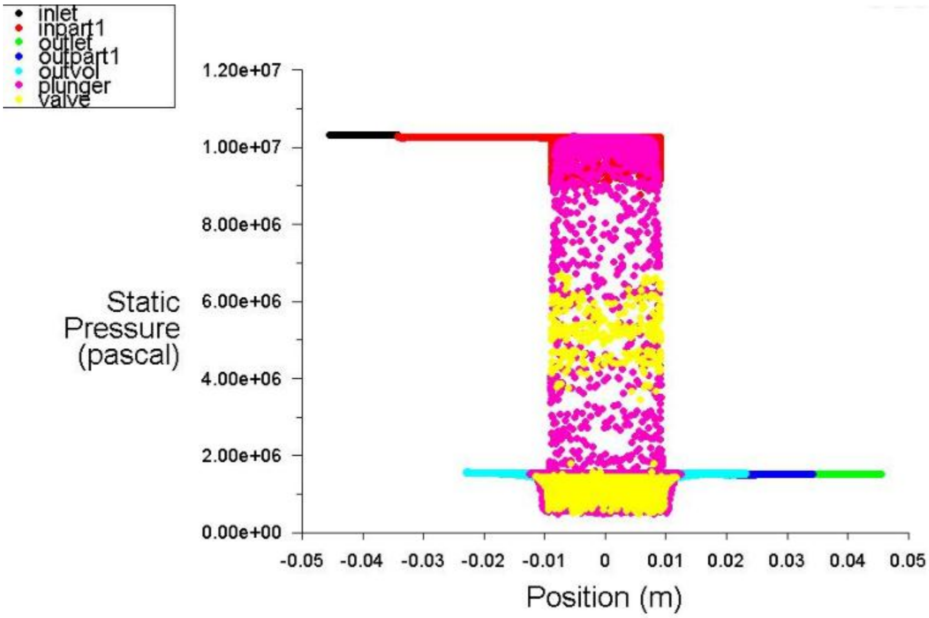

Figure 7.11 Pressure distributions inside pressure regulator from inlet to outlet

For looking the inside of pressure regulator we observe the pressure distribution in moving shaft and near valve opening. The high pressure drop is occurring near the valve opening. A minimum pressure of 4.63 bars is seen close to valve opening due to contraction of flow area near the valve. After the valve opening as flow expansion occur due to larger outlet volumes, pressure again increases and reaches to demand pressure of 15bar

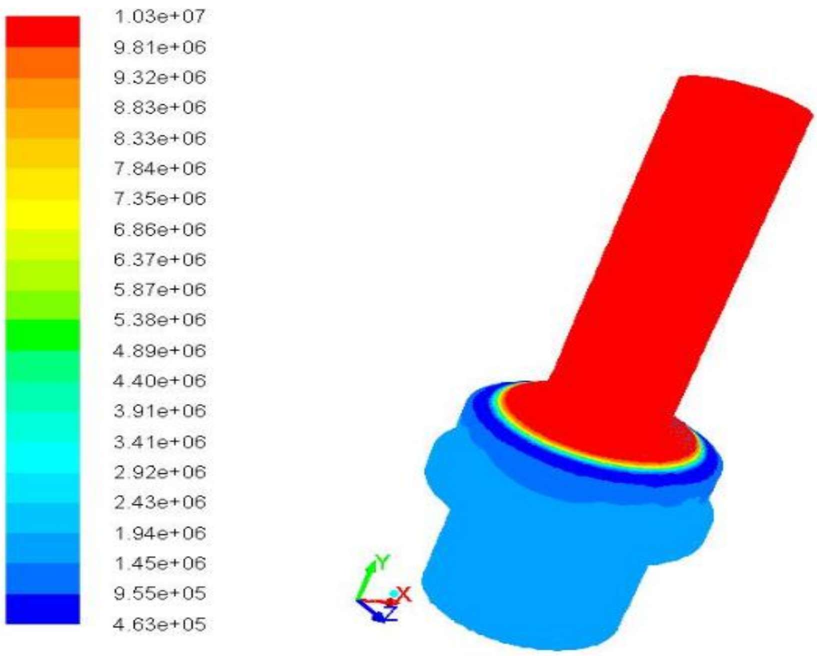

Figure 7.12 Pressure drop near valve opening

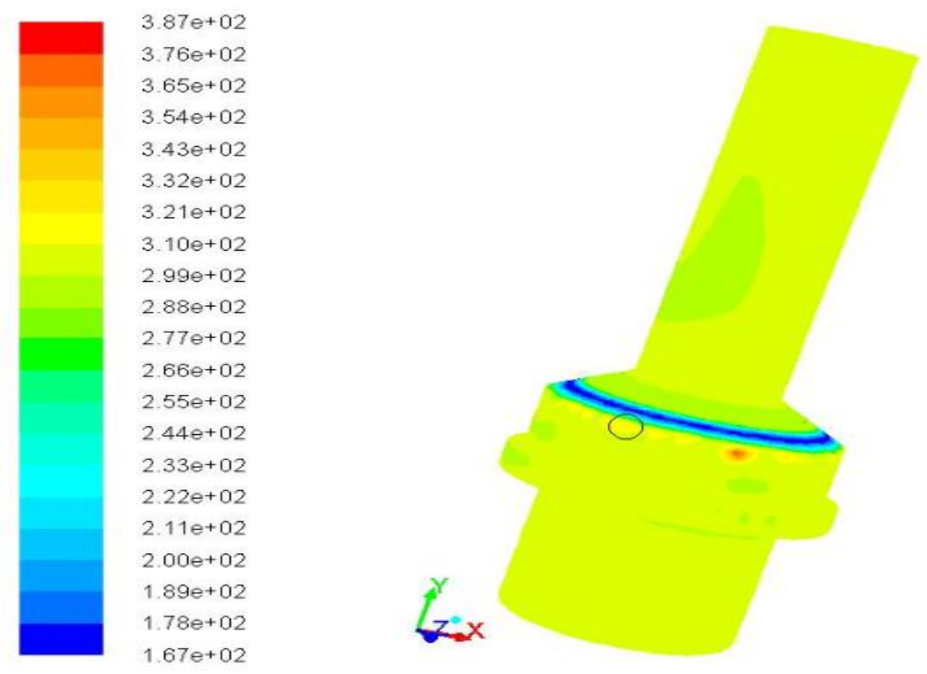

Figure 7.13 Temperature contour on moving shaft

Due to sudden drop of pressure near the valve opening and flow expansion as it cross the valve, temperature suddenly drops due to Joule Thomson effect. A minimum temperature region of 167k can be seen near valve opening in figure 7.12.

Contour of velocity magnitude is shown in figure 7.13. From the graph it is clear that nearest to narrow cross-section region of valve, the fluid is accelerated above the speed of sound while the static pressure drops according to Bernoulli's energy equation. So shock behavior can be seen near the valve after the shock behavior velocity decelerated below the speed of sound as a result the fluid is compressed to a smaller specific volume in the region near the valve as shown be seen in figure 7.14

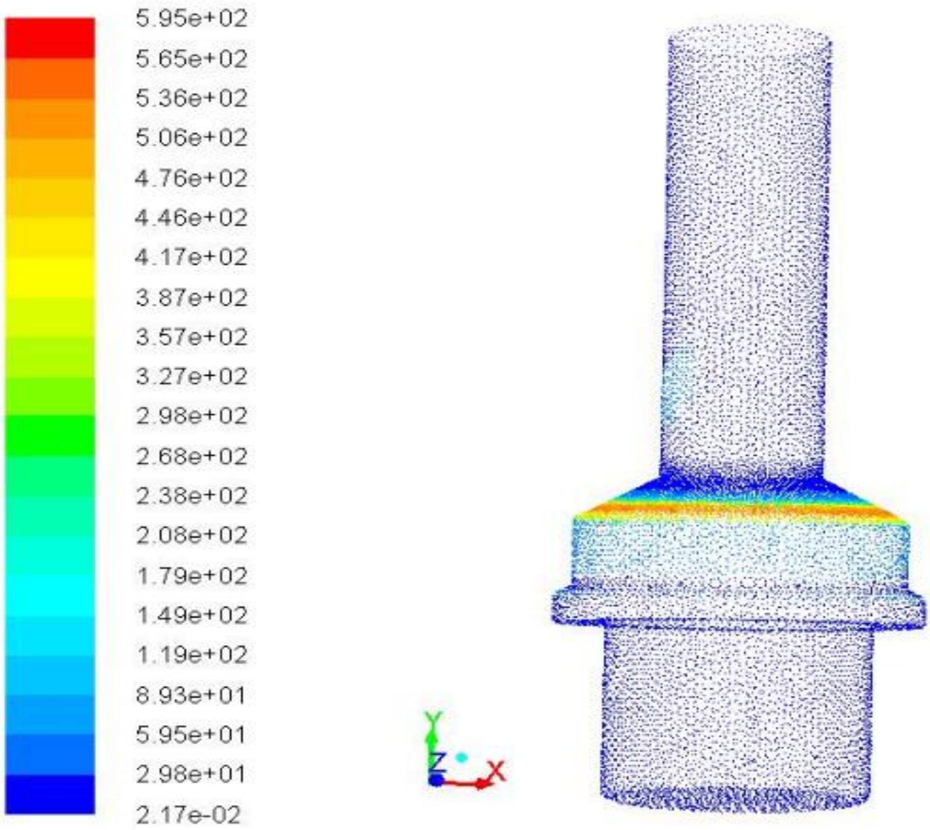

Figure 7.14 Contour of velocity vector (m/s)

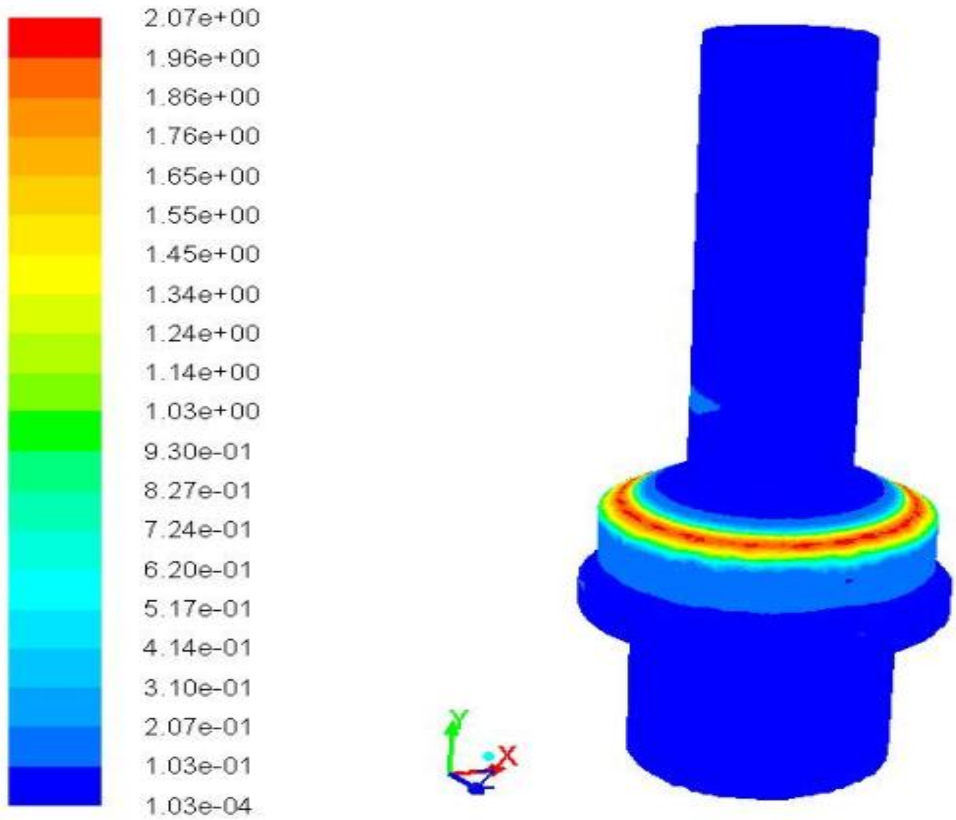

Figure 7.15 Contours of Mach number

7.8.1 2D Axis Symmetry Flow Domain

As From the above analysis it can be observed the major changing in pressure, temperature and velocity are occurring near the valve and on the moving shaft. Knowing this fact we can shorten our domain from the whole pressure regulator analysis to moving shaft analysis. For this reason we can simplified our flow geometry t0 2D axis symmetry case. In Figure 7.15 simplified 2D axis symmetry flow geometry is shown. We from now do all other analysis with this simplified flow geometry.

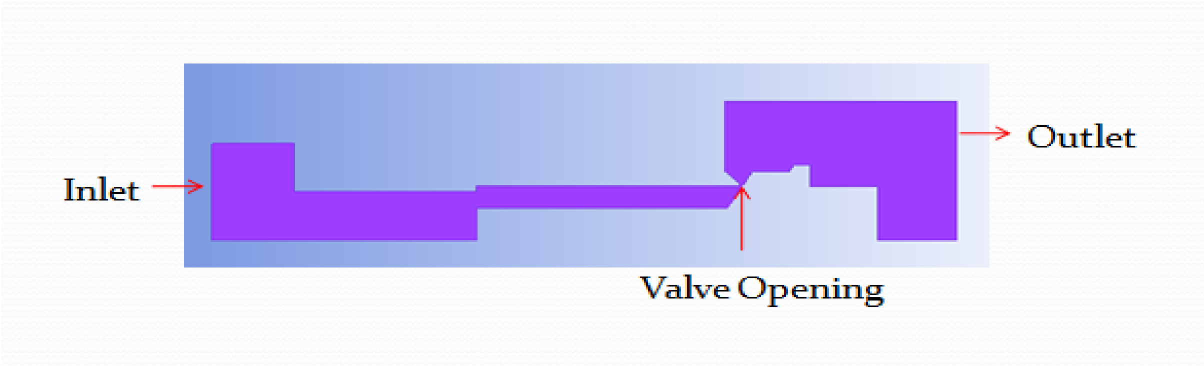

Figure 7.16 2D axis symmetry design for flow simulation on moving shaft

This simplified 2D axis symmetry geometry is designed and meshed in GAMBIT software [49]. Flow geometry is meshed with triangular meshed with the highly dense meshed near valve opening as can be seen in figure 7.16 and 7.17

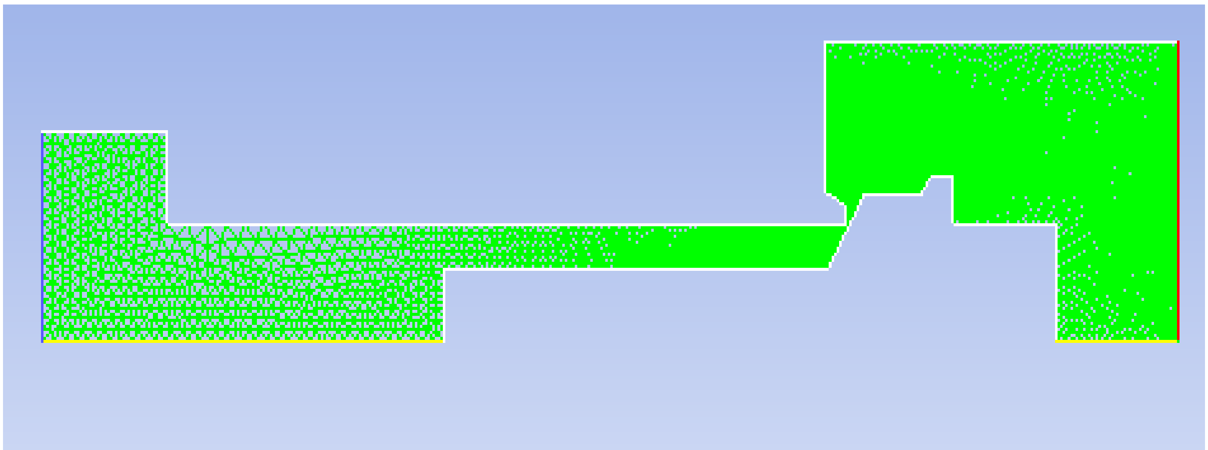

Figure 7.17 Flow geometry is meshed with triangular elements

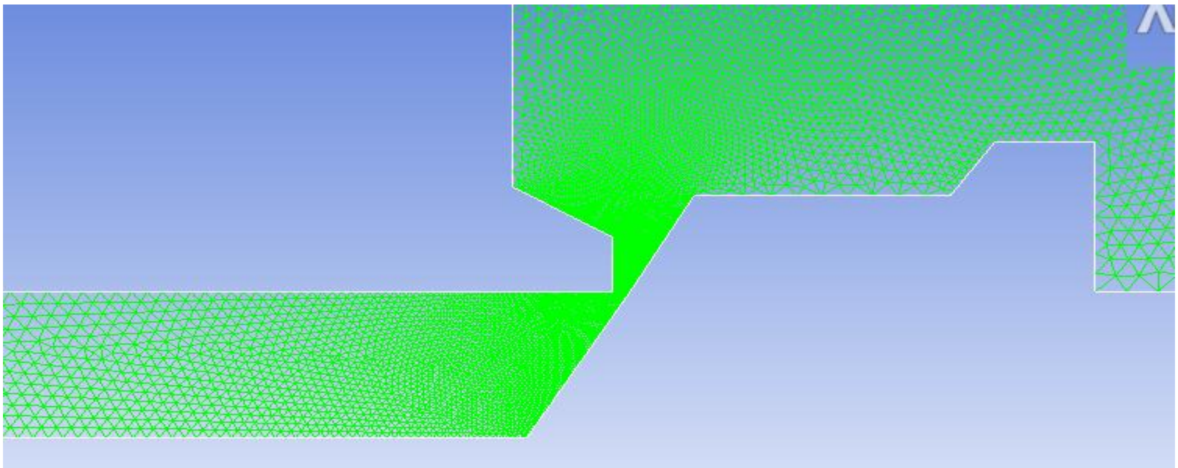

Figure 7.18 Highly dense meshed near valve opening

With the same boundary condition we simulated above 2D axis symmetric flow model in fluent. The mass flow rate achieved was same and here maximum pressure drop is seen near opening valve as can be seen in figures 7.18 and 7.19

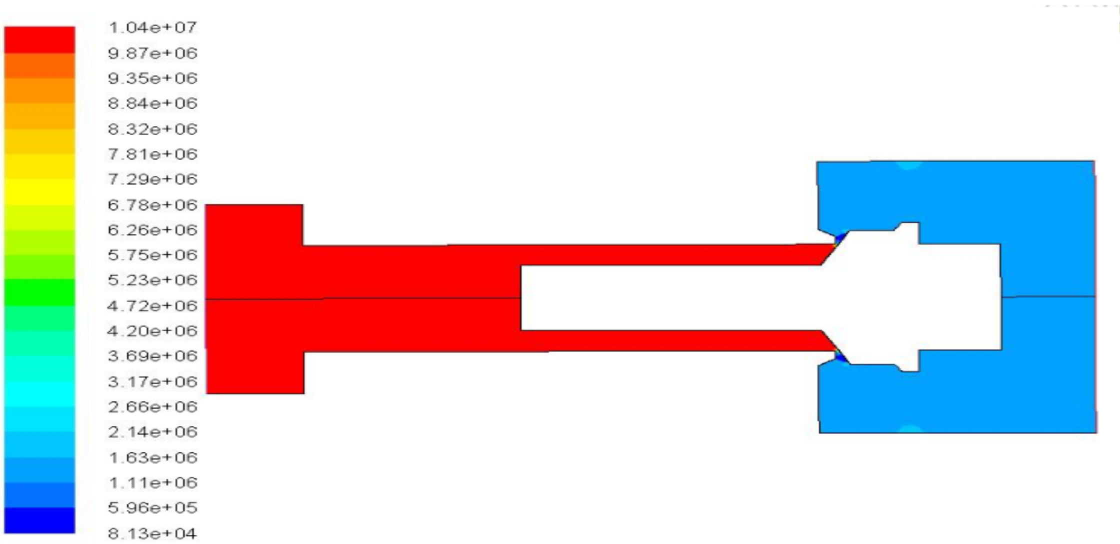

Figure 7.19 Pressure contour in moving shaft and on outlet volume

Here near the valve pressure reaches to its minimum level of 8bar and then again pressure increases due to expansion of flow area after valve opening.

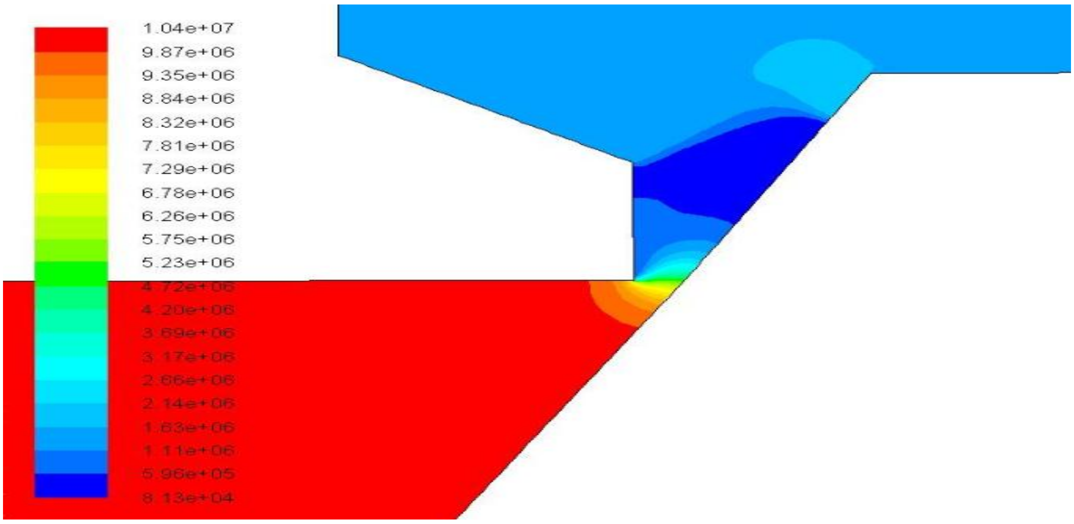

Figure 7.20 Maximum pressure drop near valve opening

A line is sketch which is passing from the valve opening to see the overall pressure change with respect to position. Pressure changes along this line is shown in following figure 7.20

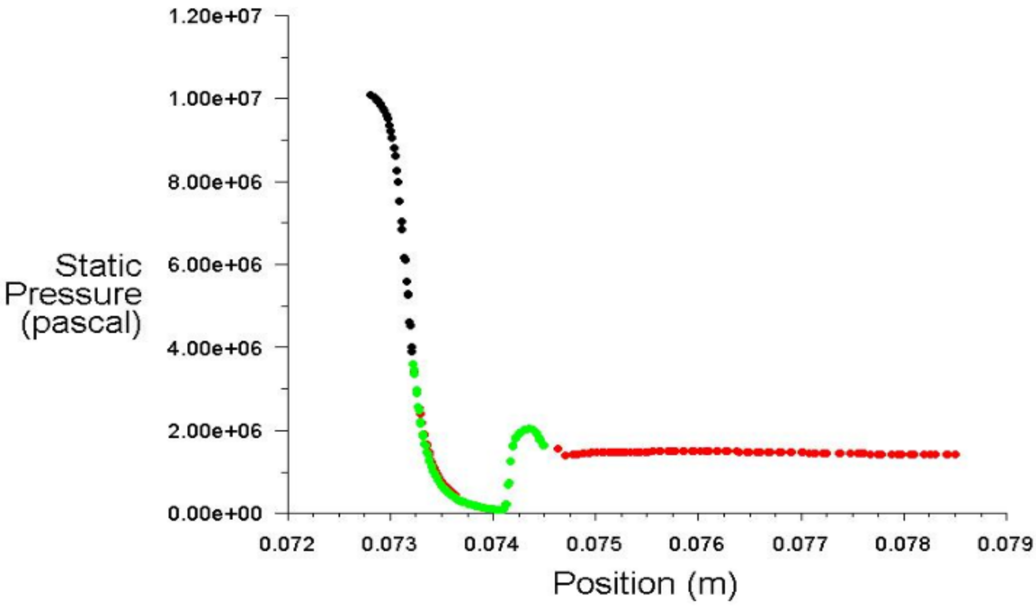

Figure 7.21 Pressure change along a line passing from the valve opening

Flow is accelerated in the contraction region near the valve opening and maximum velocity reaches to near 623m/s near the valve opening as shown in figure 7.21.and similarly mach number can be seen on line passing from the valve opening as shown in figure 7.22

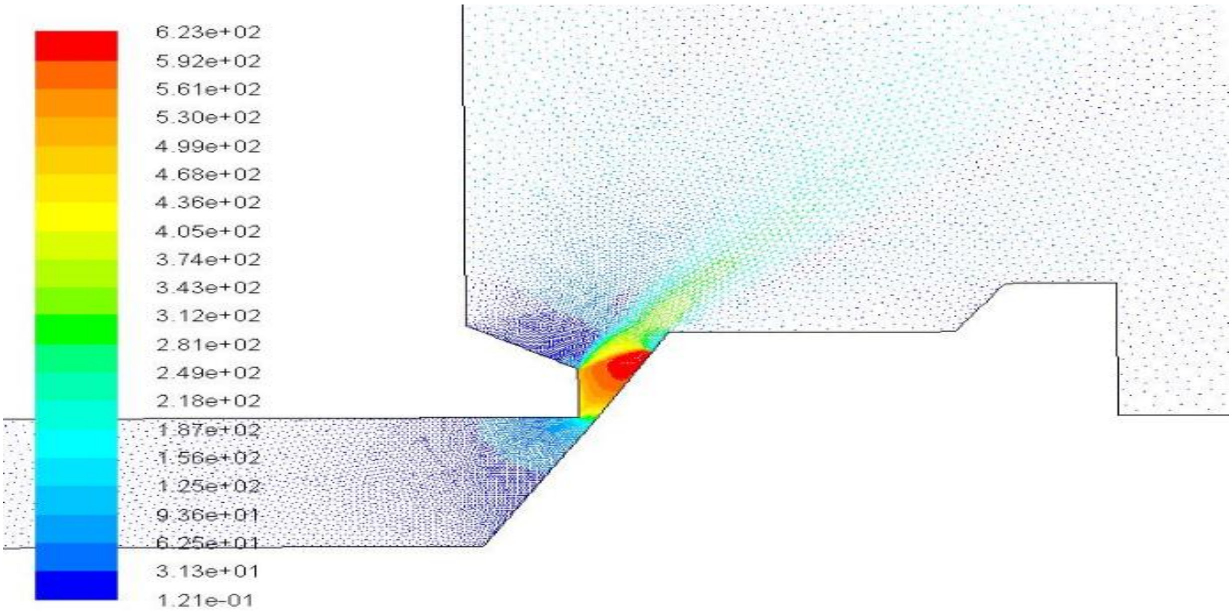

Figure 7.22 Velocity acceleration near the valve opening

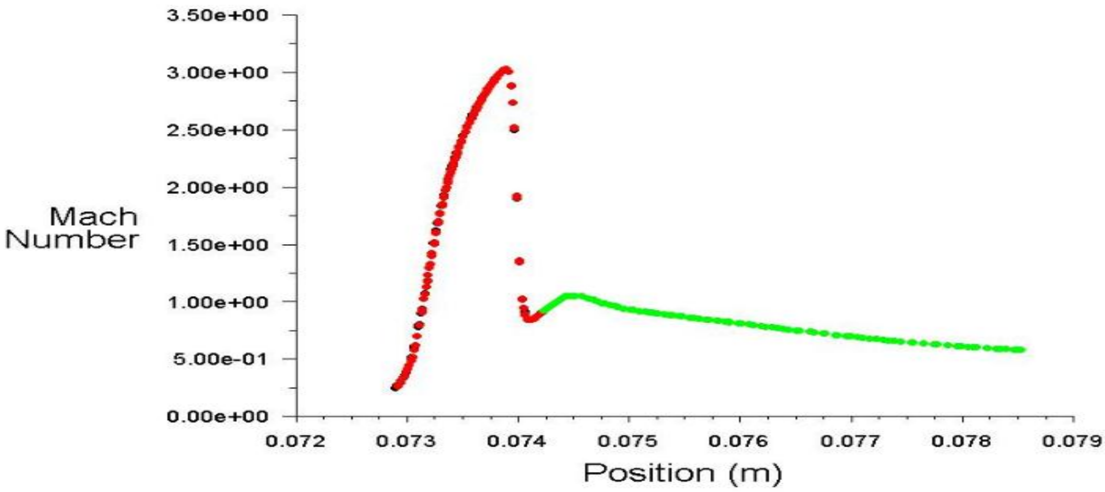

Figure 7.23 Flow acceleration along the line passing from the valve opening

Here we obtained the same result of mass flow rate, pressure and temperature distribution as in the case of complete 3D pressure regulator analysis. So we can confidently reduce over domain from 3D flow analysis to a axis symmetry flow analysis using the same design parameters

Similarly for different inlet pressures results and contour of pressures, temperature and velocity are shown in following figures.

7.8.2 Inlet Pressure 75 bar and valve opening is 0.5mm

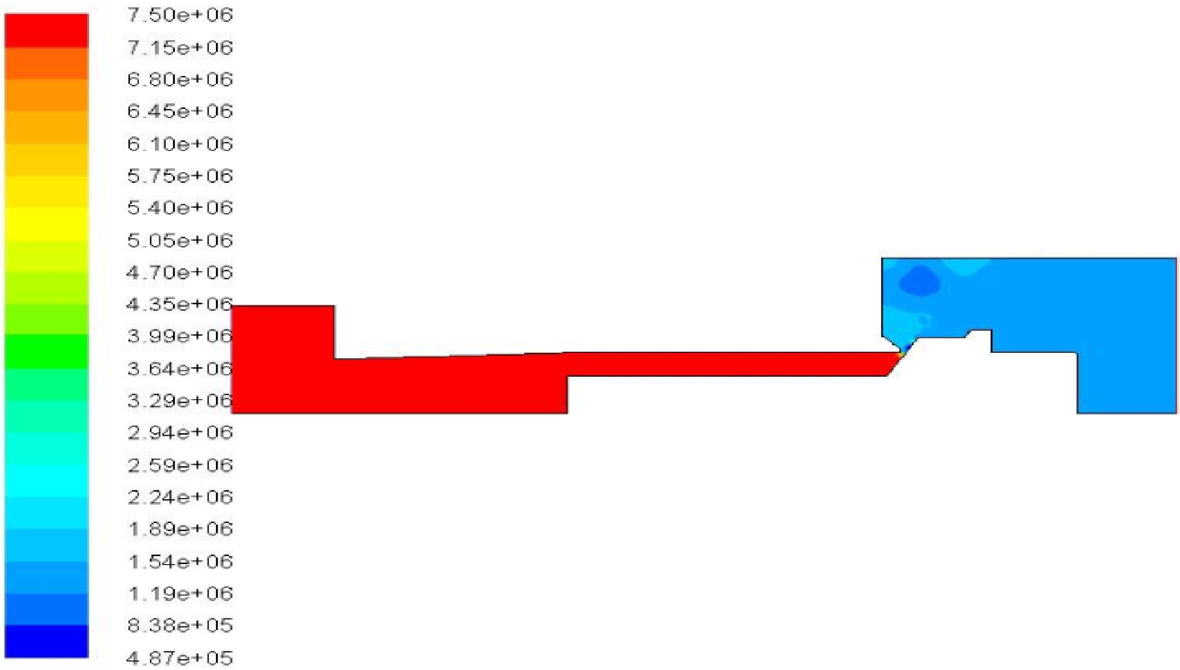

Figure 7.24 Pressure contour on moving shaft for inlet pressure of 75bar

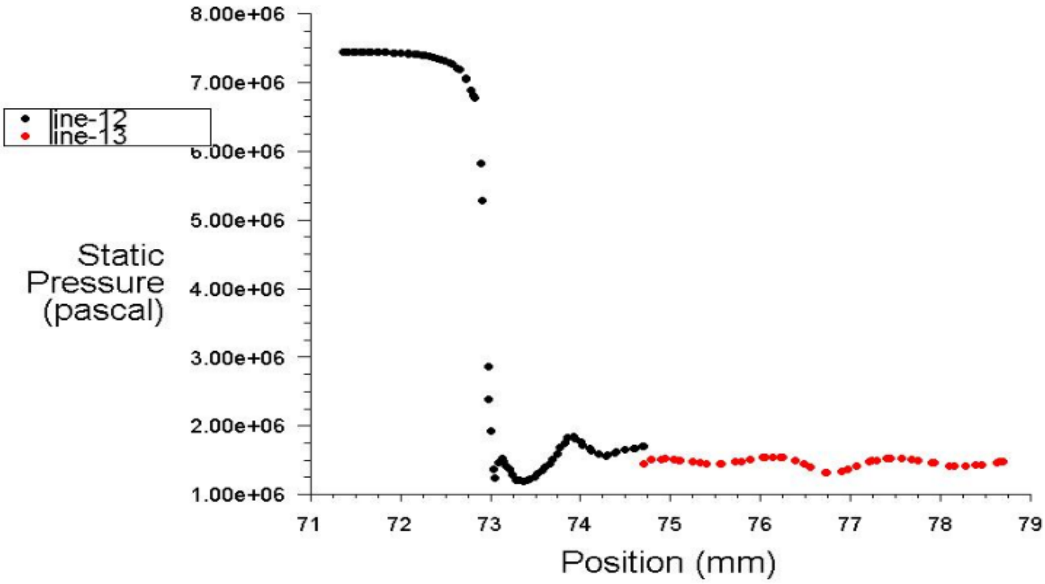

Figure 7.25 Pressure distribution along the line passing from valve opening

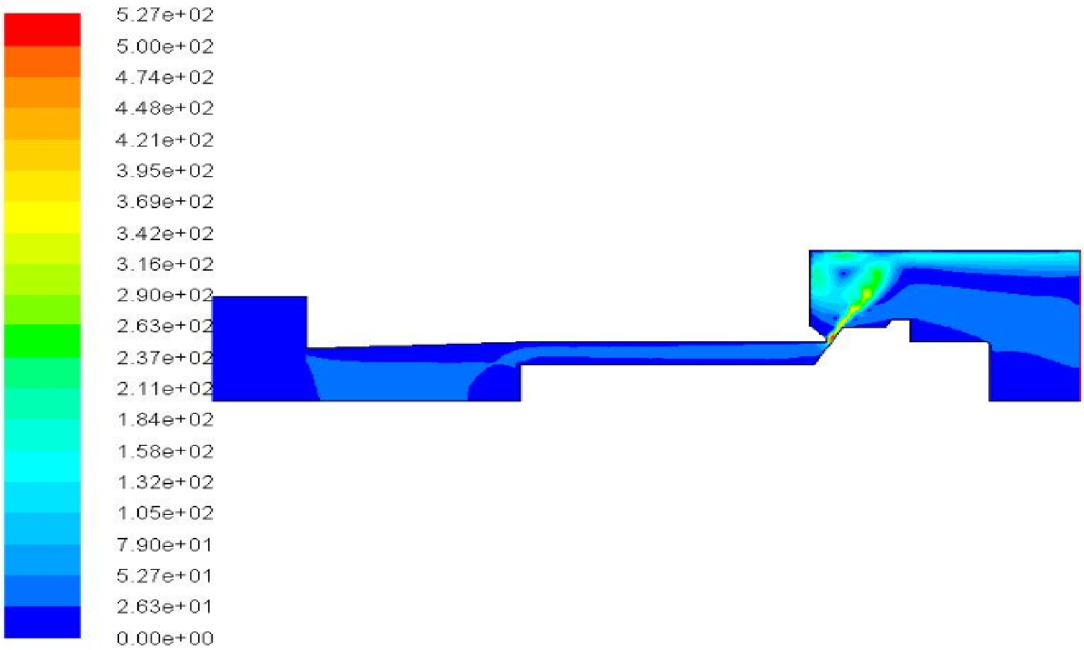

Figure 7.26 Velocity distribution for the inlet pressure of 75 bars

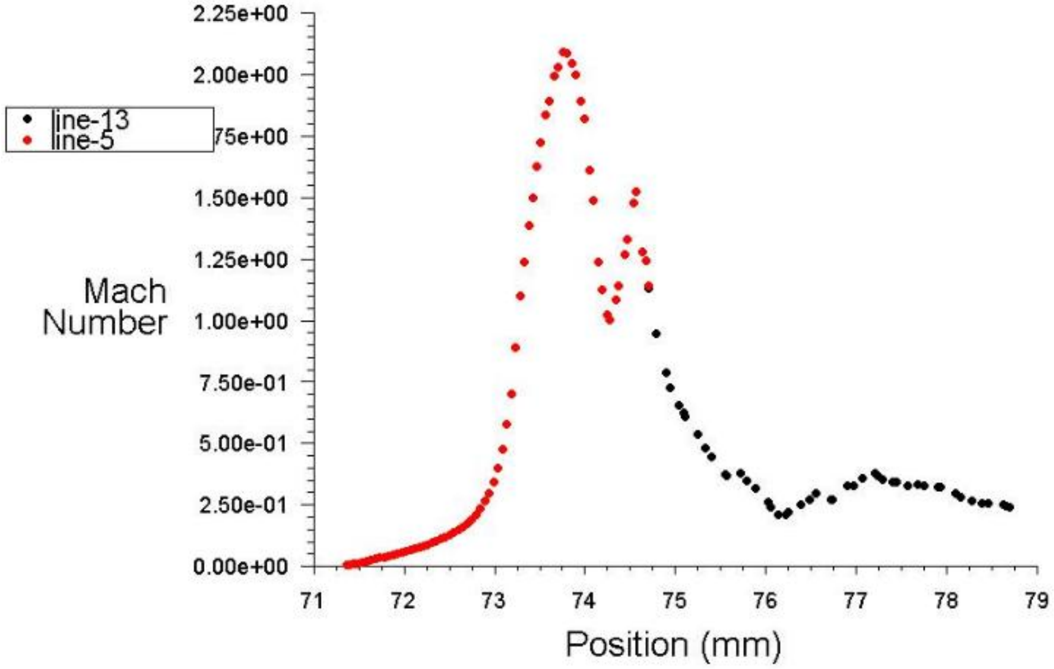

Figure 7.27 Mach number along the line passing from the valve opening position

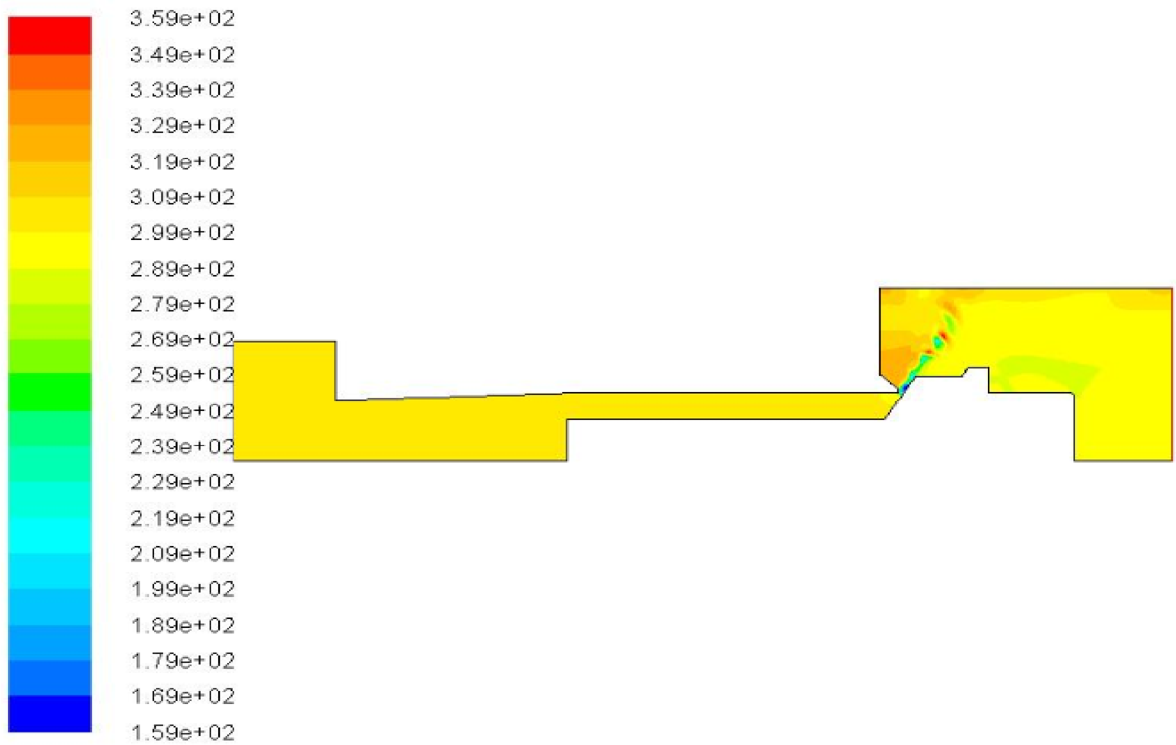

Figure 7.28 Temperature distribution for inlet pressure of 75 bars.

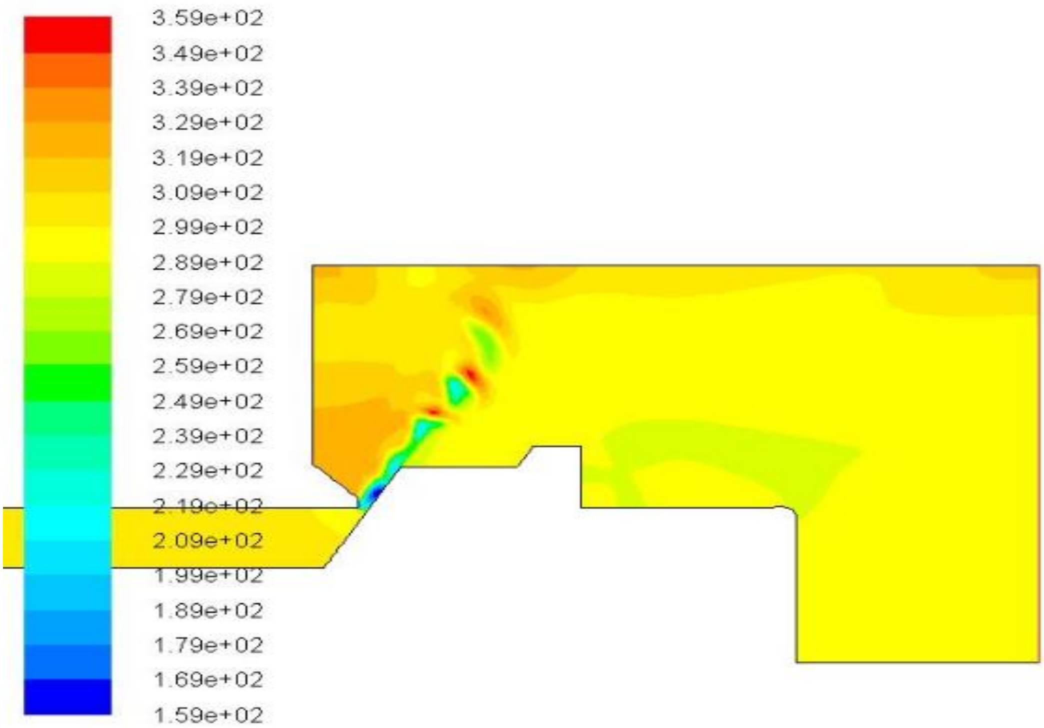

Figure 7.29 Temperature drop to minimum value near valve opening

7.8.3 Inlet Pressure 130 bar and valve opening is 0.275mm

Contour of pressure, temperature and Mach number are shown in the following graphs for the above inlet pressures

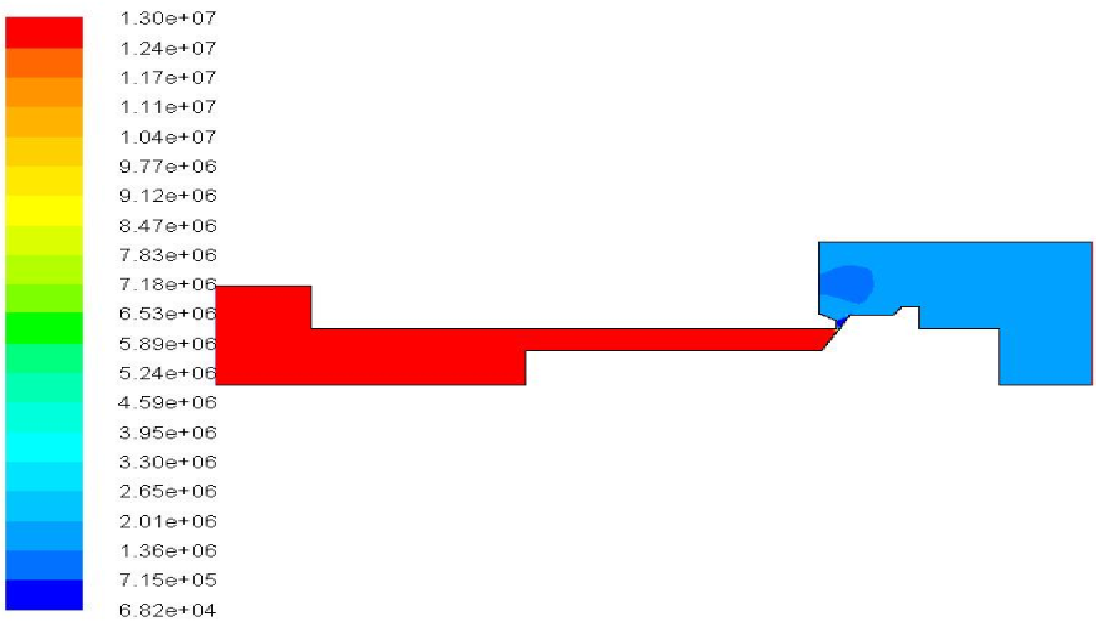

Figure 7.30 Pressure distributions for inlet pressure of 130e5

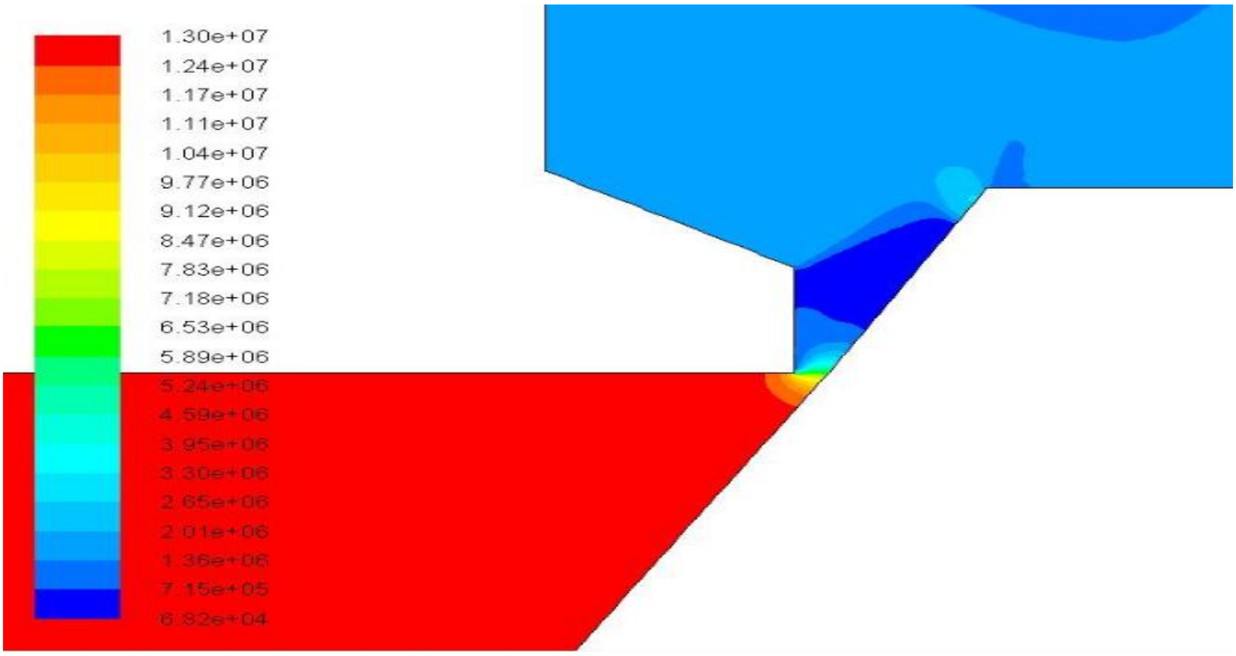

Figure 7.31 Minimum pressure near valve opening is near 6 bar

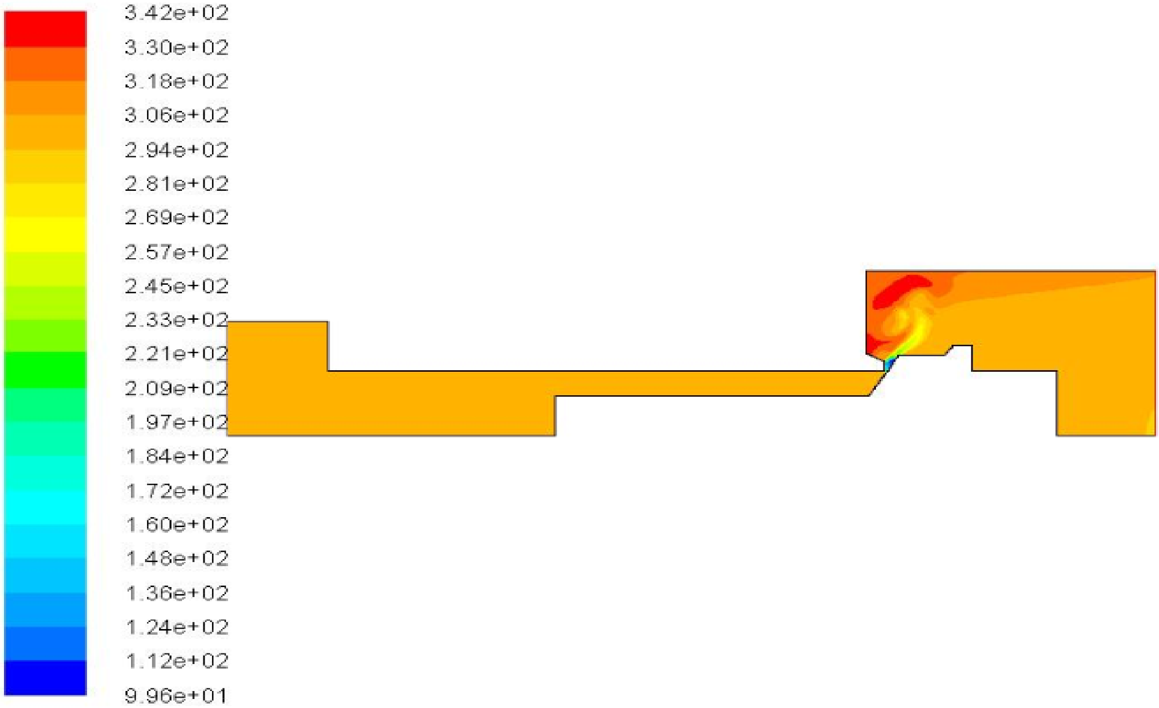

Figure 7.32 Contour of temperature distribution for inlet pressure of 130e5

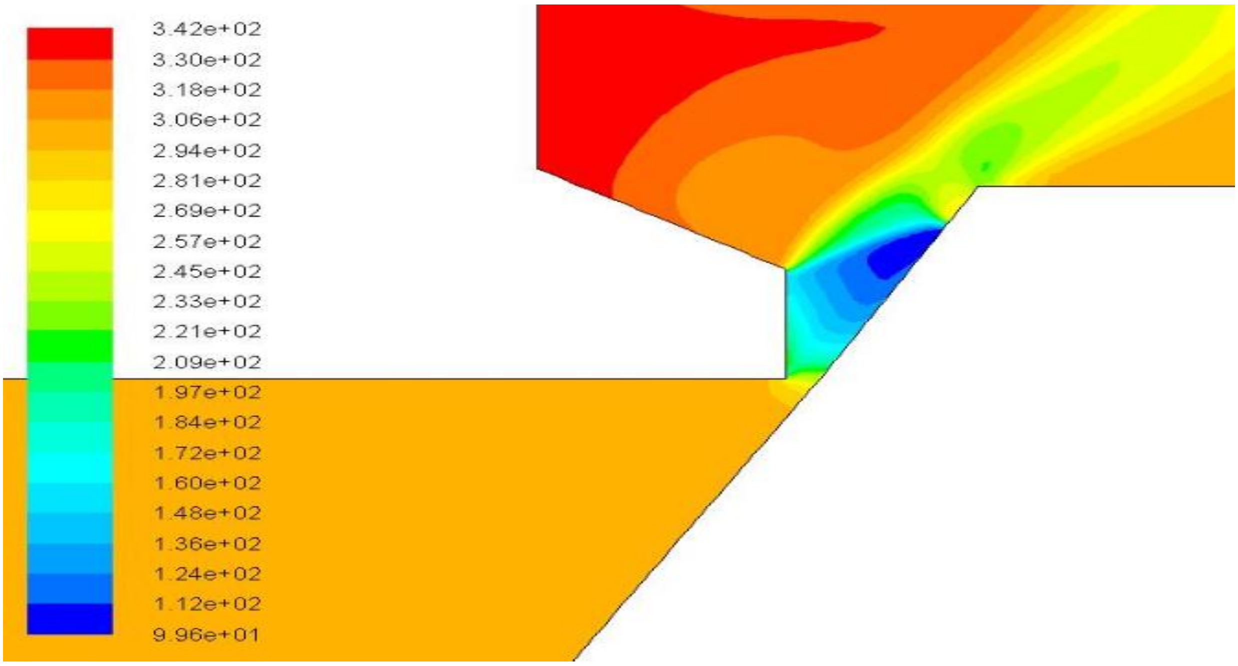

Figure 7.33 Minimum temperature reaches to 99.6k near the valve opening

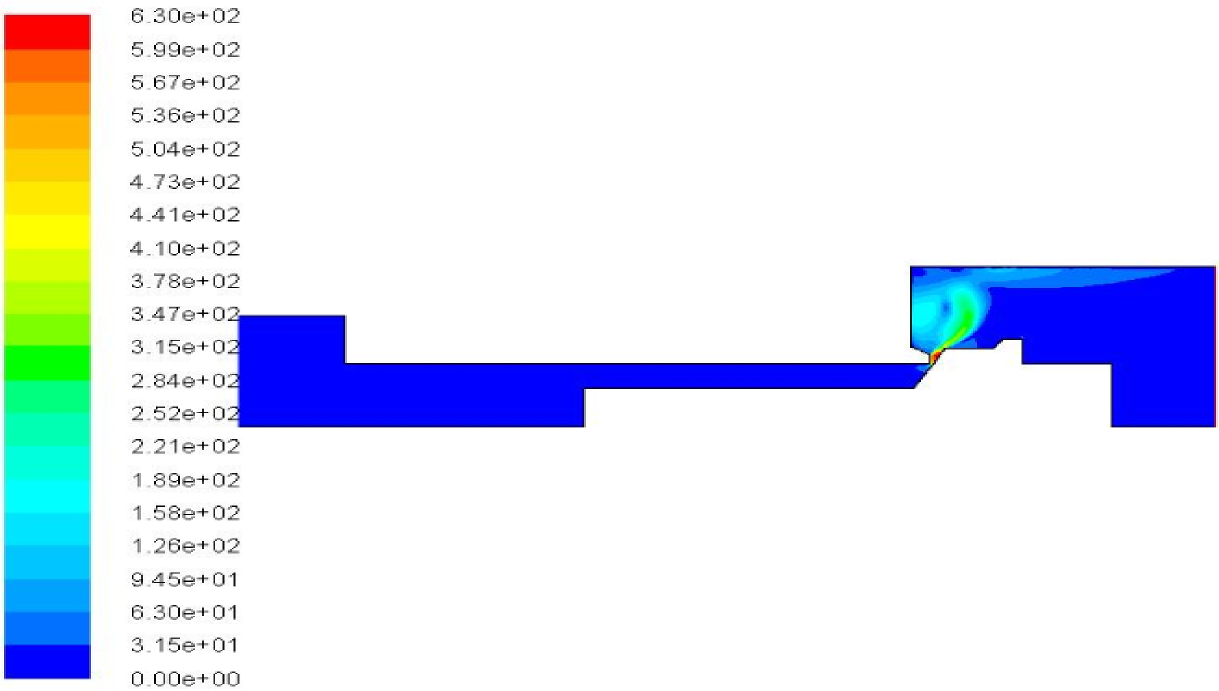

Figure 7.34 Flow accelerated near the valve up to 630m/s

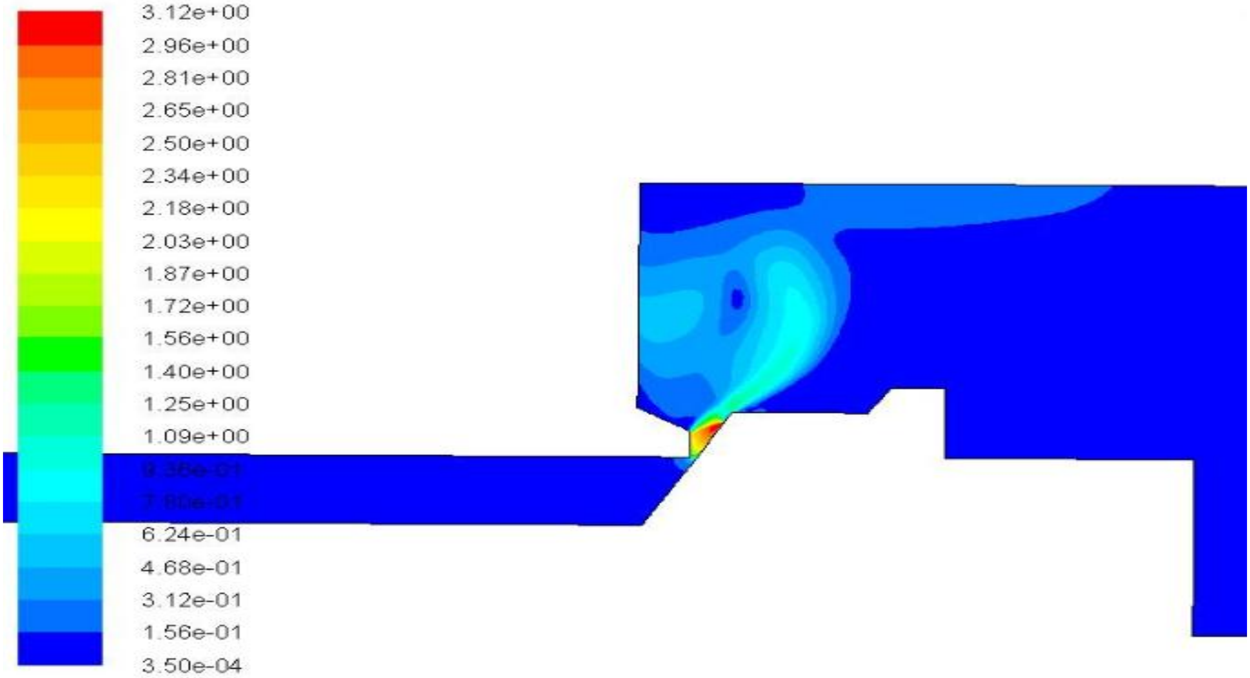

Figure 7.35 Shocks near the valve opening and Mach number distribution

Similarly for different inlet pressures CFD simulation are run and following values of mass flow rates are required for the given value of valve opening.

7.8.4 2D Axis Symmetry results for different inlet pressures from CFD Analysis

Inlet Pressure (Bar)	Outlet Pressure (Bar)	Mass Flow Rate (Kg/s)	Valve opening (mm)
65	15	0.34185	0.55
70	15	0.36419415	0.52
75	15	0.38918993	0.5
80	15	0.4054957	0.468
82.9	15	0.40577641	0.455
85	15	0.39477	0.45
90	15	0.42759642	0.42
95	15	0.39636	0.4
96.77531	15	0.40947	0.38
103.82804	15	0.395787	0.35
119.75	15	0.394587	0.3
134.55	15	0.39477	0.275
140	15	0.395787	0.256

7.9 Comparison of Numerical and CFD Results

A comparison of numerical and CFD analysis are given below. The difference in result is due to complete solution of Navier Stokes equation in CFD calculation as compared to the mathematical model of pressure regulator.

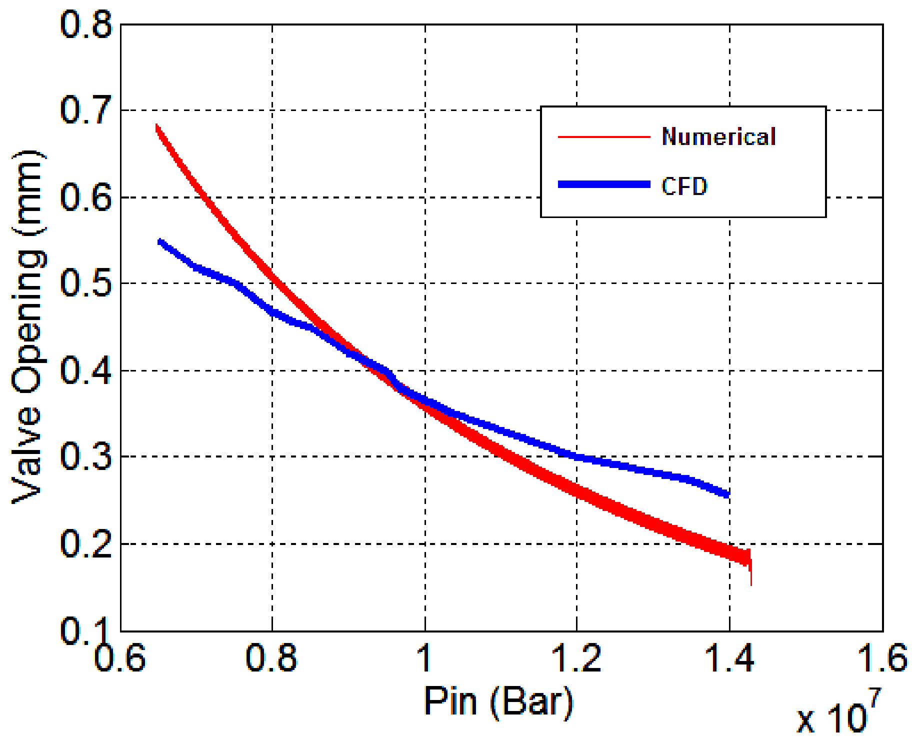

Figure 7.36 Comparison of Valve opening

For outlet pressure of 15 bars valve opening rate is found to be higher in non-linear mathematical formulation as compared to CFD.

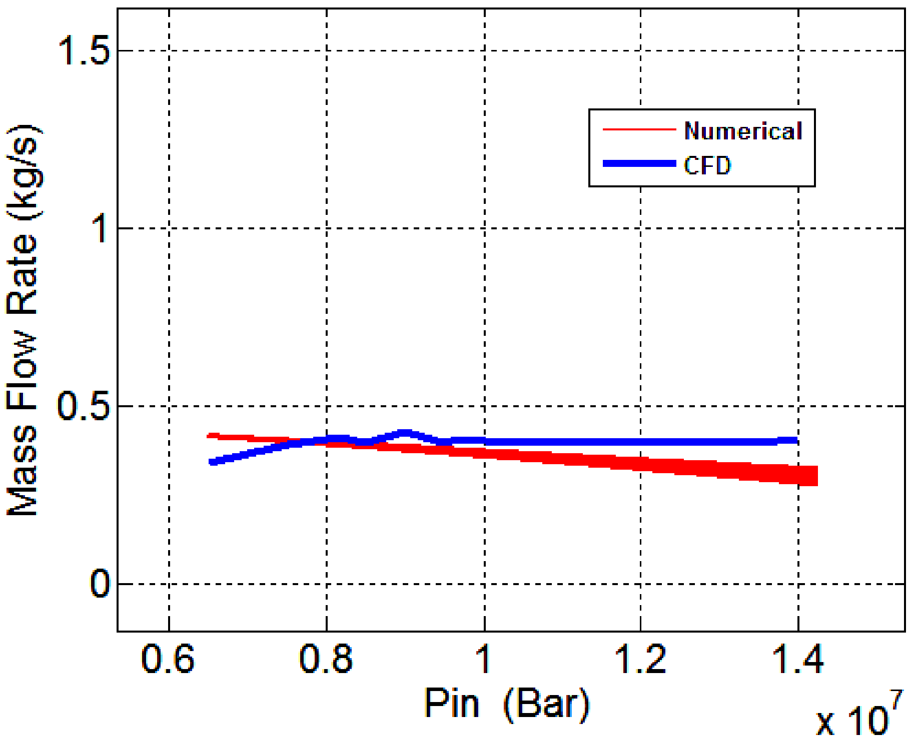

Figure 7.37 Comparison of Mass flow rate

Due to higher valve opening initially, mass flow rate found to be higher in CFD as compared to non-linear mathematical formulation.

CHAPTER 8
Conclusions and Future Work

This thesis considered the modeling and simulation of generic pressure regulator with respect to its design consideration. It mainly focuses on development of mathematical model for fluid flow in pressure regulator and its simulation for required outlet pressure. Through computational fluid dynamic a detailed simulation of fluid flow inside pressure regulator is provided. With some assumption, this thesis also provides an analytical solution for dynamical equation of pressure.

Brief introduction to pressure regulator and all its major components is provided in chapter 1. For understanding how a pressure regulator controls the outlet pressure, a detailed study is given on working of pressure regulator and on its fundamental principles. Various applications of pressure regulator in industries are briefly discussed with its particular usage in rocket feed system. Literature review on fundamental of pressure regulator, its stability analysis, its CFD study and mathematical modeling are presented in chapter 2. In chapter3 we developed the mathematical model of pressure regulator based on some assumptions. Equation of mass flow rate from regulator duct to valve opening and then to outlet port of regulator are developed. Dynamic equation of pressure and temperature are developed based on the continuity and energy equation to capture the pressure and temperature change in regulator ducts as a function of time. Equation of moving shaft is developed by Newton second law of motion and by force balancing. Computational form of flow equations are formed in chapter 4 for each regulator flow volumes. Numerical method is also presented in this chapter for finding valve clearance from equation of moving shaft. Simulation results and discussions are provided in chapter 5. Here results of both cases of inlet pressure are presented. Results include the dynamic simulation of pressure, mass flow rate and temperature as a function of time and inlet pressure. CFD studied of flow inside pressure regulator is presented in chapter 6. Both 3D and 2D flow models of pressure regulator are discussed here and contour of pressure drop, temperature drop and mass flow rate are obtained for various cases. Analytical solution of flow equation is developed in chapter 7 based on some assumption. The result of analytical solution is compared with numerical results and satisfactory results were obtained.

8.1 Future Research

Pressure regulator is very essential components of high pressure flow system. For safety of system attached with pressure regulator, pressure relief valve is also joined with outlet volume of pressure regulator. So a complete analysis of pressure regulator with pressure relief valve is also necessary for the safety of system which requires an extension of mathematical model of flow system. Now in industry mechatronical pressure regulator are also used which senses the outlet pressure with sensor attached to its outlet port and corresponding valve opening information is passed to moving shaft. For this mechatronical pressure regulator a detail research needed in order to make its mathematical model and its simulation. In CFD study of pressure regulator, a detail research is also needed which correspond to user defined function for finding valve clearance as a function of outlet pressure with the employment of dynamic meshing in Fluent.

REFERENCES

[1] Technical monograph 27 , Fundamental of Gas Pressure Regulation, Floyd D. Jury Director Education, Fisher Control International, Inc 205 south Center Street Marshalltown, Lowa 50158 USA.

[2] Lain Johnston, Emerson Process Management

[3] Kevin Shaw Actaris Metering System 970 Hwy, 127 North, Owenton, Kentucky

[4] Miles O Dustin, Analog computer study of design parmeter effects on the stability of a direct-acting gas pressure regulator, NASA TN D-6267,1971

[5] DragoljubVujic, Slobodan Radojkovic, Facta University Mechanics, Automatic Control and Robotics Vol. 3 N11, 2001, pp 269-276

[6] Jiang Yanping, ShenChibing, Simulation research on the dynamic process of gas pressure reducing valve, 46the AIAA/ASME/SAE/ASEE Joint propulsion conference & Exhibit 25-28 july, Nashville, TN

[7] Sunil S. UllekhPandey, mathematical modeling of pressure regulator for cryogenic application, proceeding of the 37th national & 4th international conference on fluid mechanics and fluid power December 16-18, 2010, IIt Madras, Chennai, India

[8] A. R. Shahani, H. Esmaili, Dynamic simulation of a high pressure regulator, Toosi University of Technology, Pardis street, mollasadra avenue, vanak square, P.O. box 19395-1999, Tehran, Iran

[9] D.J. Kukulka, A. Benzoni and J.C. Mallendorf, Digital simulation of a Pneumatic pressure regulator, Simulation Modelling , Practice and Theory, pp252-266, (1994)

[10] A. Nabi, E. Wacholder and J. Dayan, “Dyamic Model for a Dome-Loaded Pressure Regulator”, Transactions of ASME, Dynamic System, measurement, control, vol. 122,pp 290-297 (2000).

[11] NaciZafer, Greg R. Luecke, ‘‘Stability of gas pressure regulator’’,Elsevier Science Direct applied mathematical modeling.

[12] B.G. Liptak, pressure regulator, Chem. Eng (1987) 69-76

[13] E1 Golli Rami, Bezian Jean-Jacques, ‘‘Stability study and modeling of a pilot controlled regulator”, Materials Science and application, 2011,2, 859-869

[14] Binod Kumar Saha, “World Academy of Science, Engineering and Technology 77 2013”

[15] Harald Ortwig, Prod. Dr.-Ing,“Investigation and CFD simulation of flow forces inside a mehatronical pressure controller for CNG- Engines”,12th Pan-American Congress of Applied Mechanics January 02-02-2012, Port of Spain, Trinidad.

[16] AditiaOza, Sudipto Ghosh, “CFD modeling of globe valves for oxygen application”, 16the Australasian Fluid Mechanics Conference Crown Plaza, Gold Coast, Australia 2-7 December 2007

[17] G. Tamizharasi and S. Kathiresan, “CFD analysis of Butterfly valve in a compressible Fluid”, Middle-East Journal of Scientific Research 15 (12):1834-1838,2013 ISSN 1990-9233.

[18] X. Du and S. Gao, “Numerical study of complex turbulent flow through valves in a steam turbine system”, International Journals of Material, Mechanics and Manufacturing, Vol.1 No 3, August 2013

[19] Jeremy Shipman, Ashvin Hosangadi , “unsteady analysis of valve systems in rocket engine testing environments”, combustion research and flow technology inc. (Craft Tech), American Institute of Aeronautics and Astronautics.

[20] Young JoonAn, Byeong Jin Kim, “Numerical Analysis of a 3-D flow through LNG marine control valves for their advanced design”, Journal of Mechanical Science and Technology 22 (2008) 1998-2005 Springer

[21] Chang-Hoon Shin, “A numerical study on the characteristics of transient flow in a pressure regulator resulting from closure of the pressure control valve”, Journal of Mechanical Science and Technology

[22] Adeel Mehmood, “Modeling, simulation and robust control of an electro-pneumatics actuator for a variable geometry”.

[23] Perry J A (1949), “Critical Flow through Sharp- Edge Orifice”, Trans ASME 71(10): 757-764

[24] Stenning A (1954) , " An experimental Study on two-dimensional gas flow through valve-type orifices", ASME paper no 54-A-45

[25] Benedict R P (1971) Generalized contraction coefficient of an orifice for subsonic and supercritical flow. Transaction of the ASME- Journal of Basic Engineering 93 (6): 99-120

[26] Andersoon S B, Bevengut G, Eckersten j, Ek G, Kalldingb (eds) 1975 Atlas Copco Air Compendium Atlas Copco AB, Stockholm, pp 567-592

[27] Ward-Smith A J (1979) Critical Flow metering: The Characteristics of Cylindrical Nozzles with Sharp Upstream Edges. Int. J. Heat & Fluid 1 (3): 123-131

[28] Reid J, Steward C D (1988) A review of critical flow nozzles for the mass flow measurement of gases, 2nd International symposium on Fluid Control, Measurement, Mechanics and Flow Visualization FLUCOME 88, 5-9 Sept, Sheffield England pp 454-457

[29] Brower W B, Eisler E, Gilkorn E J, Gonenc J, Plati C, Stagnitti J (1993) , " on the compressible flow through an orifice. Trans ASME, Journal of Fluid Engineering 115:660-664

[30] Fleisher H (1995) , " Manual of pneumatic system operation. McGraw-Hill, New York San Fancisco Washington Auckland Bodota Caracas Lisbon London

[31] J.E. Carniro and F.G. Almeida, "Reduced-order thermodynamics models for servo pneumatic actuator chambers", Journal of system and control engineering, 220:301-314, 2006

[32] L. Guzzella and C.H. Onder, "Introduction to modeling and control of internal combustion engine system". Publisher Springer, ISBN-13:978-354022743, 2004

[33] A.J. Kotwicki and J. Russel, "Vacuum valve actuator model". International Fuels and Lubricant meeting and expositions,107,1998.

[34] Baline W. Anderson, 1979, the analysis and design of pneumatic system", John Wiley & sons Inc., Ny, USA, pp. 17-31

[35] A.F. Conteras, I. P Auiroz, and C.C. Wit, "Modeling and identification of electronic throttle body", 10th Mediterranean conference on control and automation, Lisbon Portugal, 2002

[36] L, Marton and B. Lantos, "Modeling, identification and compensation of stick-slip friction". IEEE Trans, on Industrial Electronics

[37] H. Olsson, K.J. Astrom, c. Canudas de Wit, M. Gafvet, and P. Lischinsky, "Friction models and friction compensation". European Journal of control

[38] D. Karnopp, "Computer simulation of stick-slip friction in mechanical dynamic systems", ASME journal of dynamic systems, measurement and control

[39] H. Olsson, K.J. Astrom, C. Canudas de Wit, M. Gafvert, and P. Lischinsky, "Friction models and friction compensation", European Journal of Control

[40] P.R Dahl, "Measurement of solid friction parameters of ball bearing", Sixth Annual symposium on incremental motion control systems and devices, 1977

[41] Y. rochdi, F. Giri, F.Z. Chaoui, F. Ikhouane, and J. Rodellar, "Parameter identification of non-linear hysteretic system", Journal of Nonlinear Dynamics

[42] C. Canudas de Wit, H. Olsson, J.K. Astrom, and P. Lischinsky. "A new model for control system with friction". IEEE Transactions on Automatic Control

[43] S. Thiery, " Modeling and compensation of fragmentation of linear motor". Phd thesis, EcolePolytechniqueFederale de Lausanne, 2005

[44] Z. Wenjing, Parameter identification of luger friction model in servo system based on improved particle swarm optimization algorithm", Proceedings of the 26th Chinese control conference

[45] ANSYS FLUENT-Solver theory Guide, ANSYS Inc, Release 14.0, South Pointe, 275 Technology Drive, Canonsburg, PA 15317 November 2012

[46] B.E. Launder, D.B. Spalding, "The numerical computation of turbulent flows", Computer method in applied mechanics and engineering vol.3. p. 269-289, 1974

[47] Shih TH, Liou WW, Shabbir A. Yang A, Ahu J. A new k-ε eddy-viscosity model for high Reynolds number trubulent flows-model development and validation. Computer fluids 1995; 24-227-38

[48] Chattopadhyay H, Kundu A, Saha B, K , Gangopadhyay T, analysis of Flow structure inside a spool Type pressure regulating valve energy conversion and management 2012; 53; 196-204

[49] Gambit Tutorial Guide, Gambit Fluent Inc. Release 2.4.6, 2007